AD-A058 471 HONEYWELL RADIATION CENTER LEXINGTON MASS F/G 17/5
HIGH-REJECTION TELESCOPES. UTAH STATE UNIVERSITY TELESCOPES HS---ETC(U)
JAN 77 W R WILLIAMSON F19628-72-C-0226
UNCLASSIFIED AFGL-TR-77-0099 NL

OF
AD
A058471

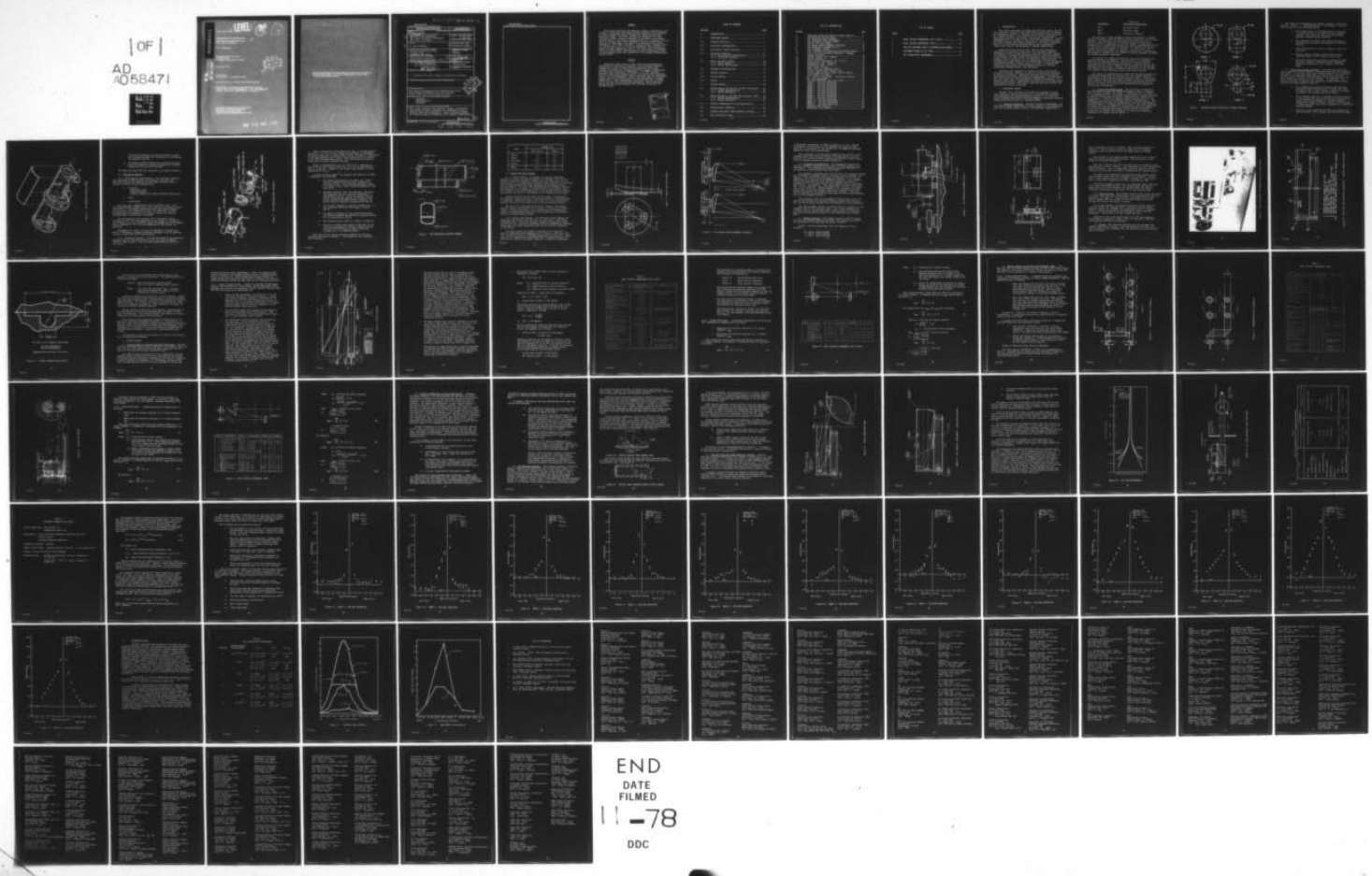

END
DATE
FILMED
11-78
DDC

AFGL-TR-77-0099

LEVEL II

HIGH-REJECTION TELESCOPES

Utah State University Telescopes HS-2, NS-2, and TPM-1

W. R. Williamson

Honeywell Radiation Center
2 Forbes Road
Lexington, Massachusetts 02173

31 January 1977

Final Report
10 April 1972 - 31 December 1976

Approved for public release; distribution unlimited

This research was sponsored by the Defense Nuclear Agency under subtask K11BAXHX534, Work Unit CDNA 0018, entitled, "High Stray Light Rejection Telescopes."

AIR FORCE GEOPHYSICS LABORATORY
AIR FORCE SYSTEMS COMMAND
UNITED STATES AIR FORCE
HANSCOM AFB, MASSACHUSETTS 01731

(1) Final rept. 10 Apr 72 - 31 Dec 76

UNCLASSIFIED

SECURITY CLASSIFICATION OF THIS PAGE (When Date Entered)

REPORT DOCUMENTATION PAGE		READ INSTRUCTIONS BEFORE COMPLETING FORM
(18) 1. REPORT NUMBER (19) AFGL-TR-77-0099	2. GOVT ACCESSION NO.	3. RECIPIENT'S CATALOG NUMBER
(6) 4. TITLE (and Subtitle) HIGH-REJECTION TELESCOPES, Utah State University Telescopes HS-2, NS-2, and TPM-1.		5. TYPE OF REPORT & PERIOD COVERED Final - 10 Apr 1972 31 Dec 1976 6. PERFORMING ORG. REPORT NUMBER
(10) 7. AUTHOR(s) W. R. Williamson		8. CONTRACT OR GRANT NUMBER(s) (15) F19628-72-C-0226
9. PERFORMING ORGANIZATION NAME AND ADDRESS Honeywell Radiation Center 2 Forbes Road Lexington, MA 02173		10. PROGRAM ELEMENT, PROJECT, TASK AREA & WORK UNIT NUMBERS 62704H CDNA15AA
11. CONTROLLING OFFICE NAME AND ADDRESS AF Geophysics Laboratory Hanscom AFB, Massachusetts 01731 Monitor/Dean Kimball/OPR	(11)	12. REPORT DATE 31 January 1977 13. NUMBER OF PAGES (12) 86 p.
14. MONITORING AGENCY NAME & ADDRESS (if different from Controlling Office) (16) K11BAXH (17) X534		15. SECURITY CLASS. (of this report) Unclassified 15a. DECLASSIFICATION/DOWNGRADING SCHEDULE

16. DISTRIBUTION STATEMENT (of this Report)

A - Approved for public release; distribution unlimited

17. DISTRIBUTION STATEMENT (of the abstract entered in Block 20, if different from Report)

DDC RELEASED SEP 12 1978 F

18. SUPPLEMENTARY NOTES

This research was sponsored by the Defense Nuclear Agency under subtask K11BAXHX534, Work Unit CDNA 0018, entitled, "High Stray Light Rejection Telescopes."

19. KEY WORDS (Continue on reverse side if necessary and identify by block number)

Cryogenic
High-Rejection
Telescope

20. ABSTRACT (Continue on reverse side if necessary and identify by block number)

This report describes the analysis, design, construction, and testing of three telescopes for radiometric sensors built by Utah State University. These telescopes operate at widely-varying IR frequencies and cryogenic temperatures.

404 486

DD FORM 1 JAN 73 1473 EDITION OF 1 NOV 65 IS OBSOLETE

UNCLASSIFIED

SECURITY CLASSIFICATION OF THIS PAGE (When Date Entered)

SUMMARY

This report describes the analysis, design, construction, and testing of telescopes with high off-axis rejection to be attached to three radiometric sensors designed and built by Utah State University (USU). The three sensors are components of a CVF (Circular Variable Filter) instrument to be flown on the SPIRE I auroral mission. One sensor designated HS-2 is a long-wave (3.6 to 16.8 μm) IR radiometer that operates at supercritical helium temperature (less than 20 Kelvin). Another sensor designated NS-2 is a short-wave (1.35 to 4.6 μm) IR radiometer that operates at liquid nitrogen temperature (80 K). The third sensor designated TPM-1 is a dual-channel photomultiplier using wavelenghs of 5000 to 7000 angstrom units that operates at non-cryogenic temperatures (above 270 K).

PREFACE

During the latter part of 1971, the Air Force Geophysics Laboratory and Utah State University (the instrument supplier) established a need for high off-axis-rejection telescopes capable of operation at cryogenic and non-cryogenic temperatures for USUs three radiometric instruments. In 1970, Honeywell Radiation Center had designed, built, and tested such telescopes as part of the TOM program. These telescopes used all-reflecting optics, had good off-axis rejection, and performed at cryogenic temperatures. AFGL subsequently contracted with HRC to design, build, and test the required USU telescopes; these telescopes follow the same design precepts that had been successful for the TOM sensor.

TABLE OF CONTENTS

LIST OF ILLUSTRATIONS

LIST OF TABLES

1. INTRODUCTION

This report describes the design and analysis, build, and off-axis rejection testing of three high off-axis rejection telescopes for radiometric sensors to be flown on the SPIRE I auroral mission. One, designated HS-2, is an LWIR (3.6-16.8 μm) CVF instrument operating at supercritical helium (<20 Kelvin) temperature. Another, designated NS-2, is a SWIR (1.35-4.6 μm) CVF instrument operating at liquid nitrogen (80 Kelvin) temperature. The third instrument, TPM-1, is a dual channel photomultiplier, with wavelengths of 5,000 Å and 7,000 Å, and operating at ambient temperatures.

During the latter part of 1971, the Air Force Geophysics Laboratory and Utah State University, the instrument supplier, established a need for high off-axis rejection telescopes capable of operation at cryogenic temperatures for the above instruments. A year before this time (1970), the Honeywell Radiation Center had designed, built, and tested an all reflecting, high rejection, cryogenically cooled sensor for the TOM Program. AFGL subsequently contracted with HRC to design, build, and test the required USU telescopes which follow the same design precepts as had been successfully demonstrated by the TOM sensor.

Tradeoffs were conducted to select the best configuration. Detailed structural, thermal, and optical analyses were performed to support the designs. Supportive off-axis rejection analyses made predictions of off-axis rejection performance. The telescopes were OAR tested and, with appropriate baffling incorporated, are judged to meet mission requirements for rejection of off-axis point and extended sources. This report describes the above efforts and summarizes the results obtained.

2. STRUCTURAL DESIGN

The HS-2, NS-2 and TPM-1 structures are designed to house their respective optical systems so as to provide the mechanism for maintaining the required spacing, decenter, tilt and stray-light shielding during any of the environmental excursions incurred during qualification test or a mission flight.

2.1 Material Selection. Because of mission requirements, the anticipated target signal must be viewed against a cold background with the telescope system cooled to the following temperatures:

Instrument	Structure Operational Temperature
HS-2	30 Kelvin (LHe)
NS-2	80 Kelvin (LN_2)
TPM-1	290 Kelvin (ambient)

As a result of these cryogenic cooling requirements, a design decision was made to make the mirror and the structure from the same material. This decision was based upon the premise that if an optical system is subjected to a uniform change in temperature, alignment will be maintained without any thermal compensation devices if the optical elements and the material that effects the spacing between the optical element is the same. In other words, the optical figure change due to a change in temperature is matched by the change in the material that spaces the optics assuming isothermal (no thermal gradient) conditions.

The choice of a common material for optics and structure was between beryllium and aluminum. The decision to use aluminum (6061-T6) was made because it satisfied all of the structural requirements and it was cheaper and easier to machine and far less expensive than beryllium. Finally, our experience in the TOM and ELS Programs gave us every confidence that mirrors of the required "low scatter" characteristics could be made from aluminum.

The choice of aluminum did not negate the ultimate possibility of beryllium being used, particularly in that future telescope requirements could involve a nuclear hardened system. This possibility imposed upon the structure and mirror design the requirement that should an all beryllium system be dictated sometime in the future, the design as it exists for aluminum would be compatible with the use of beryllium.

2.2 Structural Configuration. The structural configuration was determined by using the "GUERAP"Program[1] in order to compare four (4) basic designs; see Figure 1. Configuration 1 of Figure 1 is the TOM design with a straylight characteristic already evaluated. As relates to straylight rejection characteristics, each of Configurations 2, 3 and 4 was compared against Configuration 1. The comparison revealed that straylight rejection characteristics, due to differences in structural configuration, were not significantly different from one configuration to the other. What was significant, it turned out, was the amount of clearance between the perimeter of the circle defining the primary mirror and the structural enclosure: the greater the clearance, the better the rejection characteristic (baffle cavity effect).

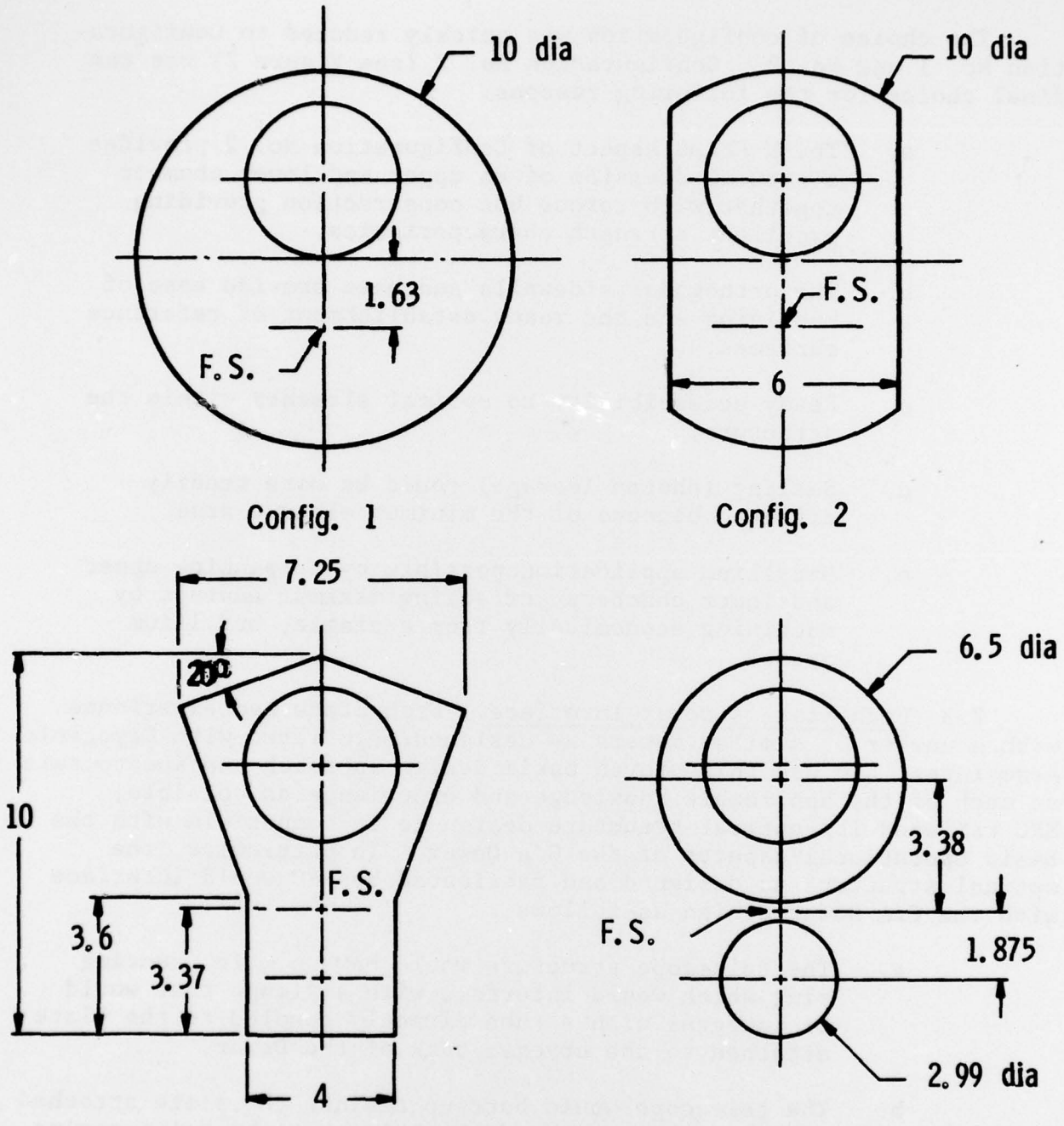

Figure 1 CANDIDATE DESIGN SUBJECTED TO GUERAP ANALYSIS.

The choice of configuration was quickly reduced to Configuration No. 1 and No. 2. Configuration No. 2 (see Figure 2) was the final choice for the following reasons:

a. The H-Frame aspect of Configuration No. 2 provides a natural division of an upper and lower chamber together with torque box construction providing excellent strength characteristics.

b. The orthogonal sidewalls and base provide ease of machining and the ready establishment of reference surfaces.

c. Ready accessibility to optical elements within the structure.

d. Sealing (photon leakage) could be more readily effected because of the minimum closure area.

e. Beryllium application possible by trepanning upper and lower chambers, effecting maximum savings by machining economically from a single, beryllium press.

2.3 Utah State's Dewar Interface. Utah State had experience with a number of similar dewars as designed/negotiated with Cryogenic Associates. To use this proven basic design approach and incorporate as much of the applicable knowledge and experience as possible, HRC tailored its optical structure design to be compatible with the basic operational aspects of the C/A Dewar. In particular, the optical structure as designed and fabricated by HRC would interface with the C/A Dewar design as follows:

a. The telescope structure would have a main mounting ring which would interface with a flange that would be integral with a tube directly coupled to the plate attached to the cryogen tank of the Dewar.

b. The telescope would butt up against the plate attached to the cryogen tank and be held there by being spring loaded (Belleville Washers) at the main mounting ring and the interface flange, using a suitable number of mounting screws, each set at assembly to a prescribed loading pressure.

c. The rear of the telescope that butted up against the plate attached to the cryogen tank would be positioned

Figure 2 USU TELESCOPE OPTICAL BENCH

by pins of sufficient size and be located to maintain alignment between the telescope as a system and the detector and CVF.

d. An indium interface between the telescope and dewar would be required to maintain maximum heat transfer between the CVF and the telescope.

The dewar interface with the telescope is as shown in Figure 3.

2.4 Structural Analysis.

2.4.1 Environmental Specification. The structural analysis was based upon an HRC generated environmental specification[2]. This specification was approved by Utah State and AFGL, and in general, consists of the following tests:

a. Vibration
   Sinusoidal Sweep
   Random Vibration
   Pressure Profile Test (Door Mechanism Evaluation)

b. Shock

c. Acceleration

Each test has a qualification and a preflight level. The CVF/Telescope/Dewar assembly was to be tested as an assembly without the benefit of subassembly evaluation other than paper analyses. All tests are to be performed in order to insure that the CVF/Telescope/Dewar is capable of surviving an ascent in a Bristal Aerospace LTD., Black Brandt 5C payload.

The qualification test consists of an "uncleaned" system evacuated to 10^{-4} Torr and submitted to test levels, as specified. The preflight test is a "cleaned" system (following the qualification test), evacuated to 10^{-5} Torr and submitted to test levels, as specified.

Throughout the tests, a failure is defined as a broken part, shift in boresight, a change in optical alignment, loss of function or loss of hold time out of specification.

2.4.2 Structural Analysis. The CVF Environmental Specification indicates that the driving function of all the tests is Random Vibration (white noise). The "g" level associated with this test is 7.75 g's.

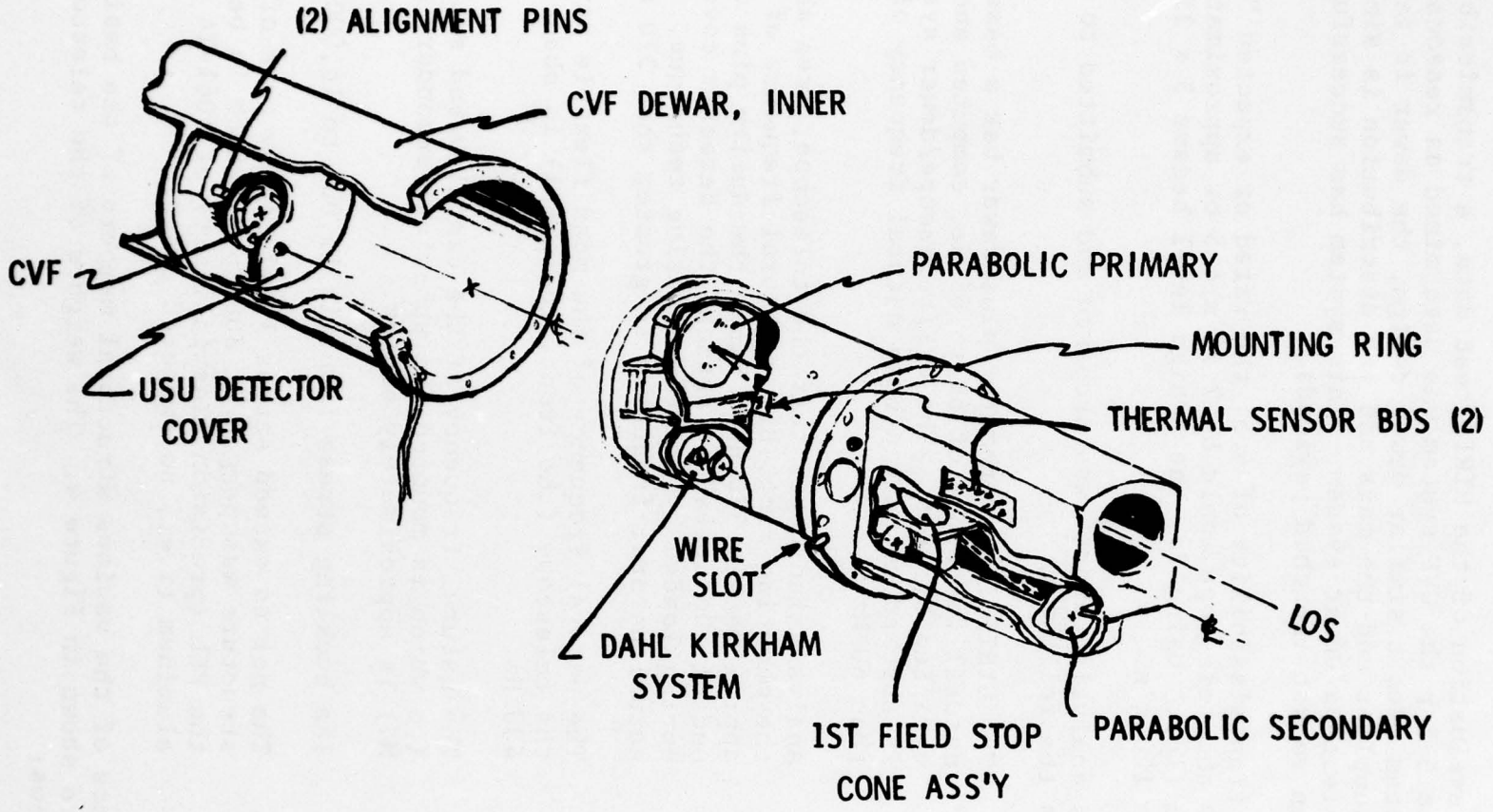

Figure 3 USU TELESCOPE/DEWAR INTERFACE

From an evaluation of the HIRIS test data, a transmissibility factor of 4 to 5 for the CVF system was determined as reasonable. The HIRIS system uses a similar dewar design, the dewar is fabricated by the same supplier and the mass and its distribution is similar to the CVF/Telescope/Dewar system. This system has successfully flown twice on rocket launched payloads.

Using a transmissibility of 4.5, the rated or expected "g" level seen by the telescope would be 7.75 x 4.5 or approximately 30 g's, 1 rms (1σ). Using 3σ, the design level became 3 x 35 or approximately 100 g's.

A stress analysis report[3] was prepared and submitted to AFGL. It highlights the following:

a. The HIRIS interferometer plus dewar has a base natural frequency of 60 to 65 Hz, computed and verified by test. The CVF/telescope/dewar system is assumed to have a base natural frequency of less than 60 Hz.

b. Analysis indicates that the telescope, free about the mounting ring, has a natural frequency of approximately 370 Hz. Since the design pins one end of the telescope against the detector cover, spring loaded by the USU mounting technique, the actual natural frequency is greater than 370 Hz.

c. The natural frequency of the most flexible part of the telescope (the front side panel) is about 400 Hz.

d. The natural frequency of the cantilevered spider (to which is mounted the spherical secondary mirror, M4) is approximately 600 Hz.

e. The buckling stress level is 15,000 to 16,000 psi.

f. The not to exceed stress level of any part of the structure was pegged at 3000 psi, which is below the PEL (precision elastic limit) of 6061-T4 aluminum (i.e., no expected creep).

The sizes of the various structural members of the basic telescope are shown in Figure 4. The weights of the telescopes are as follows:

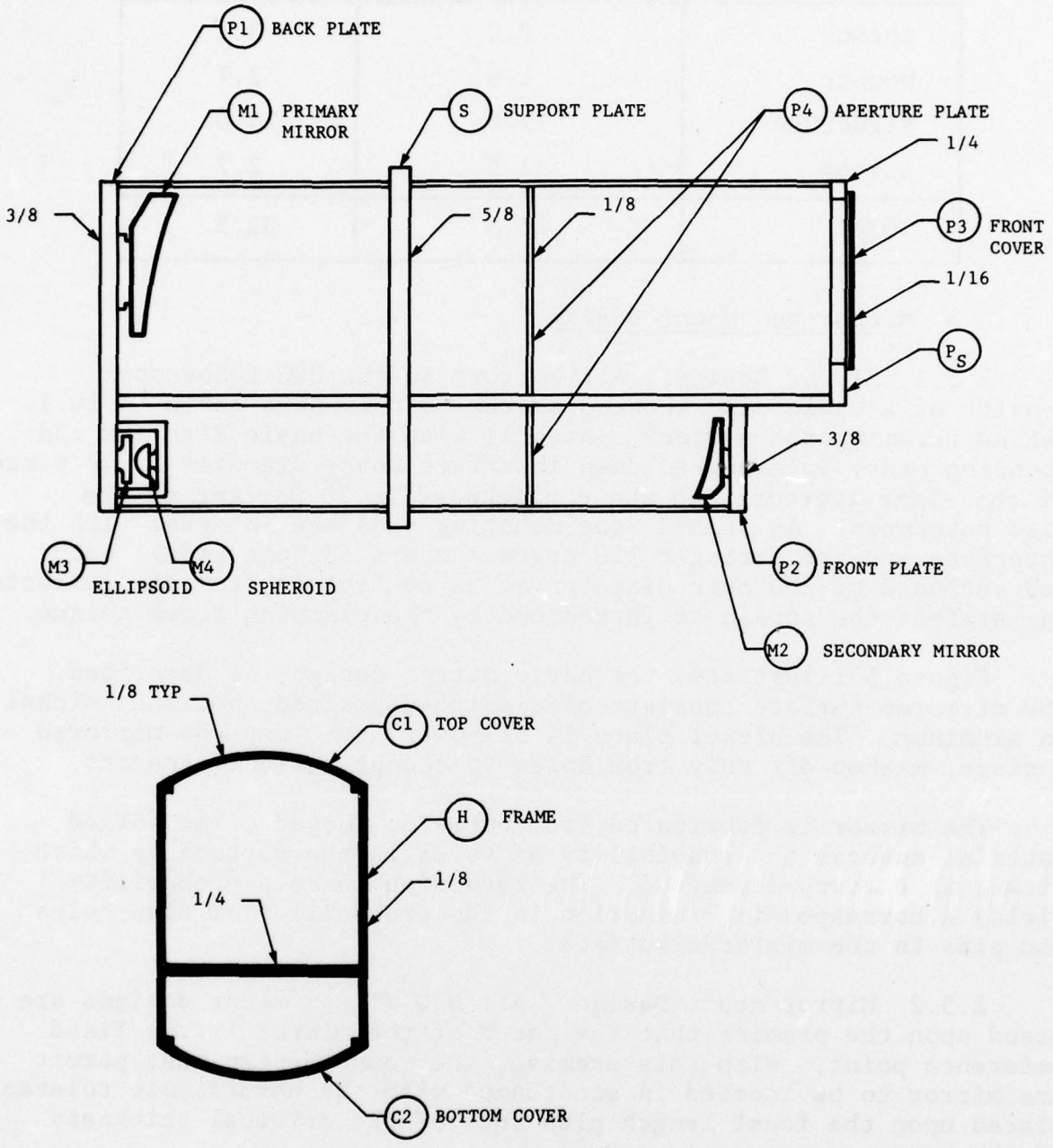

Figure 4 USU STRUCTURAL ANALYSIS SUMMARY

ITEM	WEIGHT (LB)	
	HS-2, NS-2	TPM-1
Optics	2.0	3.1
Mounts	1.0	2.7
Structure	21.0	24.0
Straps	1.5	2.7
TOTAL	25.5	32.5

2.5 Mirror and Mount Design.

2.5.1 Mirror Design. All mirrors in the USU telescopes consist of a basic disc whose diameter to thickness ratio is 10:1. Behind the mirrored surface, integral with the basic disc and the mounting pads, is a necked down interface whose diameter is 40 percent of the clear aperture and whose thickness is 20 percent of the disc thickness. As stated, the mounting pads are integral with the interface and are arranged 120 degrees apart (3 foot pads), each pad outboard of the neck diameter so as to isolate from the reflecting surface the strain as introduced by the clamping screw torque.

Figure 5 illustrates the basic mirror design, as described. The mirrored surface consists of electro-deposited, polished nickel on aluminum. The nickel plate is all over, not just the mirrored surface, masked off only from holes to accept helicoil inserts.

The mirror is fabricated from 6061-T6, forged. The forged material reduces the possibility of voids in the surface to which nickel is electro-deposited. The reduction in void probability yields a corresponding reduction in the probability of blow holes and pits in the mirrored surface.

2.5.2 Mirror Mount Design. All USU mirror mount designs are based upon the premise that the focus of the mirror is the fixed reference point. With this premise, the mount design must permit the mirror to be located in accordance with the permissible tolerance placed upon the focal length plus that of the critical thickness of the mirror.

The mount design (see Figure 6) provides for a Mount No. 1 which is undersized (see dimension "A") in order to include a shim "B" to bring the focus to a predetermined spot in space, "P". Given that the "A" dimension is determined (quite probably different for each of the 3 mirror food pads), Mount No. 2 (which is oversized)

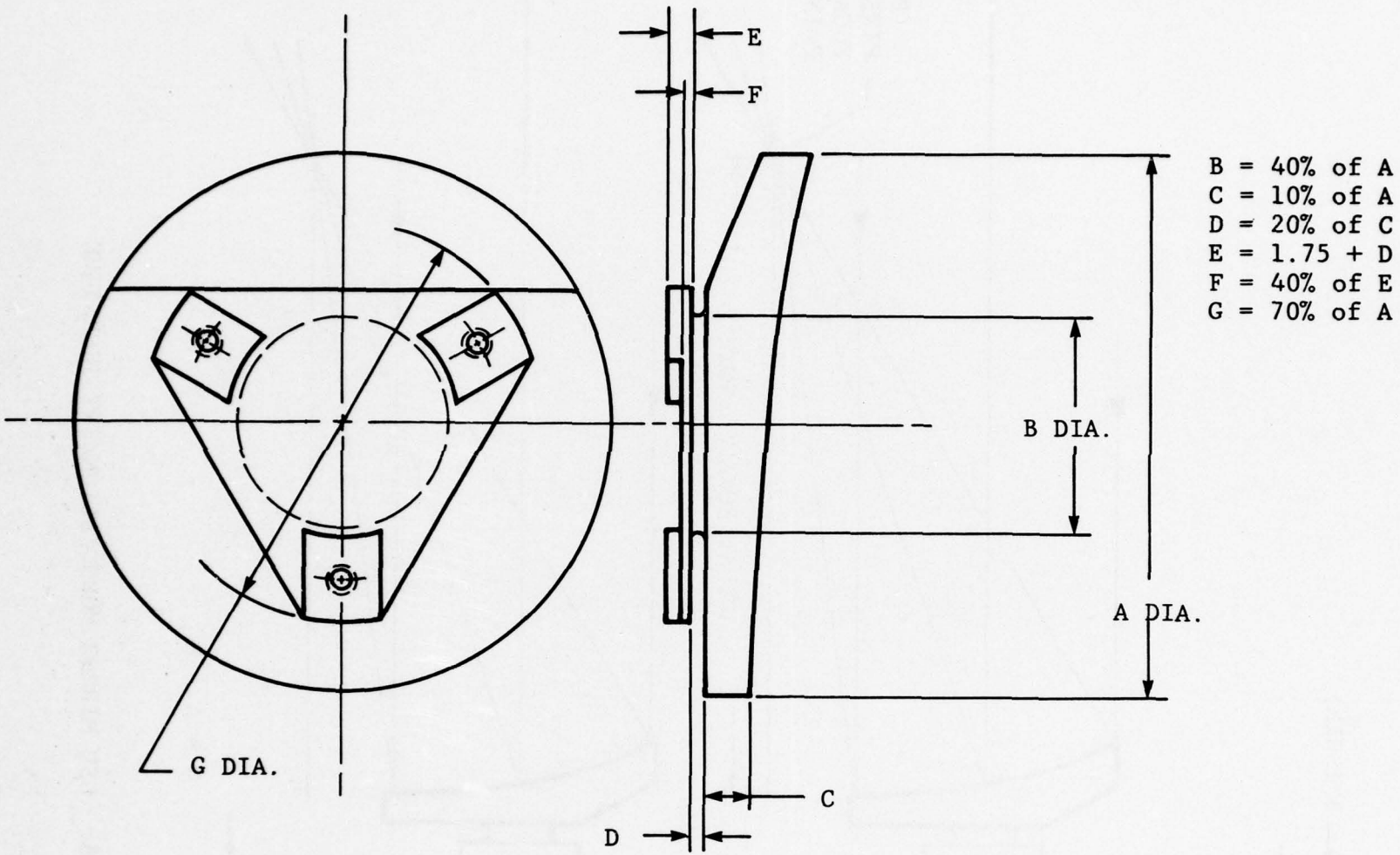

Figure 5 TYPICAL OFF-AXIS MIRROR

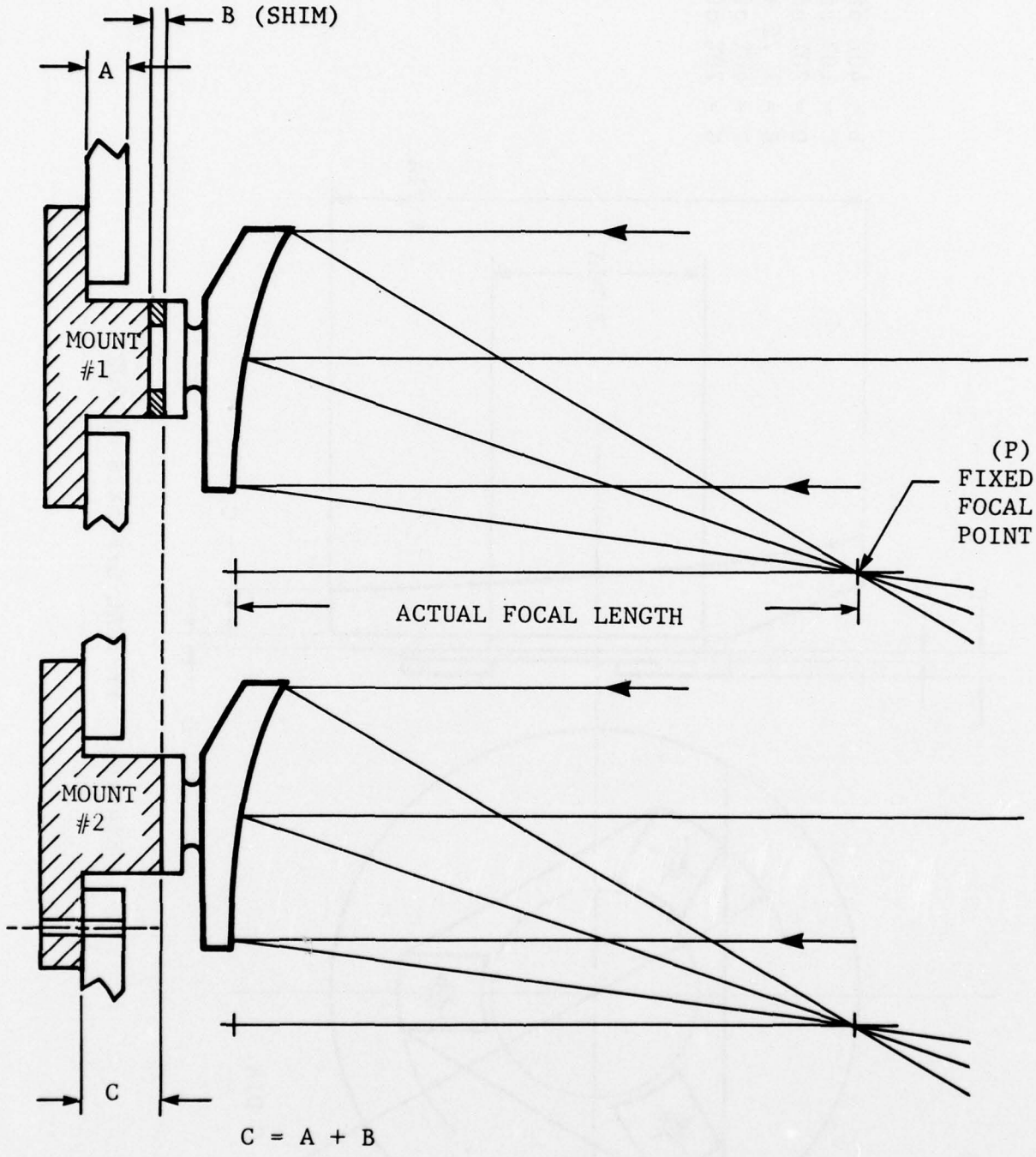

Figure 6 USU MIRROR MOUNT/ALIGNMENT TECHNIQUE

is machined to dimension "C" which is equal to (A + B). Should a difference exist in the (A + B) dimension for each foot pad, Mount No. 2 is machined to the largest (A + B) dimension and hand lapped for final focus positioning.

This technique of mirror mount eliminates the need for three separate shims (one under each mirror foot pad) which, in turn, provides for a plane to plane interface and minimal thermal transitions or maximum conductive cooling capability.

2.6 Alignment Considerations. The alignment procedure for the HS-2 and NS-2 telescopes is as specified in HRC specification 22914-ES01.[4] The alignment procedure for the Dual CVF(TPM-1) is as specified in HRC specification 22914-ES03.[5]

The alignment procedures call for the use of an alignment fixture that attaches to alignment holes in the rear of the telescope; see Figure 7. The rear of the telescope, see Surface "B", is set up perpendicular to the LOS of an alignment telescope. The alignment fixture is positioned in place and the alignment telescope is translated so as to center the 1/8-inch diameter hole in the alignment fixture, see Figure 8. This establishes the lower centerline, ℓ_2, of the telescope. Using crosshairs and a reticle, the common focal point of the two confocal parabolas is established and all mirrors are mounted and aligned within the telescope. The focus of the telescope is positioned in the plane of the 1/8-inch diameter hole in the alignment fixture.

This procedure (use of an alignment fixture) makes use of the rear of the telescope as the main reference surface and requires only two mirror mount surfaces that are machined to close tolerances.

The same alignment fixture is used by USU and is mounted on the alignment pins in the detector cover. The 1/8-inch diameter hole is used to center and position their detector which is centered and positioned precisely relative to the telescope focus requirements.

2.7 Thermal Analysis. The thermal analysis report[6] explains in detail the thermal analyses performed, the premises upon which the calculations are based and the results attained.

Briefly, the anticipated heat load was computed to be as follows:

11.3 watts, Solar Loading
4.5 watts, Earth Loading
1.7 watts, Earth Emission

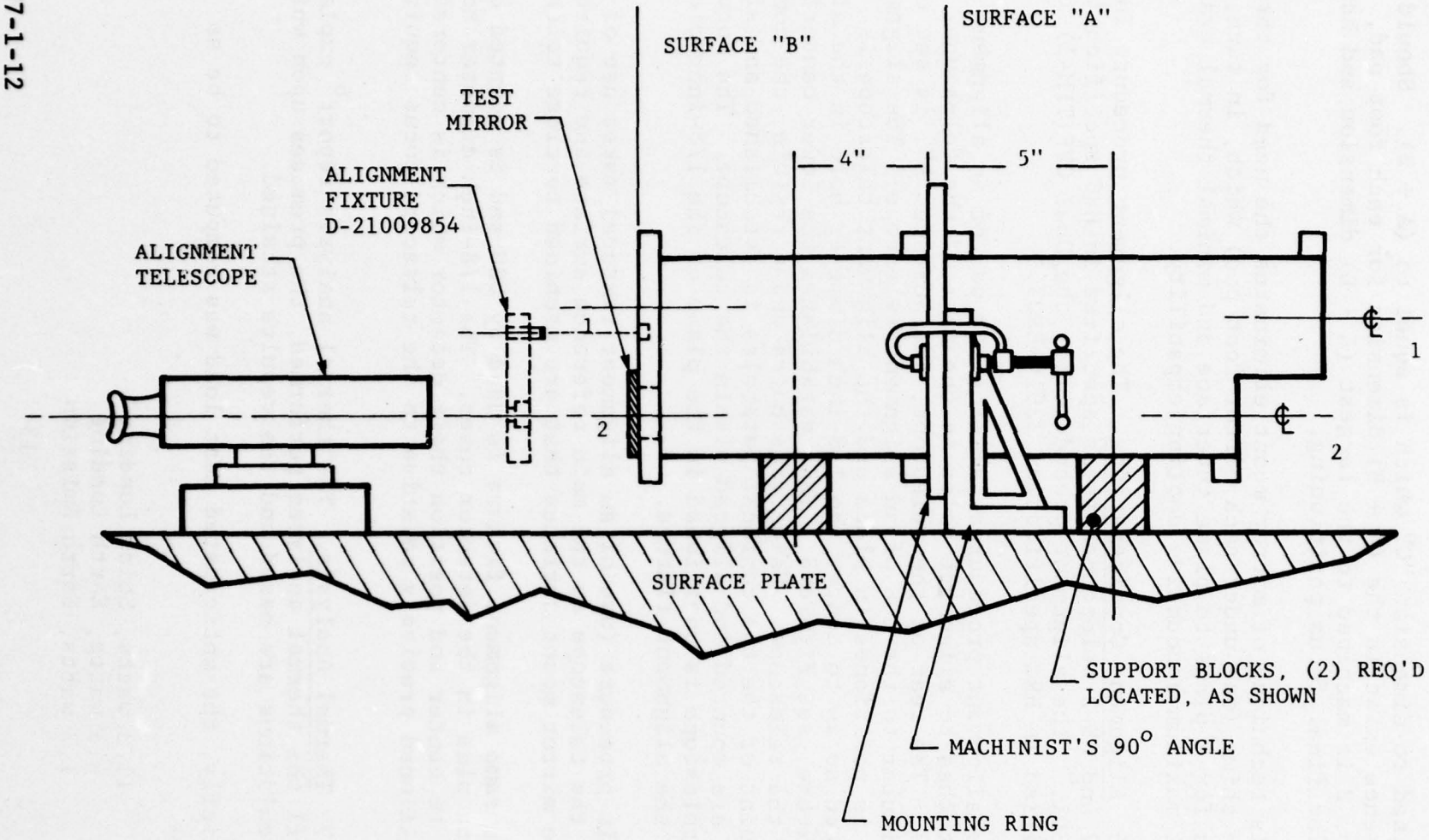

Figure 7 USU TELESCOPE ALIGNMENT SET-UP

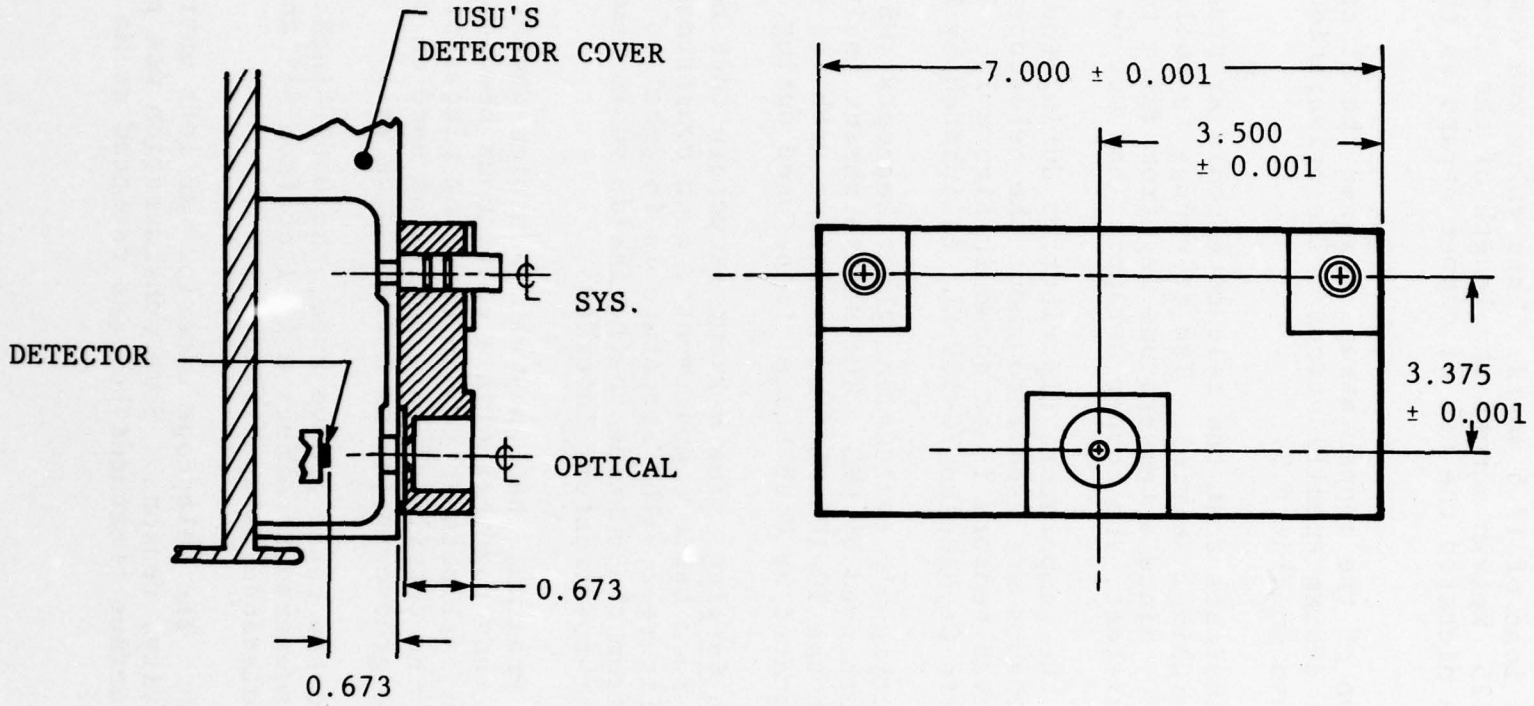

Figure 8 USU ALIGNMENT FIXTURE

for a total heat load of 17.5 watts. This value was computed to induce a ΔT of 125 Kelvin across the length of the aluminum telescope, which dictated the use of copper straps as thermal shunts.

The addition of the copper straps lowered the ΔT to 14 Kelvin which was within design specifications. The orientation of the straps is as shown in Figure 9.

USU tests indicate that the telescope cools as predicted (every measured point within 1 Kelvin). The telescope is cooled conductively within the dewar. Since a temperature lag from front to rear was virtually non-existent, the copper strapping has met design criteria.

To monitor the temperature distribution during thermal tests, seven thermal sensors are used throughout the telescope. The location of these seven sensors is as shown in Figure 10. The sensor used is Lake Shore Cryogenics TG-100-KL, calibrated by HRC.

Following cryogenic evaluation, the telescopes (HS-2, NS-2 and TPM-1) were refurbished by HRC. The refurbishment included the discontinuing of the TG-100-KLs and replacing with two carbon resistors, calibrated by Utah State, to be used during flight.

2.8 Photon Sealing. The H-frame structure that houses the optics is divided into four basic compartments, each compartment having its own cover, see Figure 2. The structure is integral so that any photon leakage from the outside to the inside would have to be through the cover-to-structure interface.

On the ELS Program, the Honeywell Radiation Center developed a groove design that together with a continuous bead of indium effects a photon seal between two interfacing pieces of aluminum. Figure 11 shows the details of this design as used on the USU telescopes. The groove is in the H-frame side wall.

Relative to the total groove area, the 0.021-inch diameter indium bead is squeezed to effect a fill of from 38% to 58% with the machining tolerance as specified.

2.9 Finish. The telescope exterior was left untreated for thermal (emissivity) reasons. Some consideration was given to a clear anodize surface treatment but was rejected as no real purpose would be served.

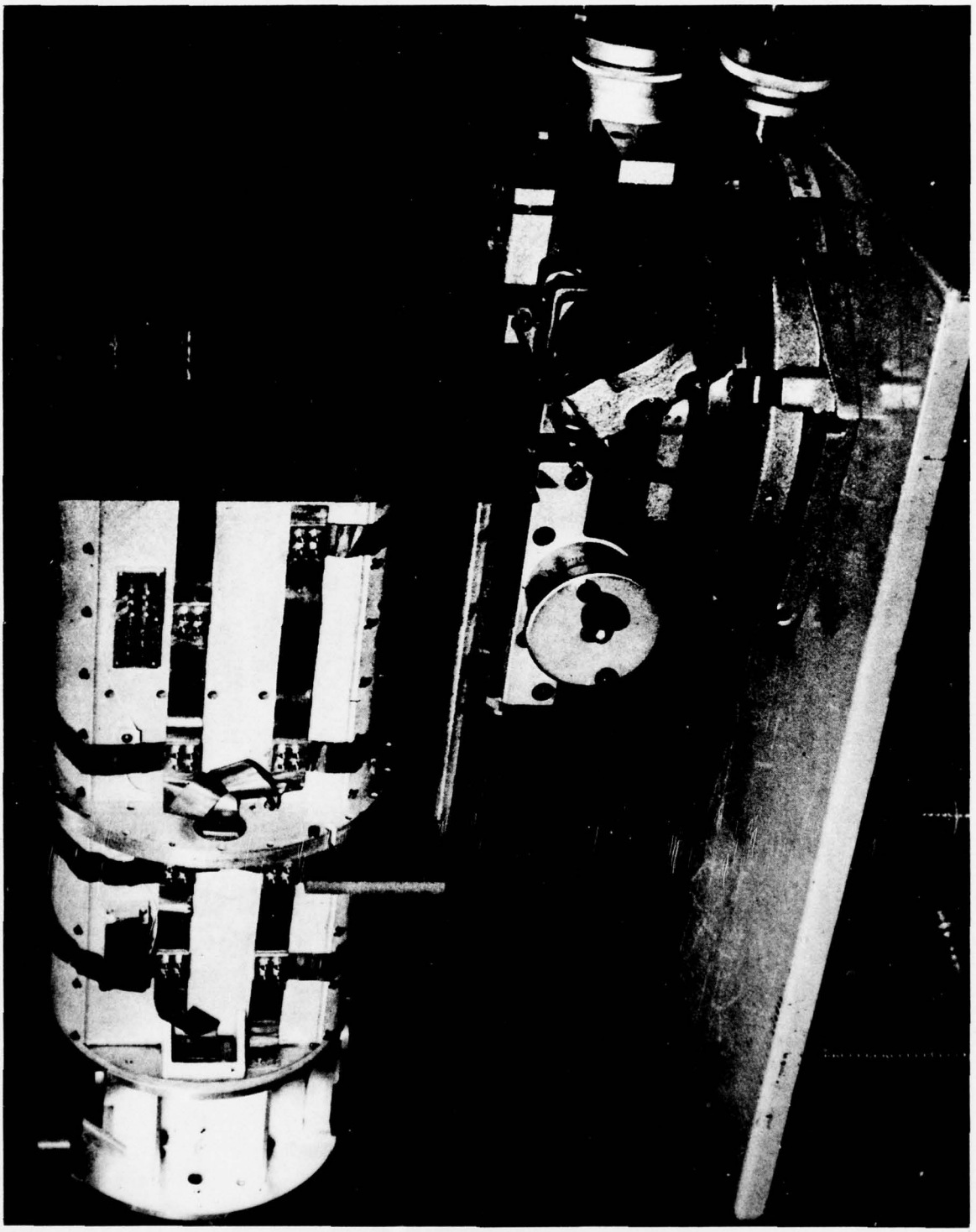

Figure 9 TPM-1 TELESCOPE ON TRANSLATOR AND ROTATOR STAGES

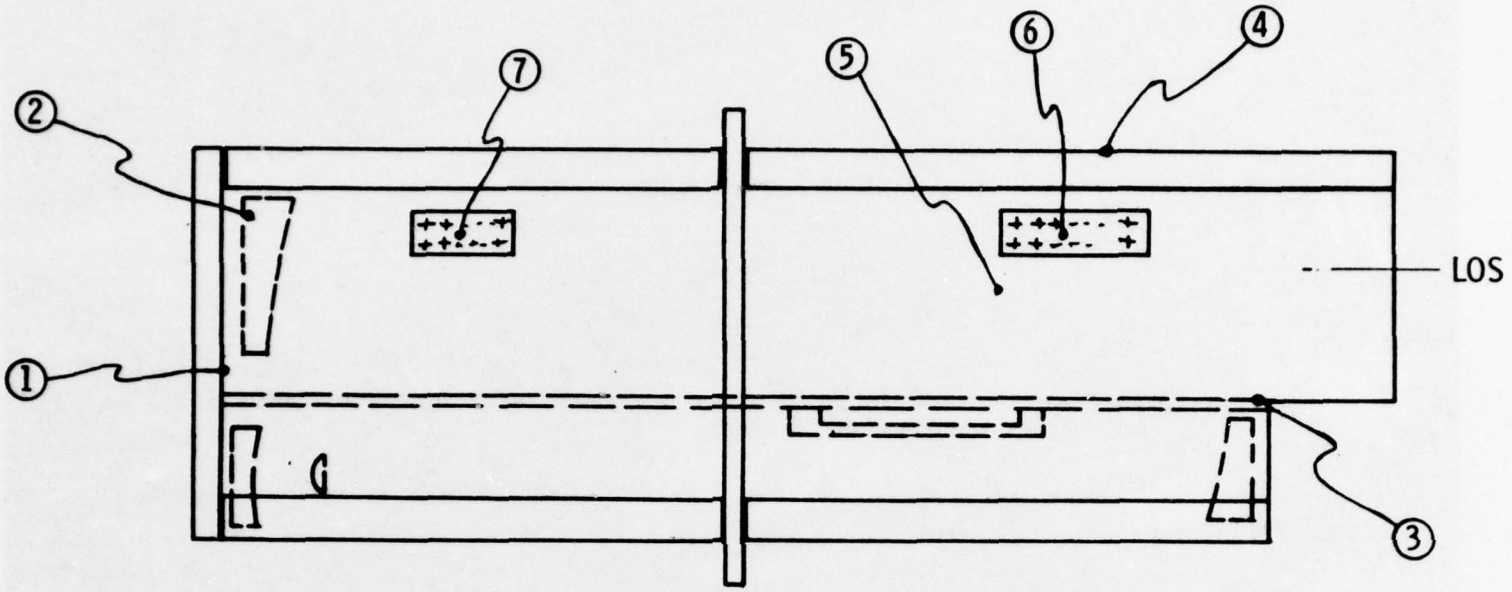

1. INSIDE TELESCOPE, LOCATED ON END PLATE.
2. LOCATED ON PRIMARY MIRROR, M.
3. INSIDE TELESCOPE, LOCATED ON DECK
4. OUTSIDE TELESCOPE, LOCATED ON TOP, FRONT COVER
5. OUTSIDE TELESCOPE, LOCATED ON SIDEPLATE

6 &7. FEED THRUS FOR HARDWIRE CONNECTION OF (5) THERMAL SENSORS.

Figure 10 USU'S-CVF HIGH REJECTION TELESCOPES - THERMAL SENSOR LOCATIONS

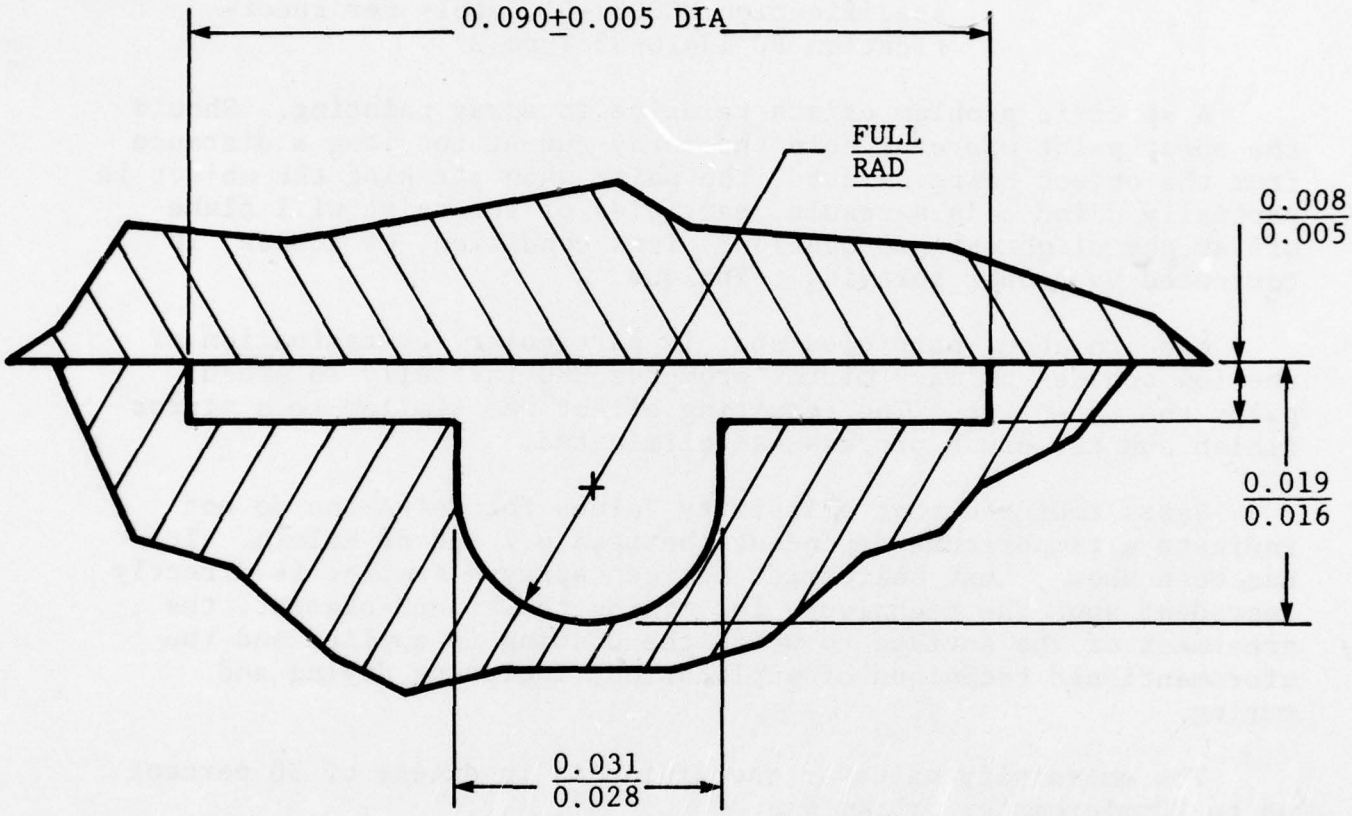

USE WITH 0.031 DIAMETER INDIUM WIRE

58% MAX COMPRESSION
38% MIN COMPRESSION

EXTRUSION WILL NOT FILL 0.090 SLOT

Figure 11 PHOTON (INDIUM) SEAL CONCEPT

The interior of the telescope was treated using a black anodize or sprayed Cat-A-Lac black paint. The specifications for both are as follows:

Anodize: Dull black anodize per MIL-A-8625 Type II, Class 2, masking where required

Paint: Cat-A-Lac 463-3-8 black (flat), material specification MC8057-01, apply per specification PC 13410-02 Type 2

A specific problem exists relative to spray painting. Should the spray paint operator hold the spray gun at too long a distance from the object being painted, the paint when striking the object is partially dried. As a result, particles of the paint will flake off at the slightest provocation. This condition, of course, is corrected by proper spraying technique.

Concern about particles and, in particular, contamination of the low scatter primary mirror prompted HRC initially to brush paint the Cat-A-Lac. The resulting effect was similar to a mirror finish and the brush process was eliminated.

Tests indicate that emissivity values for Cat-A-Lac do not indicate a temperature dependence between 4.2 and 80 Kelvin. It has been shown, that uniformity between sprayed samples is directly dependent upon the techniques for mixing the binder-pigment, the treatment of the surface to which the coating is applied and the aforementioned technique of application, including drying and curing.

The emissivity value of the finish is in excess of 90 percent up to 20-micrometer thickness.

3. OPTICAL DESIGN

3.1 Optical Design of the HS-2 and NS-2 Telescopes. The HS-2 and NS-2 telescopes are optically identical in all respects with the HS-2 used in a USU supplied helium cryogenic system and the NS-2 used in a USU supplied nitrogen cryogenic system.

The single telescope design fits into a specified 9.75-inch diameter space envelope (cross section) and provides the largest collecting aperture possible in keeping with the use of a confocal parabolic primary and secondary, all reflecting, optical system with the appropriate apertures and stops required to effect the

off-axis-rejection (OAR) requirements. After the single magnification provided by the confocal foreoptics set, collimated target energy is delivered to a Dahl-Kirkham system that focuses the target energy onto the focal plane within a defined f-cone and at a specified distance behind the rear face of the telescope structure.

3.1.1 Design Considerations. Using the original TOM Radiometer concepts and the follow on, evolutionary, Earth Limb Sensor (ELS) aperture stop concept, the design of the HS-2 and NS-2 optical train took the following course (see Figure 12):

a. Given the OAR requirement, the selection of an all reflecting foreoptics system was dictated. Using the confocal parabolic concept of TOM and ELS, the magnification of the fore telescope was set at 2:1 with the size of the primary selected at 4.00 inches diameter clear aperture and the secondary at 2.00 inches diameter clear aperture.

b. The available length of telescope was specified by USU to be contained within 22.625 inches. This restriction dictated a 12-inch primary focal length and a 6-inch secondary focal length.

c. The OAR design criteria includes the ELS aperture stop approach. Since diffraction from the entrance aperture constitutes a major portion of undesirable off-axis energy within the target signal, an "oversized" entrance aperture is placed in a plane which is perpendicular to the primary optical axis and contains the common focal point of the primary and secondary parabolic mirrors. The image of the entrance aperture edge is formed after leaving the secondary and lies approximately in the same plane containing the entrance aperture when the plane is extended below the primary optical axis. In this image plane, the lyot stop is placed such that the image formed is out board of the aperture, thus stopping (baffling) the imaged diffraction main lobes. Referring to Figure 12, the 4-inch entrance aperture is imaged to a 2-inch image diameter at the lyot stop. The selected 1.6-inch lyot stop diameter now becomes the limiting aperture and dictates an effective entrance aperture diameter of 3.2 inches, as shown, given a fore-telescope magnification of 2:1.

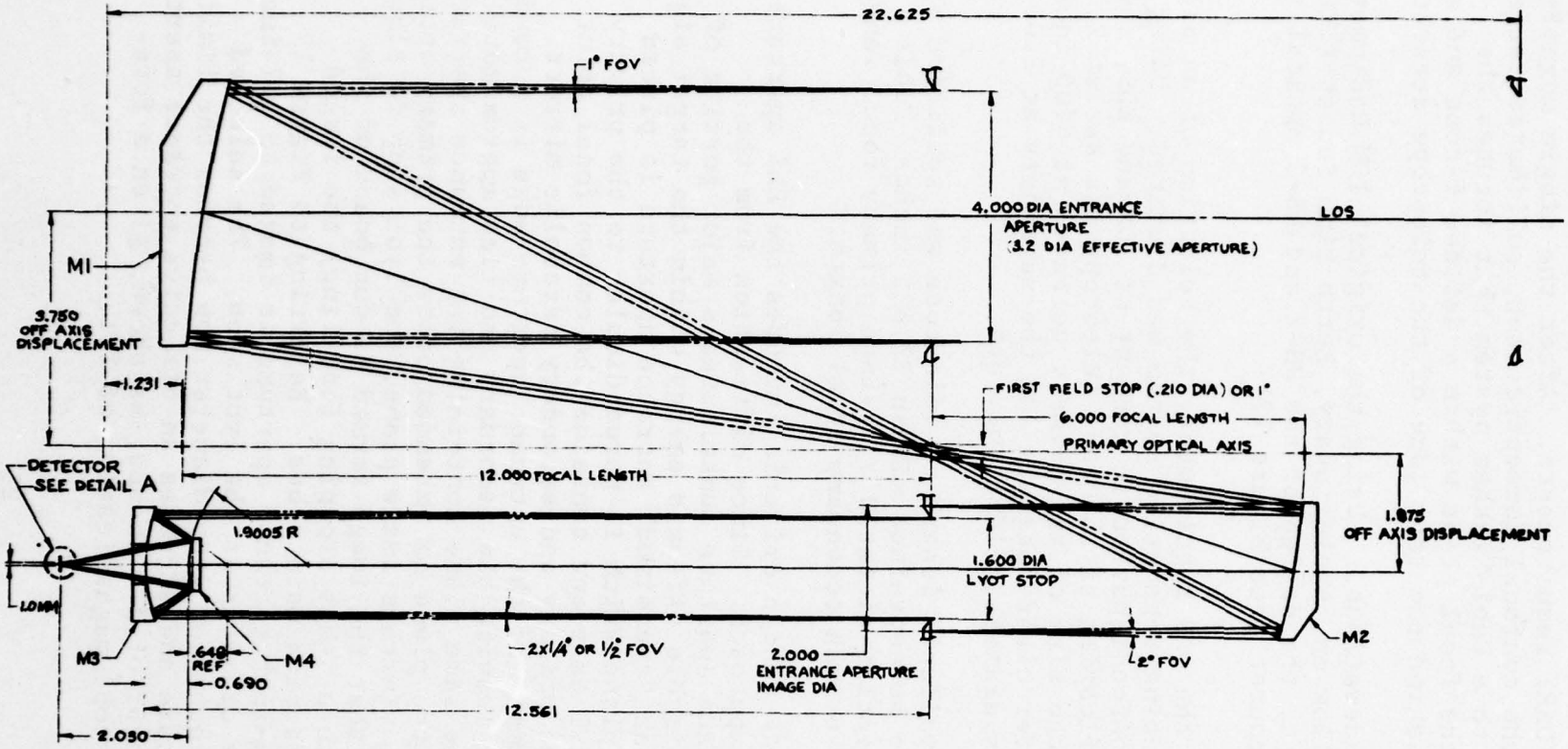

OPTICAL RAYTRACE DATA	
TELESCOPE FOV, ENTRANCE	1/4°
TELESCOPE MAGNIFICATION	2:1
M1 PARABOLOID PRIMARY	21008478
M2 PARABOLOID SECONDARY	21008479
M3 ELLIPSOID PRIMARY	21008512
M4 SPHERICAL SECONDARY	21008513

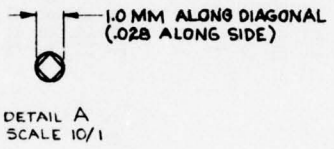

Figure 12 OPTICAL RAYTRACE

The first field stop is sized to accommodate both the OAR criteria and the blur as caused by the off-axis primary mirror. The sizing of the first field stop was set at 1 degree (0.210-inch diameter), which dictates a 1 degree FOV for the fore-telescope. The actual diameters of both the primary and secondary mirrors are governed by the 1 degree FOV, specified by the first field stop, plus a radial "roll-off" for fabrication to effect the desired 1 degree clear aperture, unimpaired by edge discrepencies due to machining and polishing. Note that the sizing of the secondary is driven by a 2 degree FOV due to the 2:1 magnification of the fore-telescope. Subsequent testing of HS-2 by USU and AFGL identified a problem in near field rejection performance, i.e., from 0.5 degree to 1 degree off-axis. A plateau of signal radiation existed which was attributed to off-axis scattering into the field of view, most probably caused by the CVF filter elements. This problem has been alleviated by reducing the first field stop size to 0.5 degree (full angle). Attendant with this change, however, is a tighter location tolerance required for the detector to avoid vignetting effects.

d. The Dahl-Kirkham (D/K) system is designed to collect the signal energy from the lyot stop and focus this energy upon the detector, located at a precise location behind the rear surface of the telescope structure, 0.673 inch, as specified by USU. Even though the fore-telescope is delivering target energy towards the D/K system with an FOV of 2 degrees, the detector is sized at approximately 1/4 degree FOV relative to object space and, therefore, "sees" 1/4 degree x 2 or 1/2 degree FOV target energy as it exits from the lyot stop. Therefore, the D/K system is sized to accept only the 1/2 degree FOV.

   Obscuration of target energy due to the D/K secondary is computed from the OD of the secondary referenced against the lyot stop diameter, plus the obscuration due to the three spokes within the 1.6 diameter supporting the hub of the spider.

e. The system focal length (SFL) of the telescope is computed as follows:

$$SFL = M_1 \times M_2 \times F_3$$

where M_1 = Magnification of the fore-telescope

M_2 = Magnification of the D/K system

F_3 = Effective focal length of the D/K primary

Referring to Table 1, Basic Optical Parameters,

$$SFL = 2 \times 3.1358 \times 1.337$$

or System Focal Length = 8.385 inches

The square detector was sized by USU as 1 mm (0.0394 inch) across the diagonal and 0.707 mm (0.28 inch) square. Using the 1 mm value, the FOV in object space is computed as follows:

$$FOV = \tan^{-1} \frac{0.0394}{8.385}$$

or FOV = 0.269 degree

If the system focal length is used with the required FOV of 0.250 degree, the detector size required across the diagonal is as follows:

Detector Size = 8.385 x an 0.250 degree

= 0.0366 inch

Expecting some tail to the image at the focal plane, the design of the optics accepts the 1 mm across the detector diagonal but to do this an increase in the FOV to 0.269 degree resulted. It should be noted that all calculations involving the telescope optical system should employ the following values:

System Focal Length = 8.385 inches

FOV (Object Space) = 0.269 degree

Table 1

BASIC OPTICAL PARAMETERS, HS-2 & NS-2

Optical Item	Optical Parameter/Spec.	Remarks
Detector Size	1 mm along diagonal (~0.028 sq)	
FOV, Entrance (1st Field Stop)	0.5 degree	
FOV, Effective Aperture (Detector)	0.269 degree using 1 mm and F_s	0.191 degree using 0.028 in. side of det
Entrance Aperture	4.0 dia	Diffracting Aperture
Effective Entrance Aperture	3.2 dia	
Primary (Parabolic) Focal length, F_1	F_1 = 12.0 inches	
Primary center ray displacement from main optical axis	3.75 inches	
Secondary (Parabolic) Focal length, F_2	F_2 = 6.0 inches	
Secondary center ray displacement from main optical axis	1.875 inches	
1st Field Stop Size	0.5 degree or 0.100 dia	0.5 degree based upon spot size and diffraction considerations
Fore-Telescope Magnification, M_1	12 ÷ 6 = 2:1 or M_1 = 2	
Lyot Stop Size	1.6 dia	
Distance from Lyot Stop to Vertex of Ellipsoid	12.561 inches	
Dahl-Kirkham Primary (Ellipsoid)	$(x^2/a^2) \times (y^2/b^2) = 1$	a = 4.78835, b = 3.57689
Effective Focal Length of D/K Primary, F_3	F_3 = 1.337 inches	0.689 + 0.648 (Virtual Image)
Dahl-Kirkham Secondary (Sphere)	Rad of Curvature = 1.90051	OD = 0.84"
D/K Primary to Secondary Spacing	0.689 inch	
D/K Secondary to Detector Spacing	2.032 inches	
Magnification of Dahl-Kirkham, M_2	M_2 = 3.1358	2.032 ÷ (1.337 - 0.689)
System Focal Length, F_s	F_s = 8.385 inches	$F_s = F_3 \times M_1 \times M_2$
L/D of Fore-Telescope	L/D = 5.35	(22.625 - 1.231) ÷ 4
Spot Size at Detector	≤0.005 inch	
Obscuration of D/K Secondary (on-axis)	29.4%	$\frac{0.785(0.84)^2 + 1.5(1.6-0.84) \times 0.032}{0.785 \times (1.6)^2} \times 100$
Cone f/No. at Detector (on-axis)	f/No. 2.5	
System Efficiency, Int.	23.6%	See discussion in text of report
System Efficiency, Eff.	36.9%	See discussion in text of report

The preceding is a narrative effort to describe the sequence and rationale behind the optical parameters and tolerances as presented in

Figure 12:	System Optical Ray Trace
Table 1:	Basic Optical Parameters
Figure 13:	Basic Optical Tolerances

The system optical raytrace (Figure 12) presents the basic limiting and effective apertures with the nominal spacing involved between elements and how the elements relate to the optical structure and the required position of the focal plane.

The basic optical parameters (Table 1) tabulates the constraints as portrayed in the optical raytrace and presents the deviation and/or rationale behind the selection or resulting value given.

The basic optical tolerances (Figure 13) identifies each element, its spacing, clear aperture and the defocus, tilt and decenter tolerance associated with each element.

3.1.2 System Efficiency. The system efficiency of the HS-2 and NS-2 telescope is computed one of two ways:

1. Based upon the entrance aperture of 4.0 inches diameter, η_{ENT}
2. Based upon the effective aperture of 3.2 inches, diameter, η_{EFF}

The system efficiency, based upon the entrance aperture of 4.0 inches diameter, is computed in accordance with the expression as follows:

$$\eta_{ENT} = \prod_{i=1}^{i=n} R_i \times \eta_L \times \eta_F \qquad (1)$$

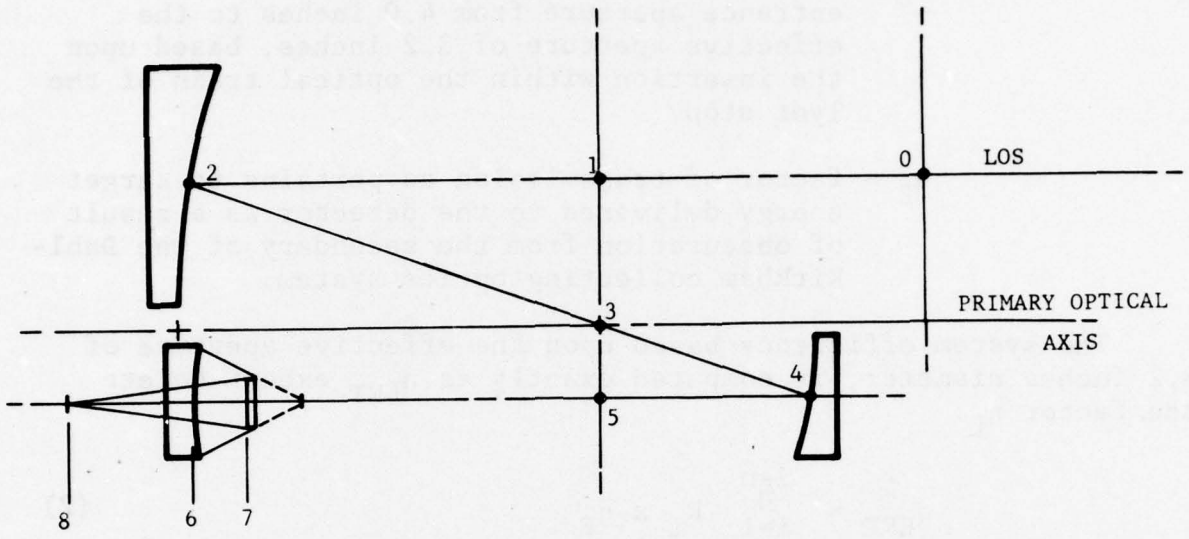

SURFACE	SURFACE GEOMETRY	SPACING	CLEAR APERTURE	(+1λ Irreg) DEFOCUS	TILT	DECANTER
0	Fore Entrance Plane	X	X	X	X	X
1	Entrance Aperture Plane	12" (1 to 2)	4" (3.2 effective)	X	X	
2	Parabolic Primary	12" (2 to 3)	4.052 dia	±0.045 in.	±0.029 degree	±0.011 in.
3	1st Field Stop Plane	6" (3 to 4)	0.100 dia	X	X	X
4	Parabolic Secondary	6" (4 to 5)	2.058 dia	±0.045 in.	±0.061 degree	±0.011 in.
5	Lyot Stop	12.561 (5 to 6)	1.6 dia	X	X	X
6	Dahl-Kirkham Elliptical Primary (FL = 1.337)	0.689 (6 to 7)	1.707 dia	±0.0087	±0.25 degree	±0.0038 in.
7	Dahl-Kirkham Spherical Secondary (R = 1.9005)	2.032 (7 to 8)	0.835 dia	±0.0087	±0.084 degree	±0.0038 in.
8	Focal Plane	X	1 mm or diagonal	X	X	X

Figure 13 BASIC OPTICAL TOLERANCES, HS-2 & NS-2

where R_i = reflectivity of mirror surface.

η_L = step reduction factor that reduces the entrance aperture from 4.0 inches to the effective aperture of 3.2 inches, based upon the insertion within the optical train of the lyot stop.

η_F = factor of transmission as pertains to target energy delivered to the detector as a result of obscuration from the secondary of the Dahl-Kirkham collecting optics system.

The system efficiency based upon the effective aperture of 3.2 inches diameter, is computed exactly as η_{ENT} except delete the factor η_L:

$$\eta_{EFF} = \prod_{i=1}^{i=n} R_i \times \eta_F \qquad (2)$$

The computations for η_{ENT} and η_{EFF} are as follows:

$$\eta_{ENT} = \prod_{i=1}^{i=4} R_i \times \eta_L \times \eta_F \qquad (3)$$

where $R_i = 0.85$ for all mirror surfaces

$$\eta_L = \left(\frac{3.2}{4.0}\right)^2 = 0.64$$

η_F = 1 - (obscuration of D/K secondary)

and $\eta_{ENT} = (0.85)^4 \times 0.64 \times (1-0.294)$

or $\boxed{\eta_{ENT} = 23.6\%}$

$$\eta_{EFF} = \prod_{i=1}^{i=4} R_i \times \eta_F \qquad (4)$$

$$= (0.85)^4 \times (1-0.294)$$

or $\boxed{\eta_{EFF} = 36.9\%}$

3.2 Optical Design of the Dual CVF Telescope, TPM-1. The Dual CVF (TPM-1) design consists of using the HS-2, NS-2 Dahl-Kirkham and adding a relay optics system that splits the aperture, directing each half of the aperture to a separate Dahl-Kirkham.

3.2.1 Design Considerations. A tradeoff study was performed that revealed the differences between two basic design approaches. The two approaches were as follows:

1. Split the energy from the lyot stop using a folding flat that collected the energy from one side of the total FOV cone and directed this energy to one Dahl-Kirkham collecting system. The uncollected energy passing under the folding flat would be collected by a second, in-line Dahl-Kirkham system.

2. Split the energy from the lyot stop using a folding flat with a hole through its center. The design was such that the energy passing through the hole, less that obscured by the secondary of the collecting Dahl-Kirkham system whose secondary was smaller in diameter than the projected hole diameter of the folding flat.

Systems No. 1 and No. 2 are shown in Figures 14 and 15, respectively. Transmission profiles are shown relative to selected points of the full field.

A design review was held at USU where System No. 2 became the selected design for the following reasons:

1. Over the FOV, System No. 2 delivers a uniform transmission over all points of the field unlike System No. 1 where the transmission varies from +30% to -12% about the on-axis transmission percentage.

2. Should the design ever be used to incorporate a larger FOV, System No. 1 would become more difficult to handle than System No. 2 even though the transmission characteristics improve.

Figure 16 shows the relay optics as designed.

The basic optical parameters of TPM-1 are as presented in Table 2. Included are the constraints as portrayed in Figure 16 and the derivation and/or rationale behind the selection or resulting value given.

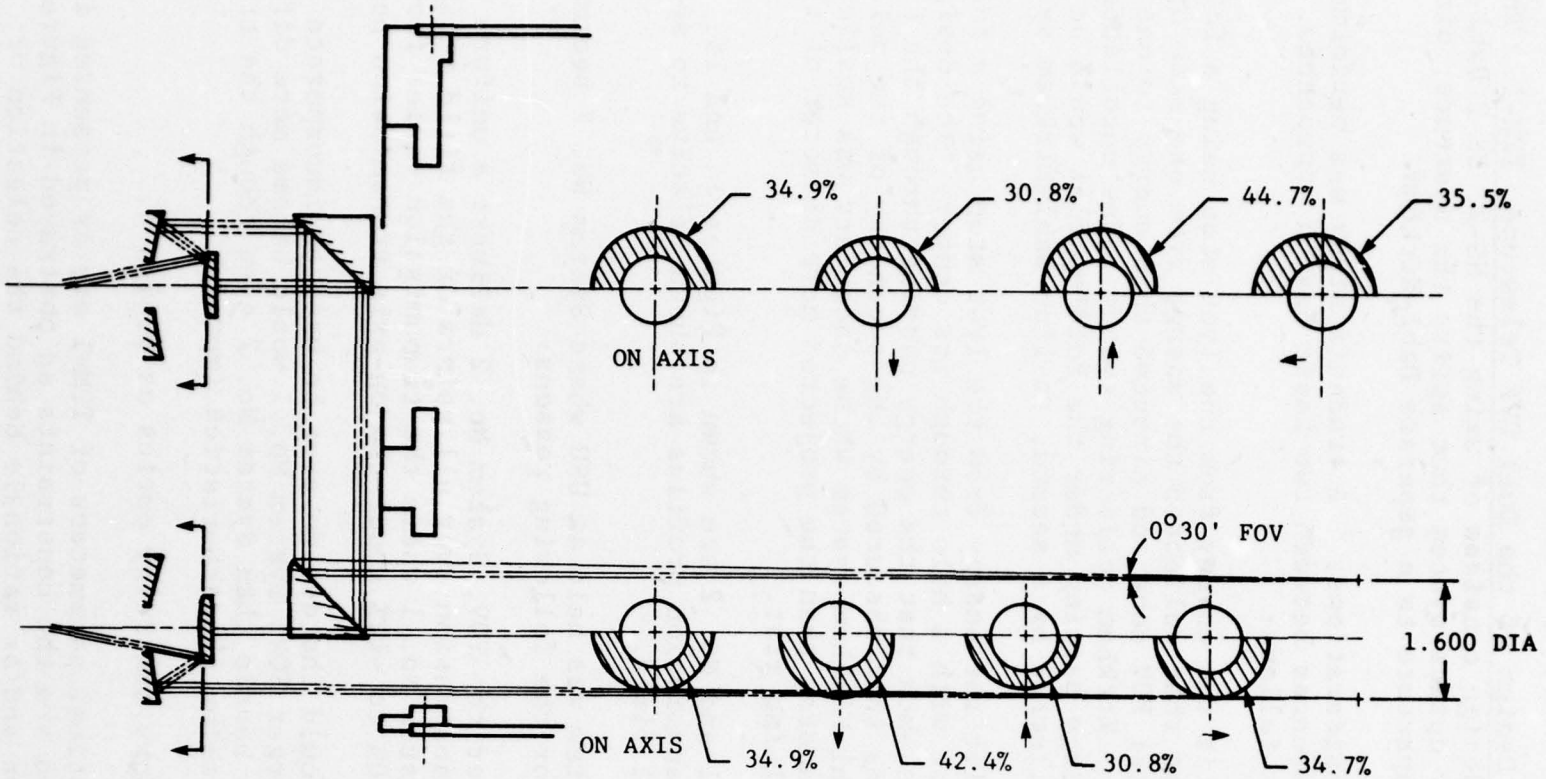

SYSTEM #1

Figure 14 OBSCURATION STUDY, SYSTEM #1

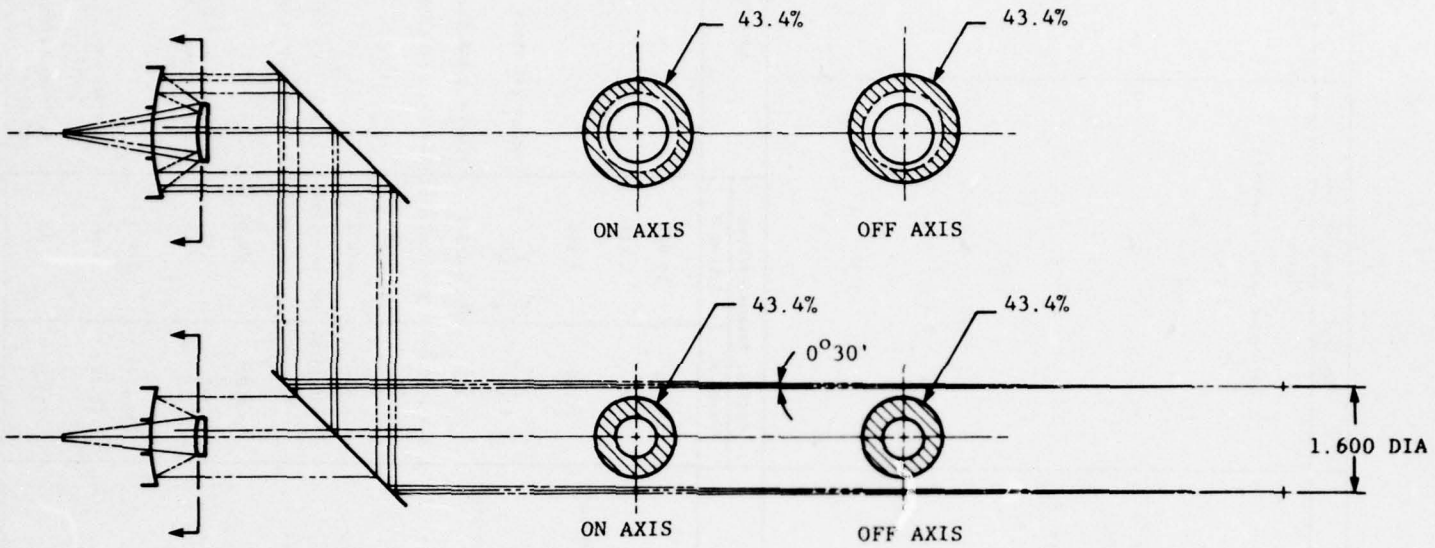

SYSTEM #2

Figure 15 OBSCURATION STUDY, SYSTEM #2

Table 2

BASIC OPTICAL PARAMETERS, TPM-1

FORE-TELESCOPE

Optical Item	Optical Parameter/Spec.	Remarks
FOV, Entrance (1st Field Stop)	1 degree	
FOV, Effective Aperture (Detector)	0.269 degree using 1 mm and F_s	
Entrance Aperture	4.0 dia	
Effective Entrance Aperture	3.2 dia	
Primary (Parabolic) Focal Length, F_1	F_1 = 12.0	
Primary Center Ray Displacement from Main Optical Axis	3.75	
Secondary (Parabolic) Focal Length, F_2	F_2 = 6.0	
Secondary Center Ray Displacement from Main Optical Axis	1.875	
1st Field Stop Size	1 degree or 0.209 dia	
Fore-Telescope Magnification, M_1	12 ÷ 6 = 2:1 or M_1 = 2	
Lyot Stop Size	1.6	
L/D of Fore-Telescope	5.35	

RELAY OPTICS

Optical Item	Optical Parameter/Spec.		Remarks
	System A	System B	
Distance from Lyot Stop to Hole in Folding Flat	14.941	14.941	
Diameter of Hole in Folding Flat	X	1.214	
Distance from Hole in Folding Flat to Vertex of Ellipsoid	7.449	2.849	
Dahl-Kirkham Primary (Ellipsoid)	$\frac{x^2}{a^2} + \frac{y^2}{b^2} = 1$	$\frac{x^2}{a^2} + \frac{y^2}{b^2} = 1$	where a=4.78835, b=3.57689
Effective Focal Length of D/K Primary, F_s	F_3 = 1.337	F_3 = 1.337	0.689 + 0.648 (Virtual Image)
Dahl-Kirkham Secondary (Spheroid)	R = 1.9005	R = 1.9005	OD = 0.84 (includes rolloff)
D/K Primary to Secondary Spacing	0.689	0.689	
D/K Secondary to Detector Spacing	2.032	2.032	
Magnification of Dahl-Kirkham, M_2	M_2 = 3.1358	M_2 = 3.1358	2.032 ÷ (1.337 - 0.689)
System Focal Length, F_s	F_s = 8.385	F_s = 8.385	$F_s = F_3 \times M_1 \times M_2$
Spot Size at Detector	≤0.005	≤0.005	
Obscuration of D/K Secondary On-axis	59%	28%	Obscurations significantly different but energy split is identical
Cone f/# at Detector, on-axis	f/# 2.55	f/# 3.4	
Efficiency of System, Ent.	10.2%	14.4%	See discussion in text of report
Efficiency of System, Eff.	15.8%	22.4%	See discussion in text of report

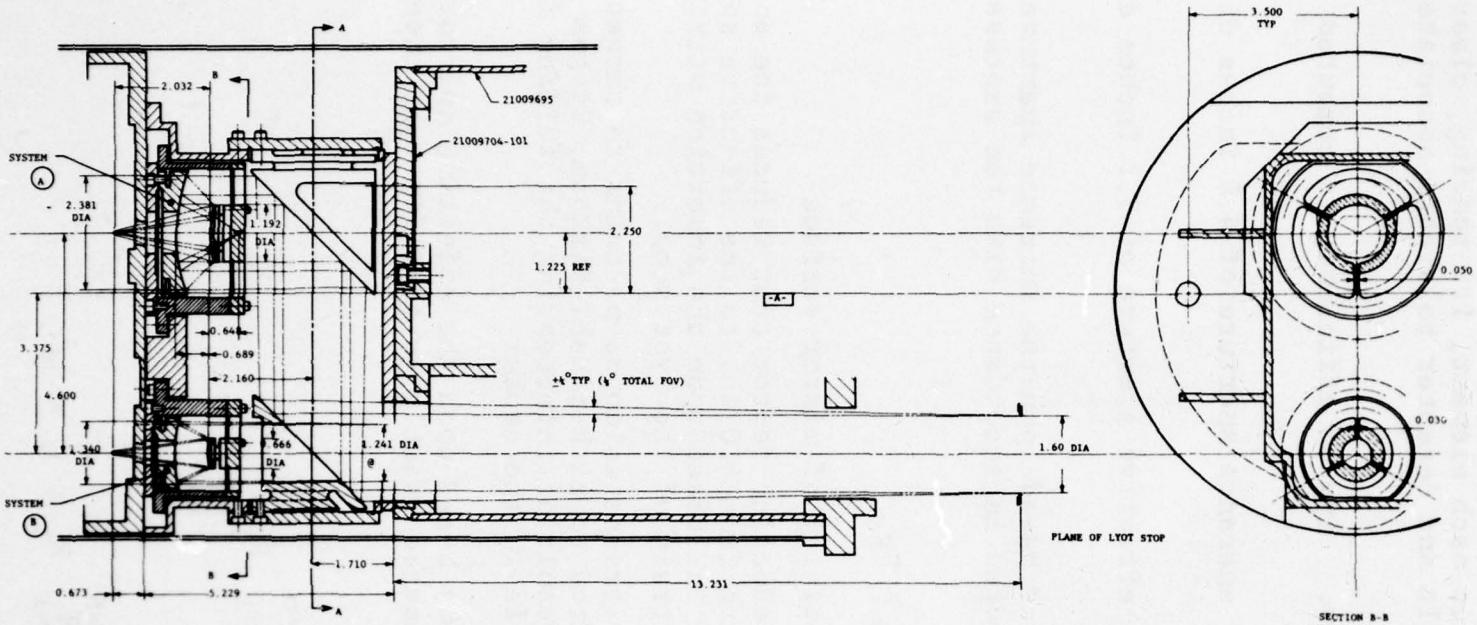

Figure 16 RELAY OPTICS DESIGN

The basic optical tolerances of TPM-1 are as presented in Figure 17 which identifies each element, its spacing, clear aperture and the defocus, tilt and decenter tolerance associated with each element.

3.2.2 System Efficiency. System efficiency is computed one of two ways:

1. Based upon the entrance aperture of 4.0 inches diameter, η_{ENT}
2. Based upon the effective aperture of 3.2 inches diameter, η_{EFF}

The system efficiency based upon the entrance aperture of 4.0 inches diameter, is computed in accordance with the expression, as follows:

$$\eta_{ENT} = \prod_{i-1}^{i=n} R_i \times \eta_L \times \eta_F \qquad (5)$$

where R_i = reflectivity of mirror surface

η_L = step reduction factor that reduces the entrance aperture from 4.0 in. to the effective aperture of 3.2 in. based upon the insertion within the optical train of the lyot stop.

η_F = factor transmission as pertains to target energy delivered to either Dahl-Kirkham, System A or B, as a result of intercepting the folding flat with the hole in the center

The system efficiency based upon the effective aperture of 3.2 inches, diameter, is computed exactly as that for η_{ENT} except delete the factor η_L:

$$\eta_{EFF} = \prod_{i=1}^{i=n} R_i \times \eta_F \qquad (6)$$

For System A:

$$\eta_{ENT} = \prod_{i=1}^{i=6} R_i \times \eta_L \times \eta_F \qquad (7)$$

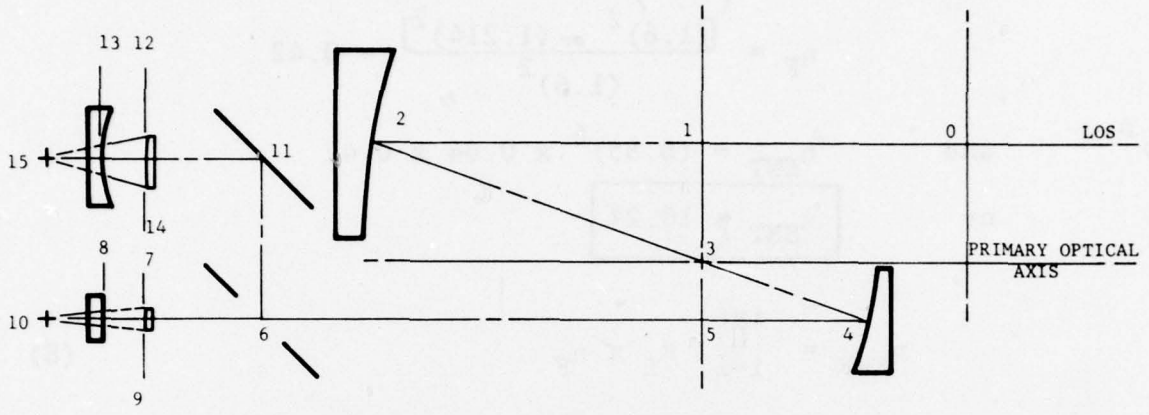

SURFACE		SURFACE GEOMETRY	SPACING	CLEAR APERTURE	DEFOCUS	TILT	DECENTER
0		Fore Entrance Aper. Plane	12.0(1-2)		X	X	X
1		Entrance Aper. Plane	12.0(1-2)	4"(3.2 effective)	±.097(2λ)	±.17°	±.00in
2		Parabolic Primary	12.0(2-3)	4.052 Dia.	±.00(2λ)	±4°	±.067in
3		1st Field Stop	6.0(3-4)	0.209 Dia.	X	X	X
4		Parabolic Secondary	6.0(4-5)	2.058 Dia.	X	X	X
5		Lyot Stop Plane	14.94(5-6)	1.600 Dia.	X	X	X
6		Folding Flat with Hole	2.160(6-7)	1.211 Dia. (Hole)			
				1.729 O.D. (Proj.	X	X	X
7	SYS B	Plane of D/K Secondary	0.689(7-8)	X	X	X	X
8	SYS B	Elliptical Primary	0.689(8-9)	1.239 Dia.	±.020(5λ)	±.5°	±.010in
9	SYS B	Spherical Secondary	2.032(9-10)	0.601 Dia.	±.002	±.3°	±.010
10	SYS B	Image	X	X	X	X	X
11	SYS A	Folding Flat	4.600(6-11)	X	X	X	X
12	SYS A	Plane of D/K Secondary	2.160(11-12)	X	X	X	X
13	SYS A	Elliptical Primary	0.689(12-13)	1.795	±.020(5λ)	±.5°	±.010in
14	SYS A	Spherical Secondary	0.689(13-14)	0.876	±.002in	±.3°	±.010in
15	SYS A	Image	2.032(14-15)	X	X	X	X

Figure 17 BASIC OPTICAL TOLERANCES, TPM-1

where $R_i = 0.85$ for all mirror surfaces

$$\eta_L = \left(\frac{3.2}{4.0}\right)^2 = 0.64$$

$$\eta_F = \frac{\left[(1.6)^2 - (1.214)^2\right]}{(1.6)^2} = 0.42$$

and $\eta_{ENT} = (0.85)^6 \times 0.64 \times 0.42$

or $\boxed{\eta_{ENT} = 10.2\%}$

$$\eta_{EFF} = \prod_{i=1}^{i=6} R_i \times \eta_F \qquad (8)$$

$$= (0.85)^6 \times 0.42$$

or $\boxed{\eta_{EFF} = 15.8\%}$

For System B:

$$\eta_{ENT} = \prod_{i=1}^{i=4} R_i \times \eta_L \times \eta_F \qquad (9)$$

where $R_i = 0.85$ for all mirror surfaces

$$\eta_L = 0.64$$

$$\eta_F = \frac{\left[(1.214)^2 - (0.61)^2\right]}{(1.6)^2} = 0.43$$

and $\eta_{ENT} = (0.85)^4 \times 0.64 \times 0.43$

or $\boxed{\eta_{ENT} = 14.4\%}$

$$\eta_{EFF} = \prod_{i=1}^{i=4} R_i \times \eta_F \qquad (10)$$

$$= (0.85)^4 \times 0.43$$

or $\boxed{\eta_{EFF} = 22.4\%}$

3.3 Scatter Coefficient of the Primary Mirror. Cryogenic E-O sensor designs at HRC have followed the approach of mirrors and mating structures to be fabricated from the same base material. The material selected for the USU telescope design was 6061-T6 aluminum. The general procedure used for the structure was to machine to the approximate dimension, stress relieve, machine to the final dimension, then lap where required. Mirrors were machined to the approximate configuration desired, stress relieved, the entire surface coated with an electroless deposition of nickel, and with final figuring and polish, a low scatter reflecting surface was effected. A number of problems have existed with both fabrication and testing of low scatter mirrors. The fabrication techniques have ranged over the use of aluminum, beryllium, nickel, steel etc. as a base metal, with or without a nickel overcoat, as required, depending upon whether nuclear hardening was a requirement and the material needed to be transmissive to soft xrays.

Claims of suppliers as to what type of fabrication technique to use, what constituted a low scatter surface, and what was, in fact, achievable, became more and more uncertain as each user had their own method of measurement. Consistency in the measurement methods became critical in assessing and evaluating mirror scatter characteristics.

In an attempt to bring order to the situation, the Air Force sponsored the following programs:

1) A determination of the state-of-the-art of low scatter mirror surfaces.

2) Development of a low scatter test station at ARO, Inc., Tullahoma, Tenn., under the direction of Ray Young.

3) A "Round Robin" test sequence, to be performed by Ray Young, such that a survey was conducted of all contributing private and government low scatter test facilities with test results referenced against "controlled" data.

4) A mirror contamination amelioration program.

The results of these programs were significant. Today, the low scatter mirror measurement and test effort has matured beyond the "black art" past to a situation of understanding and credibility. Approved setups for low scatter test and evaluation exist in virtually all major facilities that have a need for low scatter mirrors.

Correlation between testing facilities exists as every accredited facility is referenced against Tullohoma's mirror test samples and data.[7]

In summary, fabrication and test capabilities exist that can achieve the following:

a) test facilities exist that can reliably check for low scatter coefficients in the order of 10^{-7} at one degree off-axis.

b) low scatter mirrors less than 4½ inches in diameter can now be fabricated to achieve a low scatter coefficient of 1×10^{-5} on a repeatable basis. The mirror substrate is either aluminum or beryllium and has an electroless nickel deposition over the surface to be polished. The USU telescope mirrors attained a scatter coefficient on the order of $1\text{-}2 \times 10^{-4}$.

c) low scatter mirrors greater than 10 inches in diameter can now be fabricated to achieve a low scatter coefficient of 1×10^{-4} on a repeatable basis.

d) achieving a 10^{-6} scatter coefficient in a reproducible manner on any diameter surface is seen only as a future possibility. This quality surface will probably be attainable only on a tilted sphere, not an off-axis parabola.

Finally, the low scatter surface contamination problem due to improper cleanliness and/or cleaning procedures is still a major concern. Only exceptional diligence in adherence to established, experience proven procedures of handling eliminates contamination as a problem.

3.4 Foretelescope Baffling. The original telescope forebaffle design premise for the TOM Sensor was to keep baffle edges to a minimum. Baffle edge effects were felt to be a greater source of off-axis noise than a straight, painted forebarrel wall. This design philosophy became incorporated into the initial design of the ELS, ELMS and the three Utah State CVF Telescope Systems. Honeywell's "GUERAP" analysis (Ref 1) indicated that the USU telescope design, as conceived, should yield a 3.9×10^{-9} reduction of off-axis energy at the detector from ½ degree energy source incident angles.

This prediction was based upon no baffles other than aperture and field stops. However, the analysis made the assumption that reflection off of structural surfaces was perfectly diffuse.

Continued system analyses and eventual subsystem and system tests have indicated that off-axis grazing energy from an extended source impinging upon the telescope forebarrel could introduce a substantial increase in the off-axis scattered radiation striking the primary and becoming a part of the "target" signal. A change in our design philosophy came about with a greater understanding of grazing effects and the realization that surface grazing energy could produce an effect far worse than the baffle edges that we were trying to avoid.

Surface scatter experiments conducted at HRC have shown that given a grazing angle ($90^{o} - \theta$), where θ is the angle of incidence, a reflected specular angle exists that includes a lobe of specular reflection; and the angle that includes this lobe may be upwards to double the grazing angle. The specular reflection angle includes energy which is a function of the grazing angle and the reflectivity and scatter characteristics of the paint. See Figure 18.

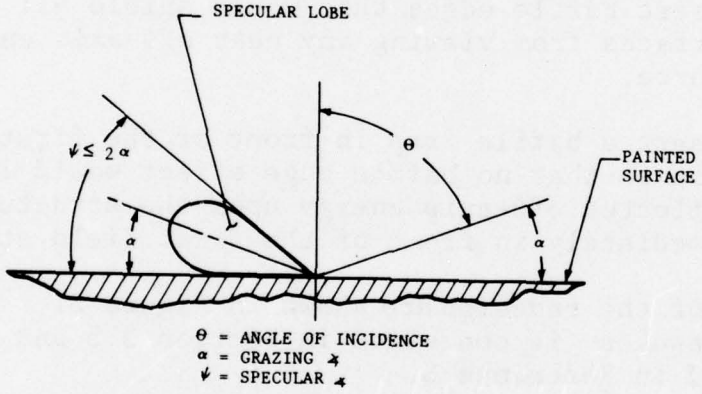

Figure 18 TYPICAL GRAZING ANGLE ENERGY LOBE

The current baffle design for high off-axis rejection systems is based upon the criteria that no specular reflection will exit from the specular trap. See Figure 19.

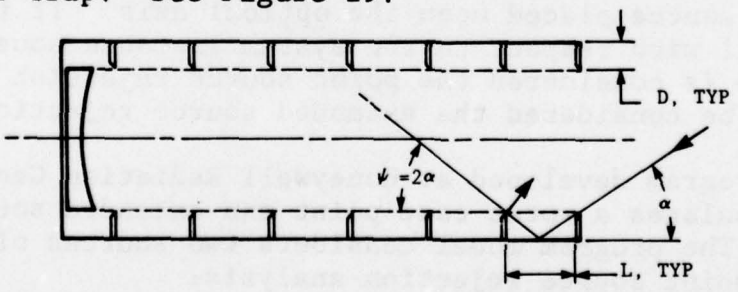

Figure 19 TYPICAL FORE TELESCOPE BAFFLE CAVITY DESIGN

From the preceding, the attenuation of out-of-field, off-axis energy impinging upon the telescope forebarrel at grazing angles of less than 20 degrees is usually accomplished by inserting baffles that accommodate a specular angle that is equal to or less than twice the grazing angle.

When the USU telescopes were initially tested for off-axis-rejection (OAR) capability, it was shown that the OAR characteristic was 1½ orders of magnitude away from meeting predicted performance. A ray trace, as shown in Figure 20, showed how the specular lobe was entering the first field stop and illuminating the field. The use of a helium neon laser illuminating on and off the suspect surfaces confirmed the structure areas needing to be baffled.

Having defined visually what was happening, a baffle system was designed that could be inserted so as to shield certain structure surfaces from off-axis energy. In particular the baffle system was devised to perform the following functions:

a) Insert baffle edges that would shield all bulkhead surfaces from viewing any near off-axis energy source.

b) Insert a baffle trap in front of the first field stop so that no baffle edge effect would impinge reflected off-axis energy upon the structure surface immediately in front of the first field stop.

The results of the redesign are shown in Figure 21. A summary of the OAR test results is contained in Section 3.5 and the testing is fully described in Reference 8.

3.5 Off-Axis Rejection (OAR) Analysis, Testing. Off-Axis rejection describes the ability of a system to attenuate out of field non-signal energy. It is simply the ratio of flux incident upon the detector element due to an off-axis source to that produced by the same unobstructed source placed upon the optical axis. If the target divergence is small with respect to the system instantaneous field of view, the ratio is considered the point source rejection ratio; otherwise it must be considered the extended source rejection ratio.

A computer program developed at Honeywell Radiation Center entitled SCAT calculates a worst case point and extended source rejection ratio. The program model considers two sources of scattered radiation in its point source rejection analysis:

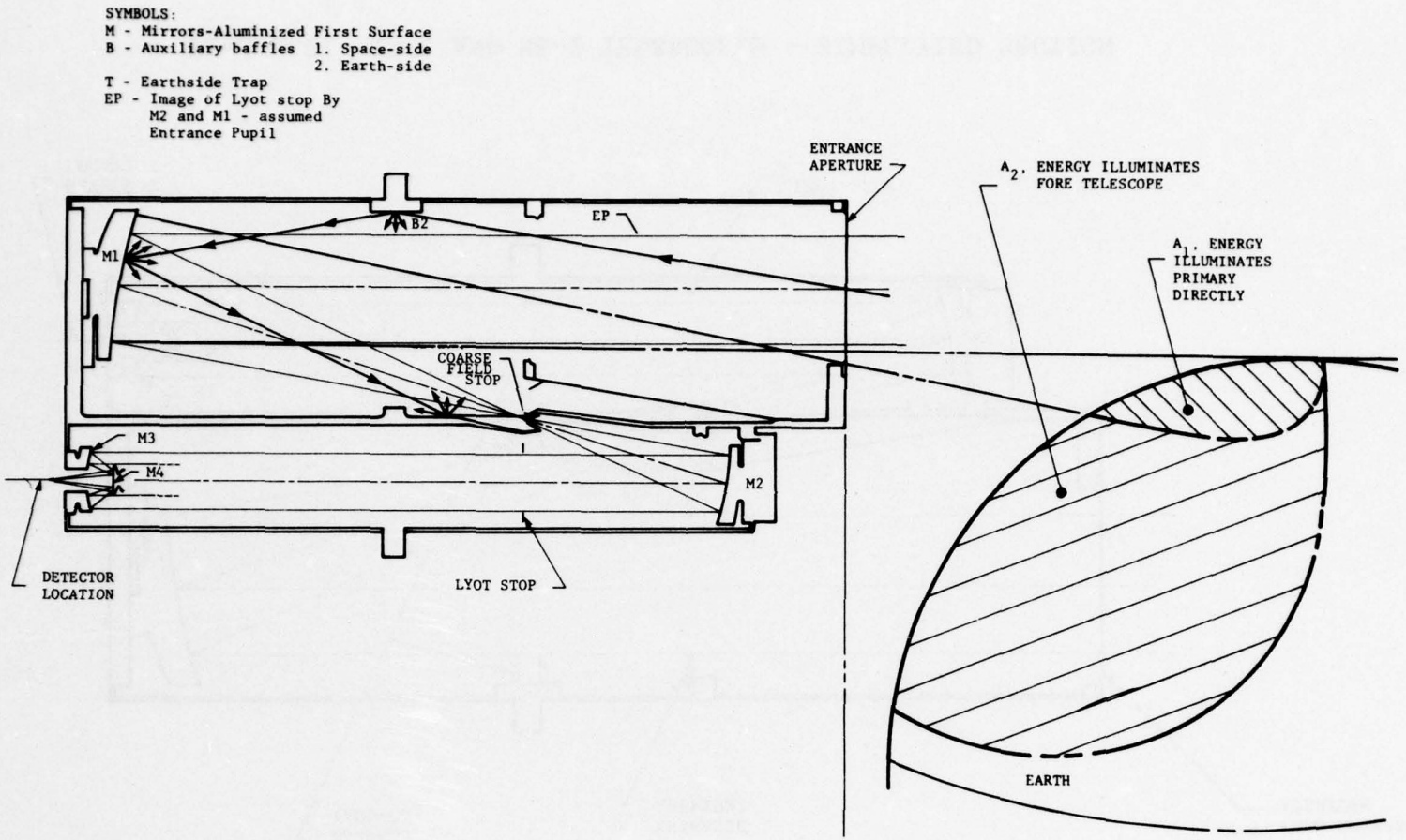

Figure 20 FALSE TARGET RAY TRACE

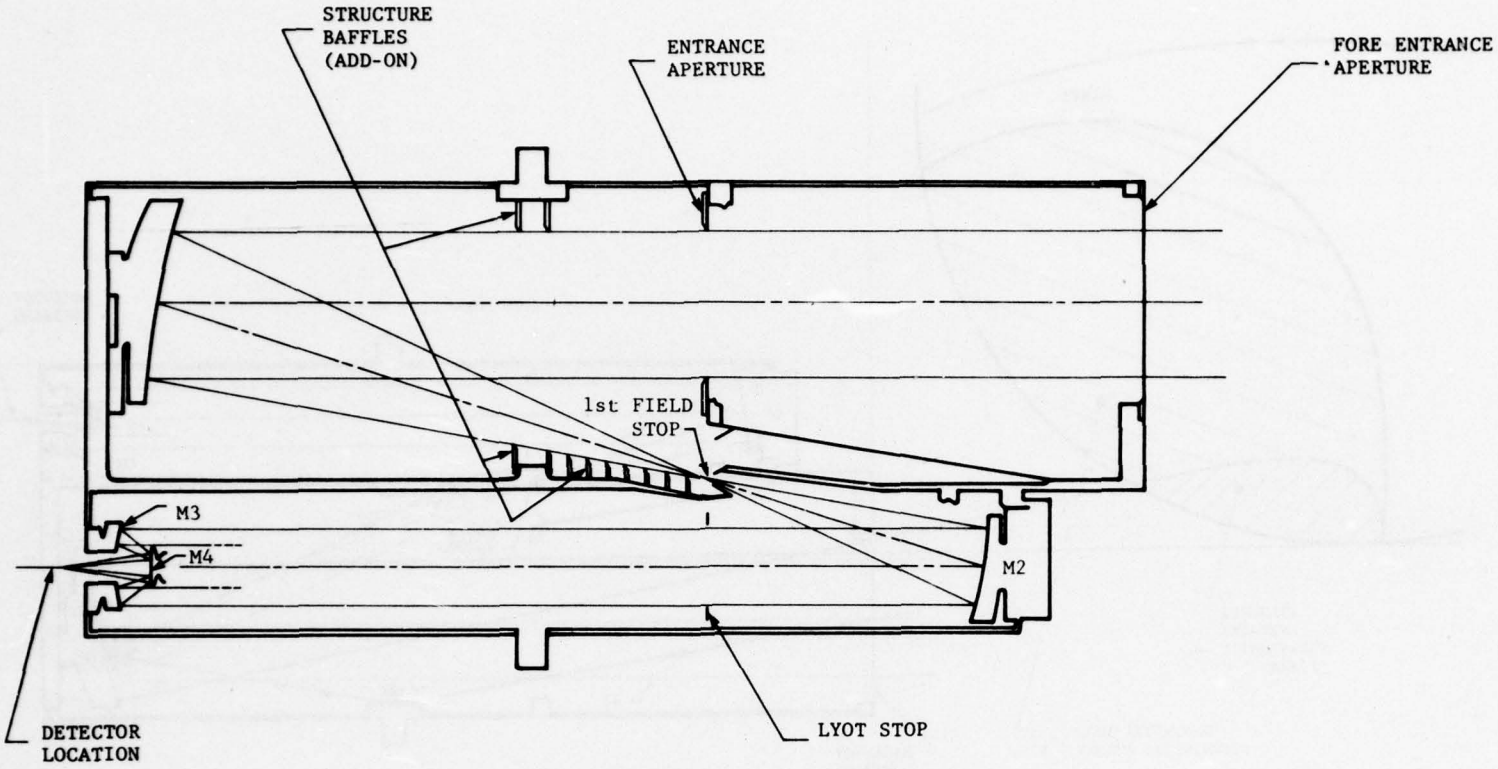

Figure 21 HS-2 AND NS-2 TELESCOPES - SIMPLIFIED SECTION

- scatter by primary optics into the detector field of view

- out-of-field scatter by flat baffle edges (extreme model) rescattered by primary optics into the detector field of view.

The degree of scatter exhibited by the optics as well as the baffle edges must be supplied to SCAT as inputs. While scatter by optical elements is a measurable system parameter, edge specular scatter must be evaluated analytically.

Given these scattering inputs as well as shade geometry and field-of-view information, the program determines the system point source rejection ratio by means of view factors. Figure 22 shows the predicted off-axis rejection of the HS-2 telescope as computed by SCAT.

The Honeywell Systems and Research Center OAR test facility is depicted schematically in Figure 23. A test laser output (10.6 μm or 1.06 μm available) is first passed through a chopper, into a specially fabricated attenuator stack and then into confocal off-axis paraboloids. The collimated output is then propagated through an iris to flood the test telescope entrance aperture, simulating a point source target.

Auxiliary mirrors are provided to allow injection of a visible tracer beam and to measure the test laser power level following attenuation. Tables 3 and 4 serve to further detail the test system components.

The attenuators are reflective metal films on substrate discs (Inconel on IRTRAN-2 at 10.6 μm and chromium on Homosil at 1.06 μm). The discs are mounted snugly, but without binding or bonding in metal rectangular holders. The holders slide in slots arranged to hold the filter surface normals $\approx$40 degrees from the laser beam direction. Carbon cones within the cylinders absorb the unwanted reflected energy. The discs are half-moon coated on the first surface so that two slide positions are created; one presents the substrate only to the laser beam and the other inserts the substrate and the reflective coat in the beam. This minimizes both the effects of thermal transients and laser beam deflections when the attenuators are inserted or removed. The alternating orientations of the filters also reduce net beam deflection.

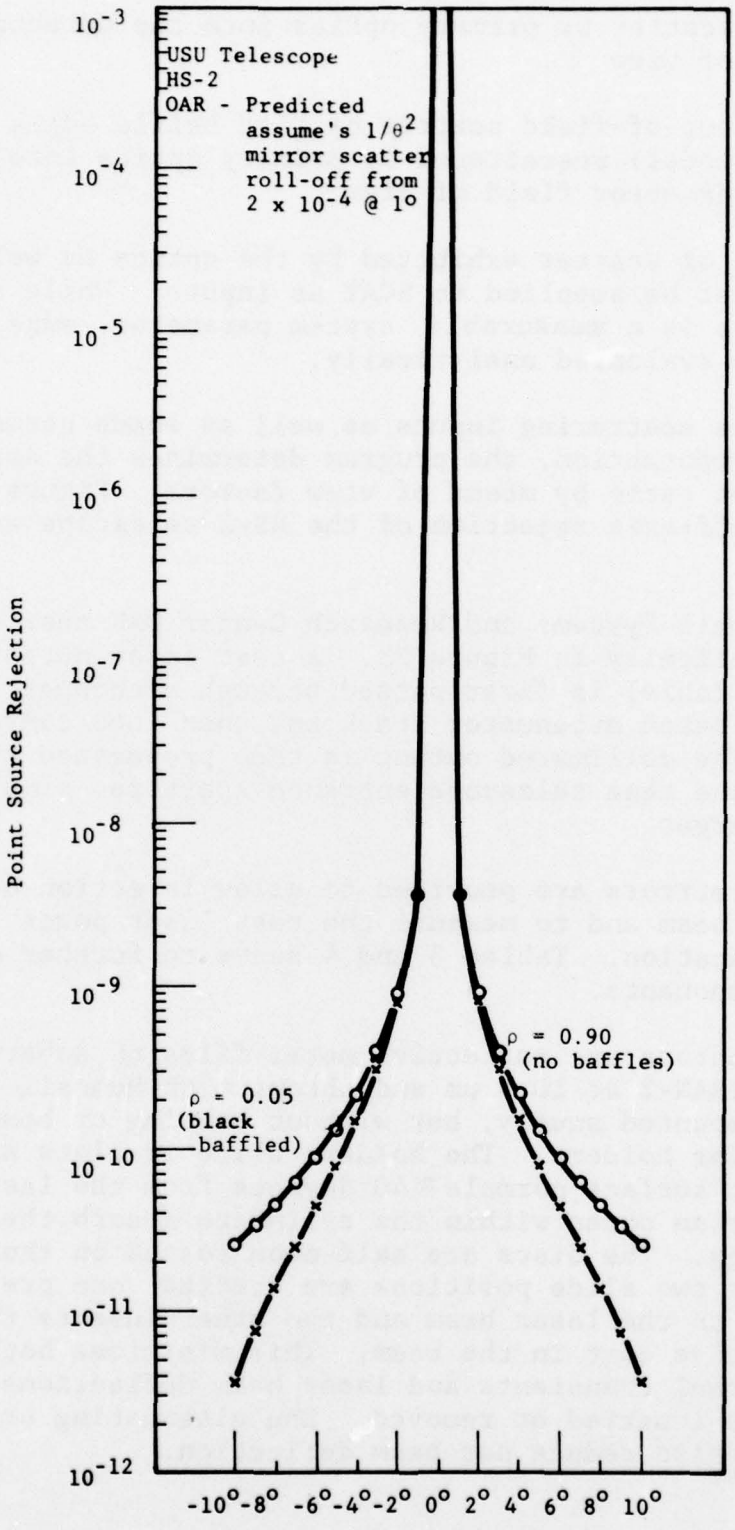

Figure 22 HS-2 OAR PERFORMANCE

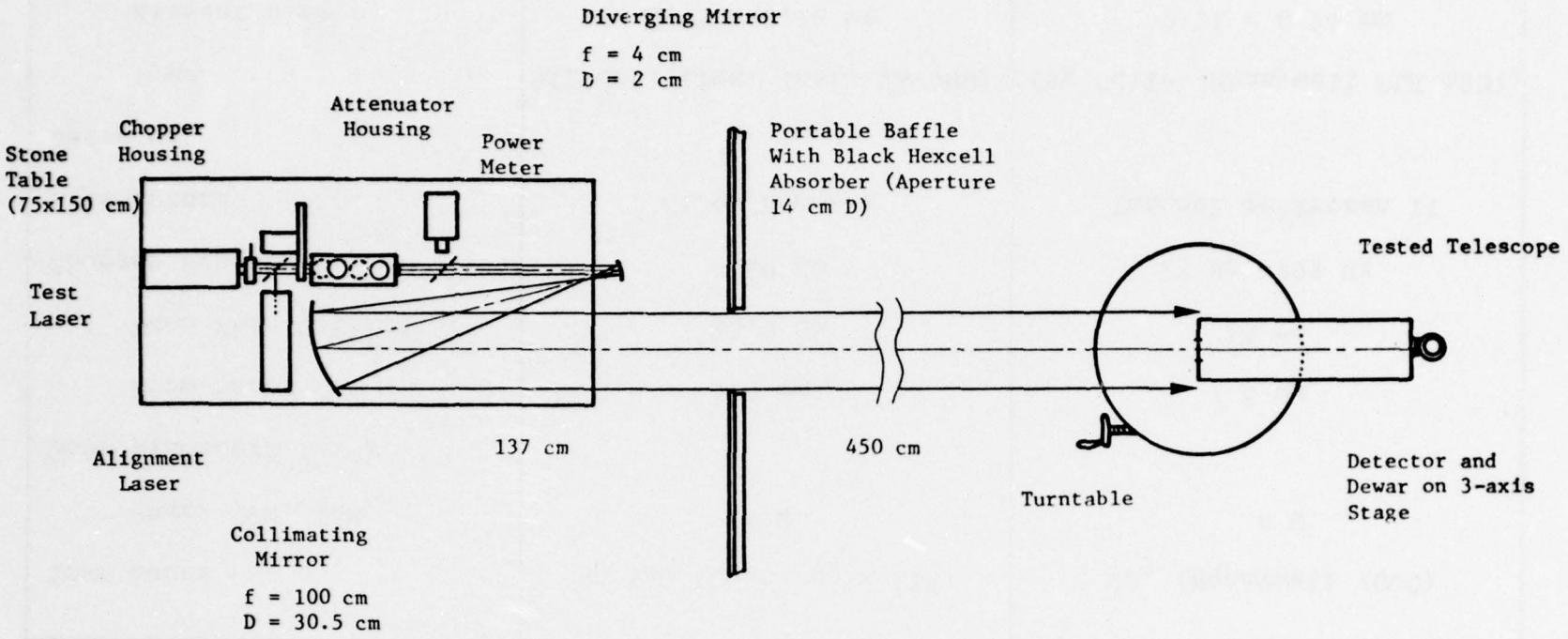

Figure 23 OFF-AXIS REJECTION (OAR) TEST SETUP

Table 3

DATA ON EQUIPMENT USED AT DIFFERENT WAVELENGTHS

Item	Wavelength	
	1.06 μm	10.6 μm
Test Laser	Nd:YAG (Quantronix 114)	CO_2 (Honeywell 7000)
Power (CW, TEM_{oo})	4 W	4 W
Beam Diameters (e^{-2})		
From Laser	5.4 mm	6 mm
From Main Collimator	13.5 cm	15 cm
Chopper Frequency	140 Hz	13 Hz, 999 Hz
Attenuators	Cr on Homosil	Inconel on Irtran II
Detector		
Type	Silicon, (Tex. Inst. LS-400)	(Hg,Cd)Te (Honeywell DLK 63D7)
Element Size	0.51 x 0.76 mm	0.71 x 0.74 mm
Operating Temperature	293 K	77 K

Table 4

EQUIPMENT COMMON TO ALL TESTS

Lock-in Amplifier:	Brower Model 132
	Preamplifier Model 261
Power Meters:	Laser Precision Radiometer Model Rk-3440 with RkP-345 Probe
	Coherent Radiation Model 201
Alignment Telescope - Gaertner	
Liquid Crystal Sheet - Edmund Scientific Stock No. 71,137, Range 20-25C	
Chopper:	Brower with Model 500 Programmer
Telescope Mount:	Hofmann dividing head, 30 cm D, readable to 0.1 min arc
	Cross-slide, 2-axis, 8" travel, readable to 0.0001 in.

The attenuators were calibrated using both the test telescope with its detector, where possible, and a power meter. The 10.6 μm (Hg,Cd)Te detector response was measured with a blackbody source and geometric power variation (aperture and distance). This detector behaves reasonably over 4 to 5 orders of magnitude, but its curve is nonlinear. When used with the IRTRAN-2 attenuators and the Brower lockin amplifier, the following expressions were used:

$$Vo = 1.39 \times 10^{3} \, V_{1,3}^{1.054} \text{ microvolts} \quad (11)$$

$$Vo = 39.99 \, V_{3}^{1.243} \text{ microvolts} \quad (12)$$

The symbols are:

Vo - signal expected without attenuators (μV)

$V_{1,3}$ - signal measured using attenuators 1 and 3 (μV)

V_3 - signal measured using attenuator 3 (μV)

Similar treatment was not effective for the silicon detector used with the 1.06 μm Nd:YAG laser. However, power meter measurements of the attenuation were internally consistent. The transmittance value 5.4×10^{-5} was measured and applied for the three attenuator combination used.

No attenuators were required for signals measured at angles $\geq 0^{o}40'$ off-axis. Due to the physical limitations of the test setup, the telescope primary views the collimator mirror directly for angles less than 1 degree off-axis. Thus, to ensure absence of collimator mirror effects no off-axis data were considered to be due only to telescope scatter at angles less than 1 degree. Therefore, laser attenuation was required only at 0^{o}, and the data reduction included an application of a normalizing factor, NF.

For the 10.6 μm data the NF divided into each off-axis signal reading was computed from Equation(11) or(12), depending on the attenuators used. The 1.06 μm data were normalized by:

$$NF = (5.4 \times 10^{-5})^{-1} \, V_{ABC} = 1.85 \times 10^{4} \, V_{ABC}$$

where V_{ABC} is the axial signal measured using attenuators A,B and C cascaded.

The entire apparatus is mounted upon an isolation table within a class 10,000 clean room. In an effort to limit sources of scatter, the walls of the test room are lined with black fiberglass hexcell absorbing sheets while the floor is coated with black epoxy.

The following test procedure was adopted:

1. With attenuators in the system, zero was established by maximizing the detector output. Record the signal output. Close the telescope and/or shutter the laser to read the noise.

2. Test for room scatter by inserting a lightly sand blasted aluminum plate into the telescope field of view with the telescope turned aside at several angles. Radical rises in signal indicates room scatter level is excessive.

3. Rotate the telescope to the maximum negative angle (-16 degree for some runs; later -25 degree).

4. Rotate the telescope in prescribed increments to +16 degrees or +25 degrees using attenuators as necessary near zero.

5. Return the telescope to zero with attenuators and repeat the maximum signal and the noise readings.

Figures 24 through 35 depict the measured off-axis characteristics of the three telescopes. The improved system (with baffles) does not yet match the theoretical worst case curves supplied by the SCAT computer program. Several possible sources of error are given below:

- SCAT does not accurately predict point source rejection ratios for off-axis angles of ± 1 degree or less.
- The 10.6 μm data was limited by a relatively high noise floor (low S/N ratio) which prohibited measurement of OAR comparative to theoretical values.
- The test laser is subject to instabilities or drift.
- Detector/attenuator non-linearity
- Meter inaccuracies
- Plant environment

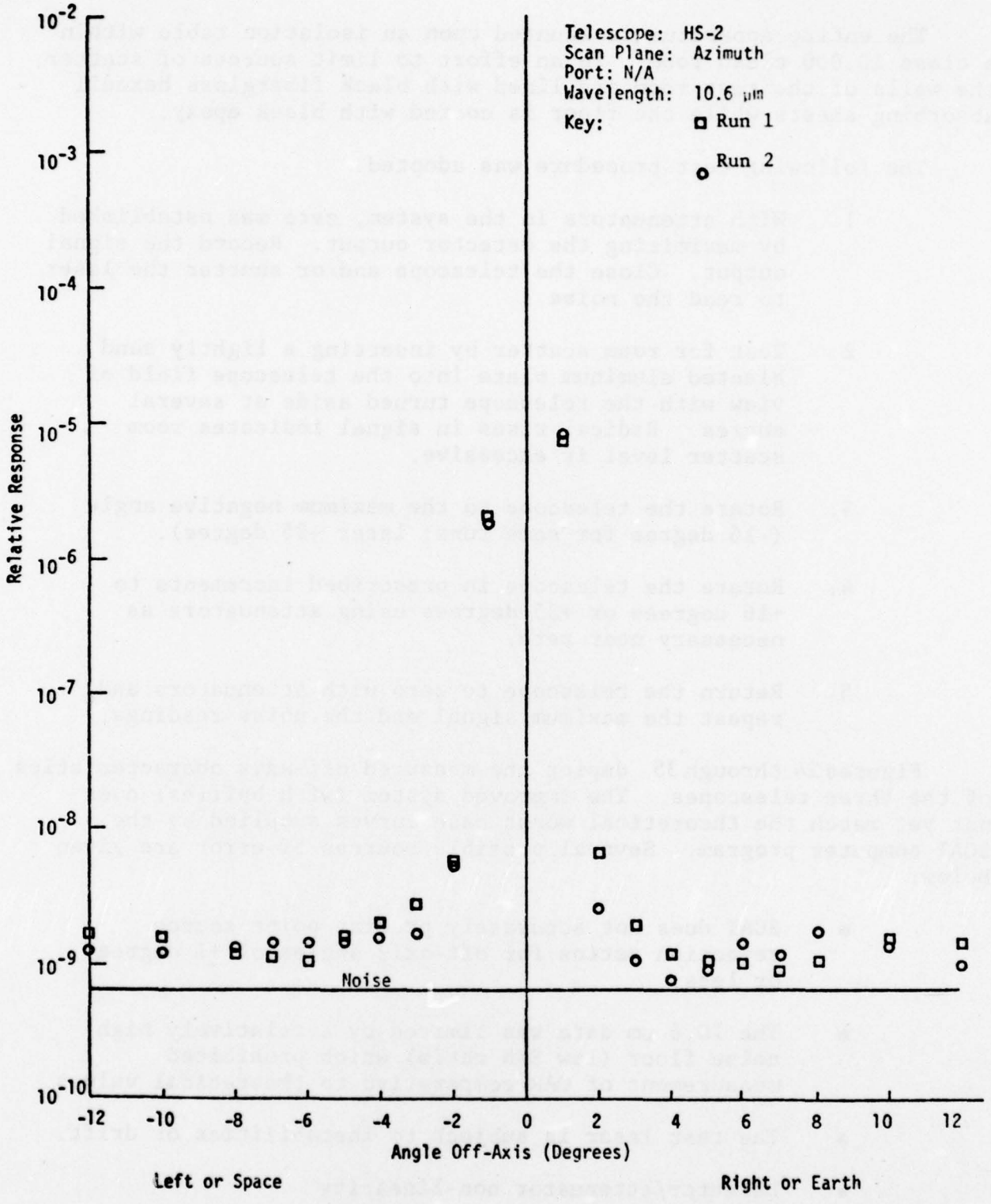

Figure 24 GRAPH 1 - OFF-AXIS REJECTION

77-1-12

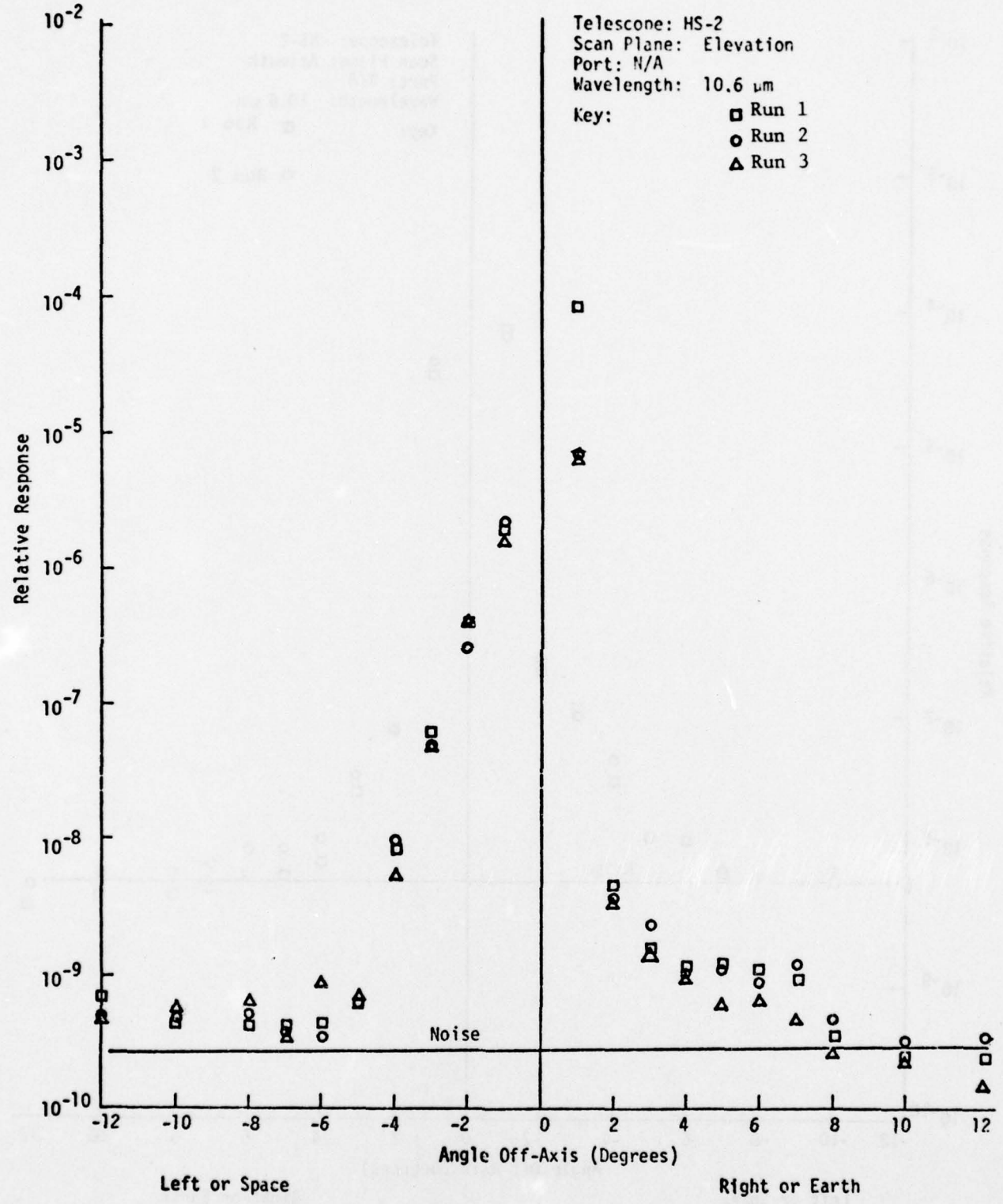

Figure 25 GRAPH 2 - OFF-AXIS REJECTION

77-1-12

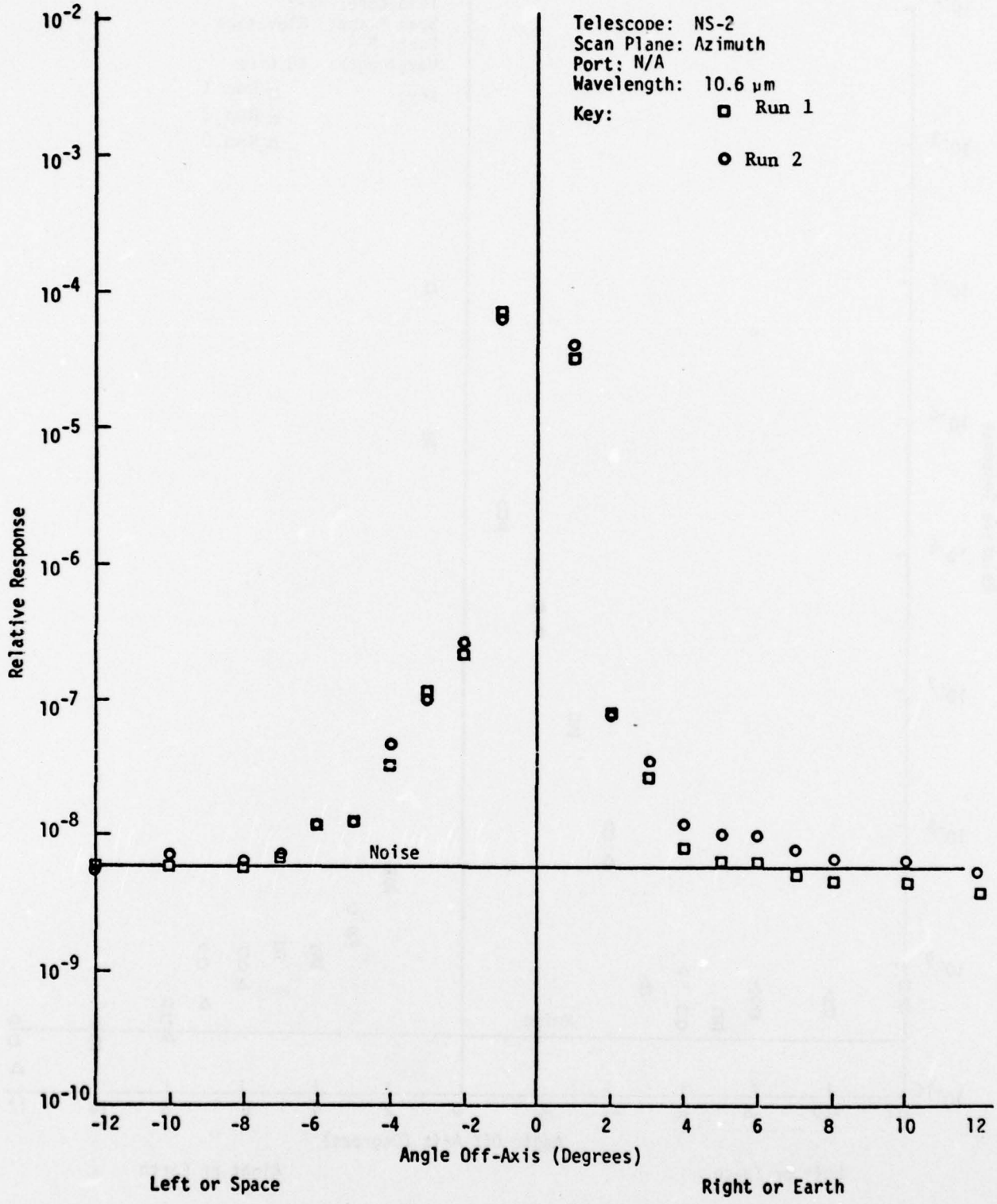

Figure 26 GRAPH 3 - OFF-AXIS REJECTION

77-1-12

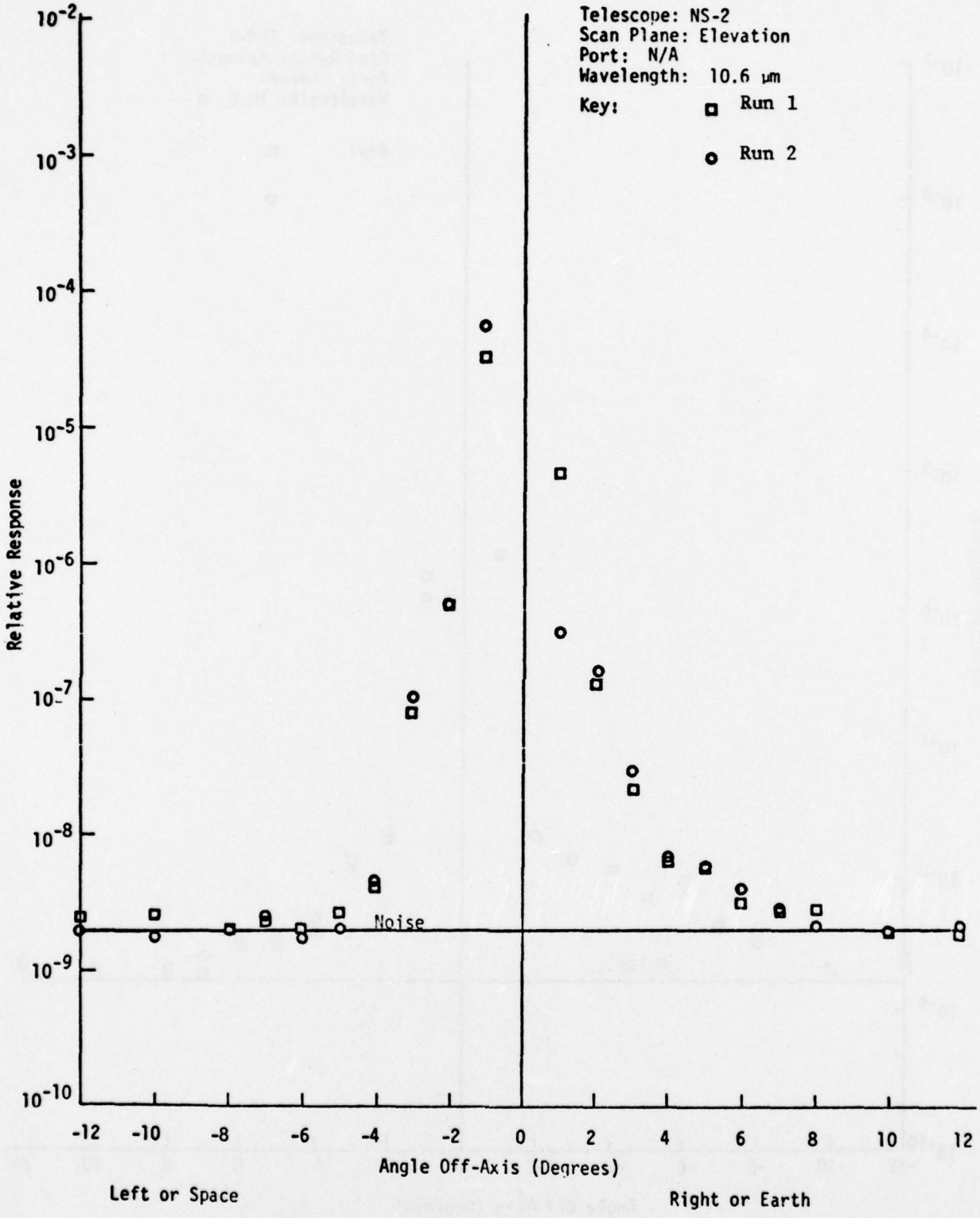

Figure 27 GRAPH 4 - OFF-AXIS REJECTION

77-1-12

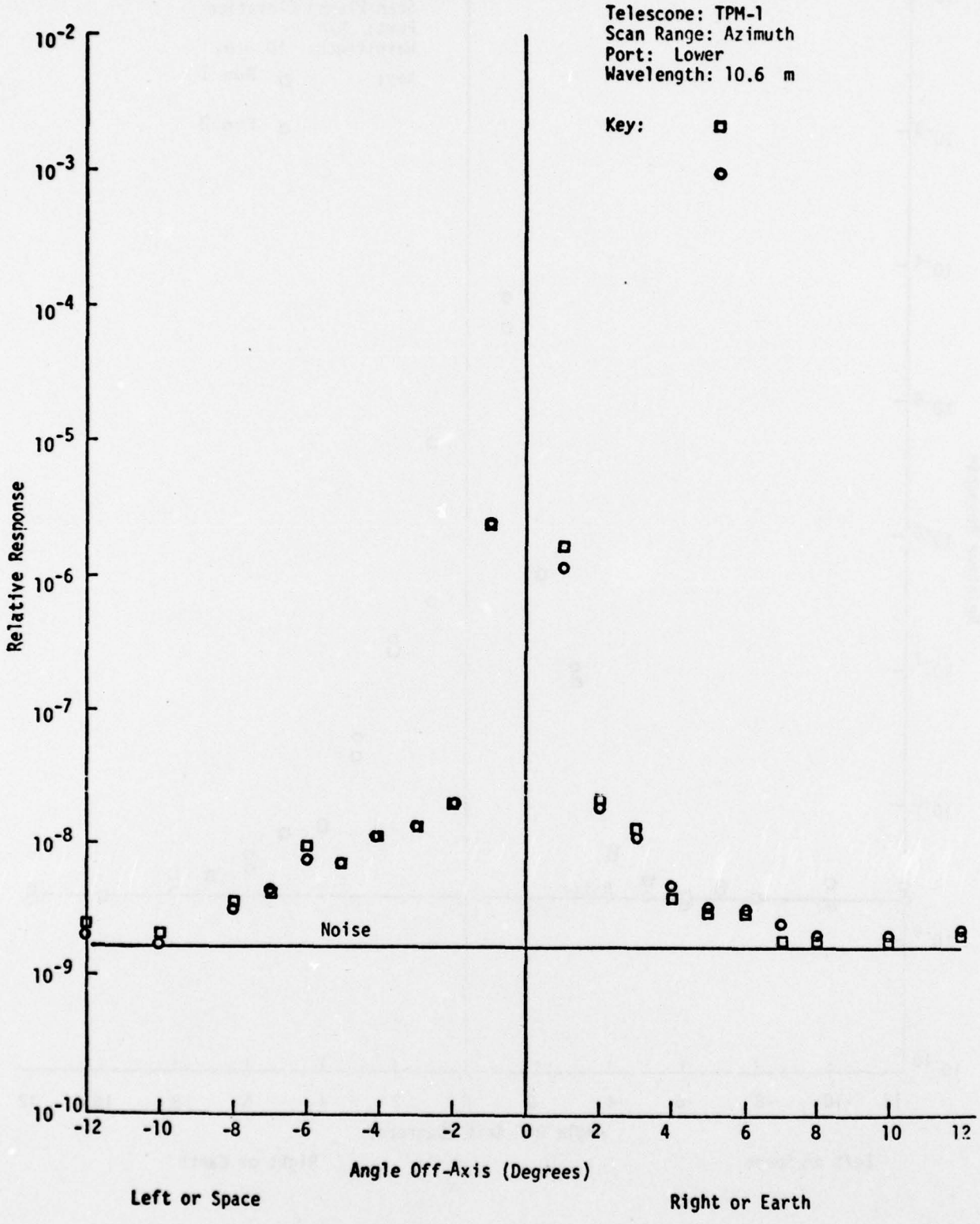

Figure 28 GRAPH 5 - OFF-AXIS REJECTION

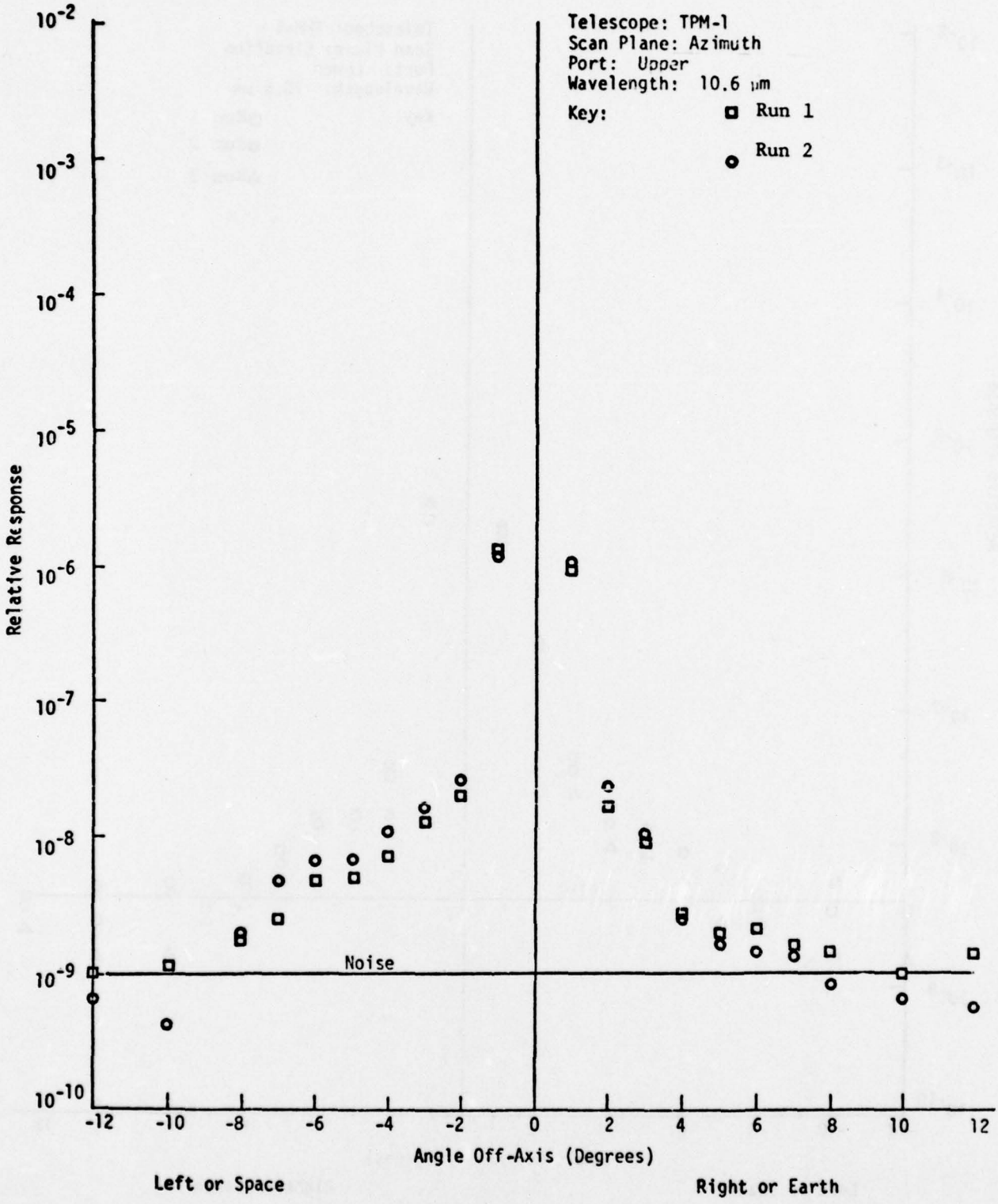

Figure 29 GRAPH 6 - OFF-AXIS REJECTION

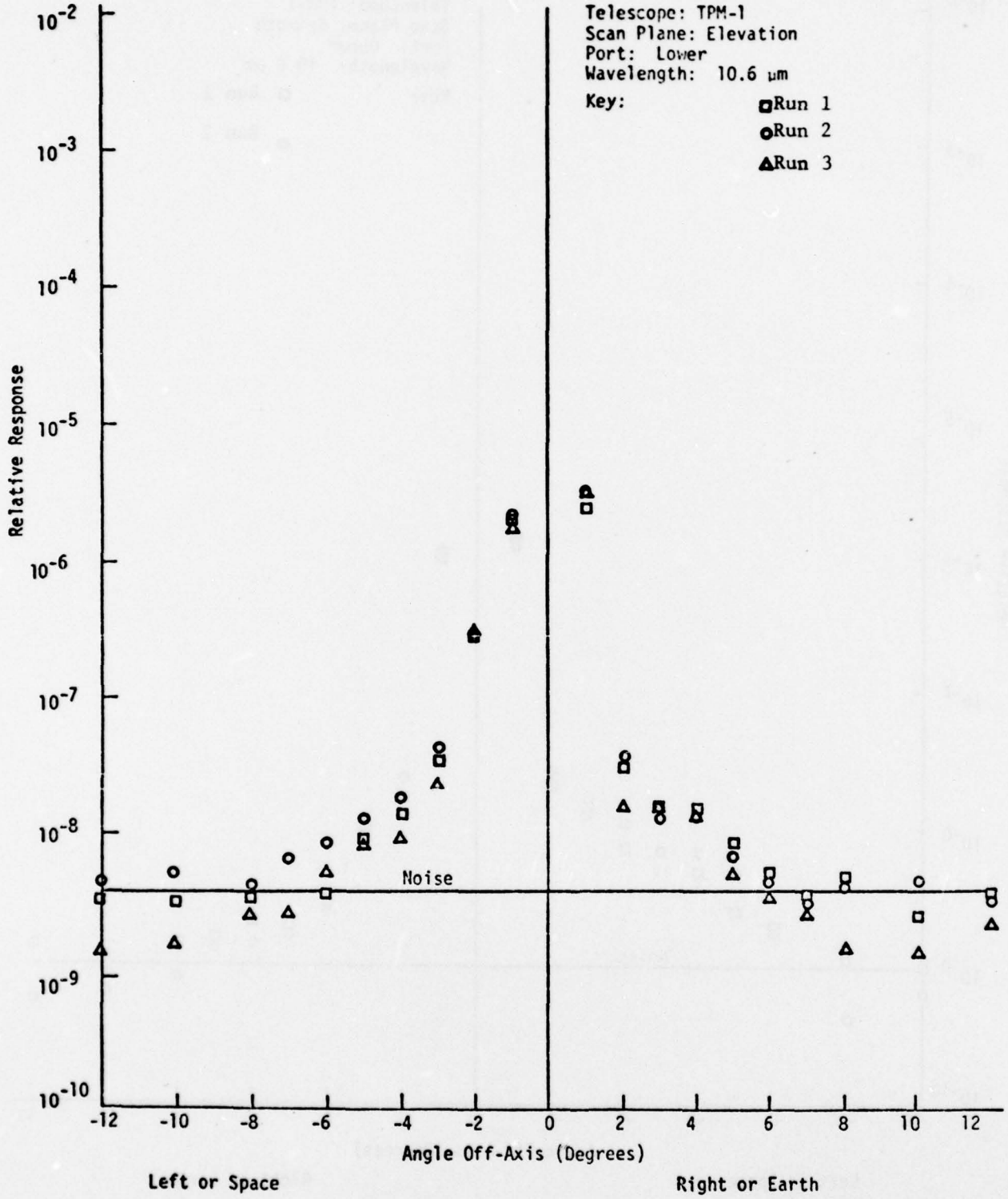

Figure 30 GRAPH 7 - OFF-AXIS REJECTION

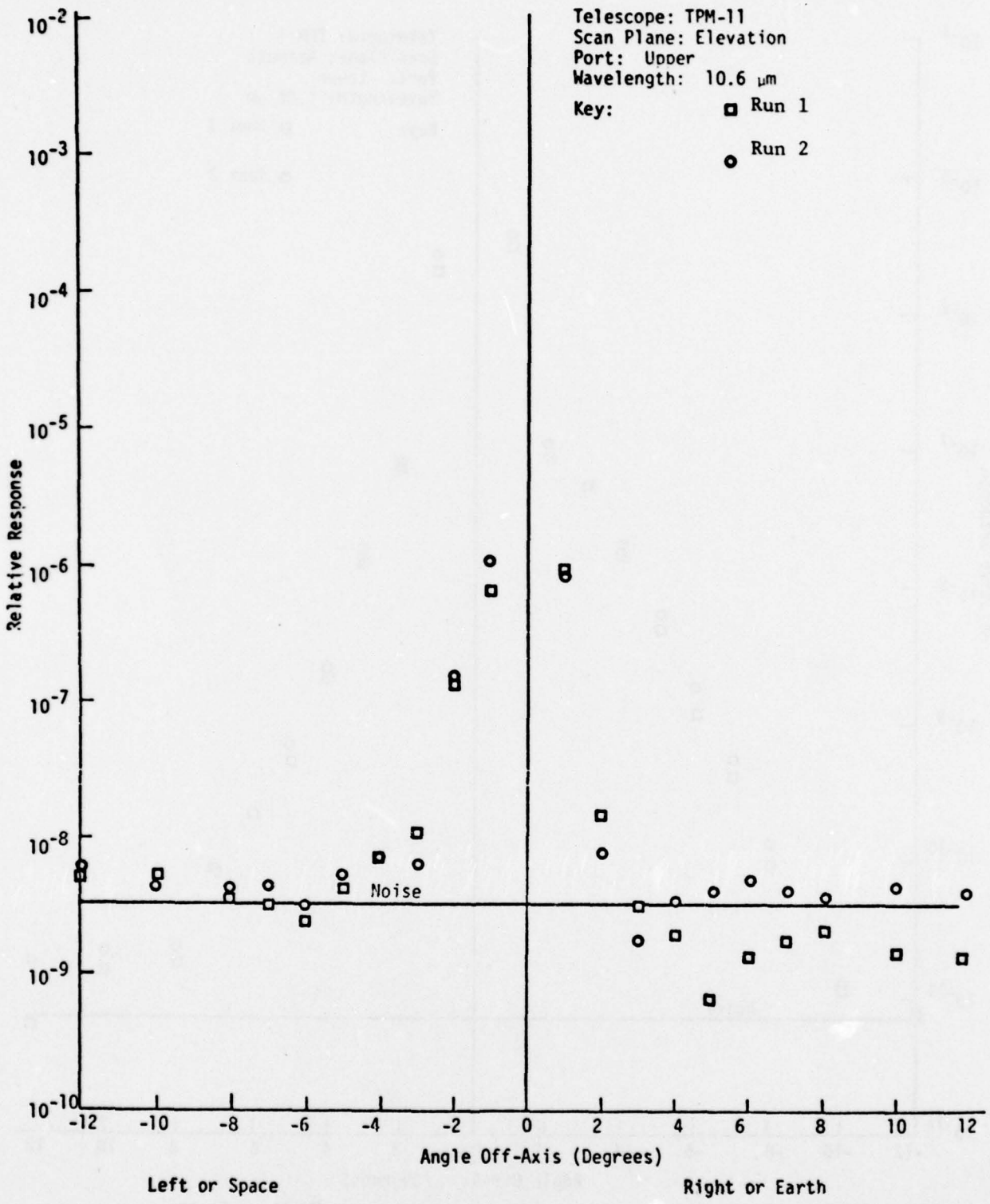

Figure 31 GRAPH 8 - OFF-AXIS REJECTION

77-1-12

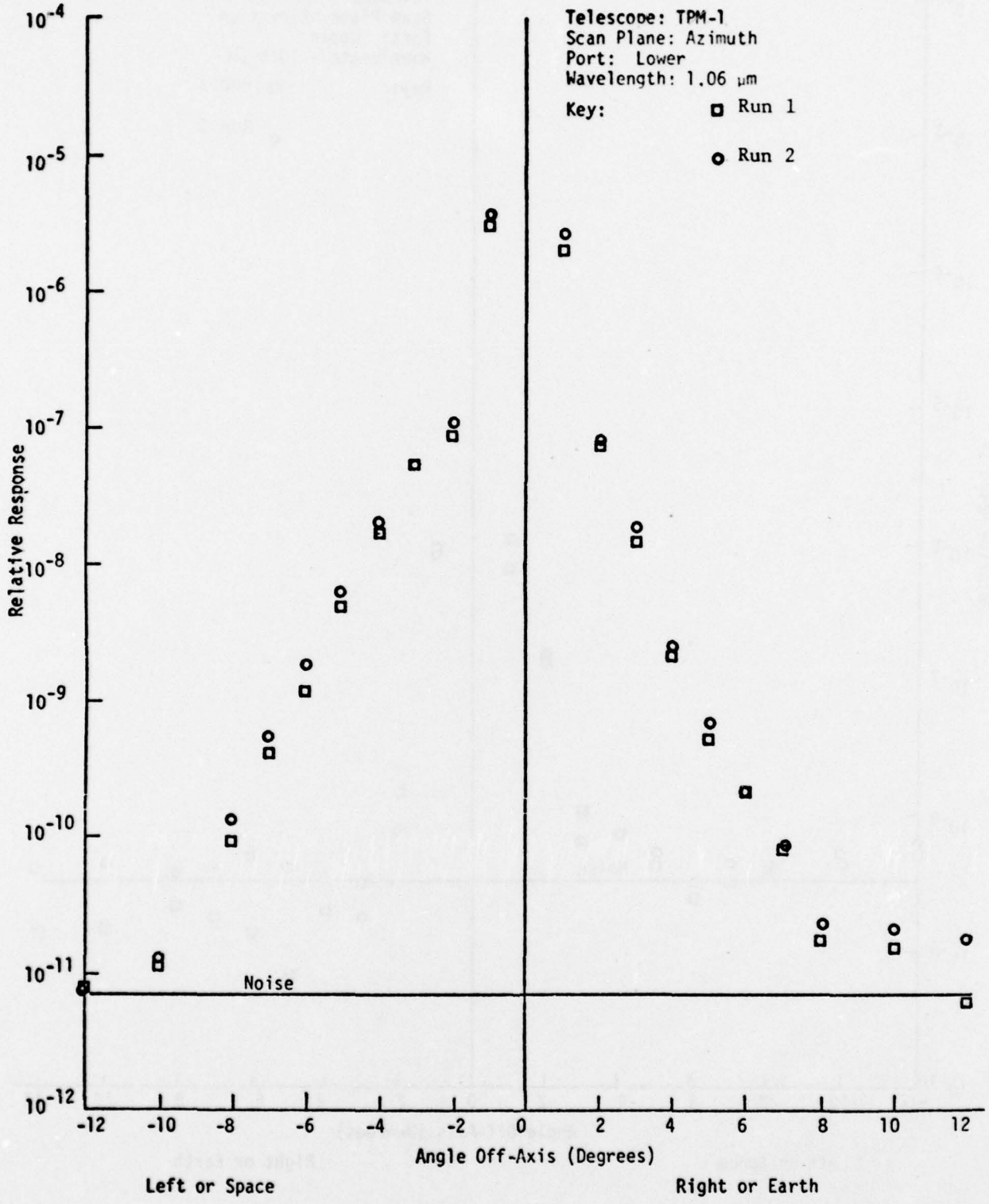

Figure 32 GRAPH 9 - OFF-AXIS REJECTION

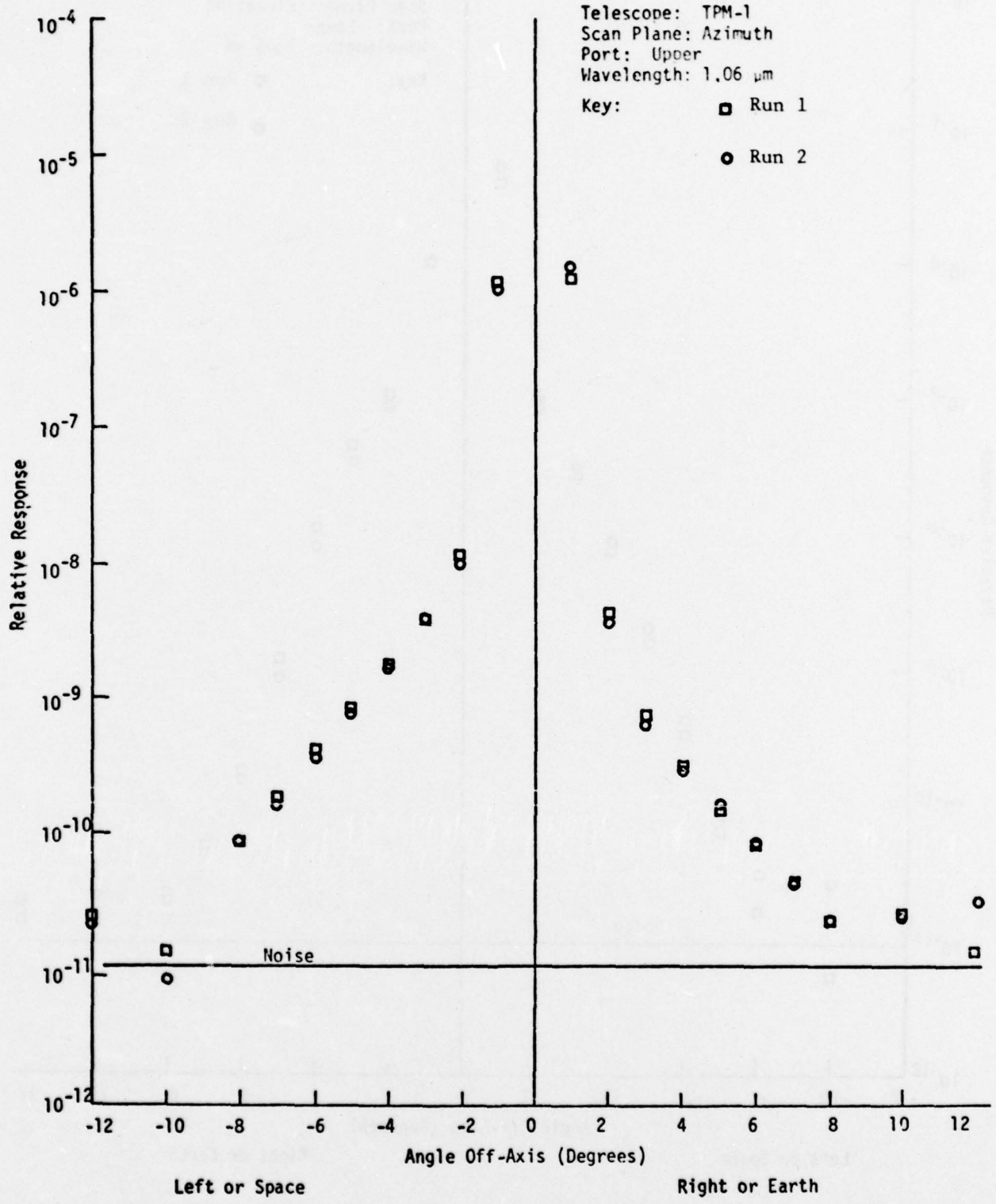

Figure 33 GRAPH 10 - OFF-AXIS REJECTION

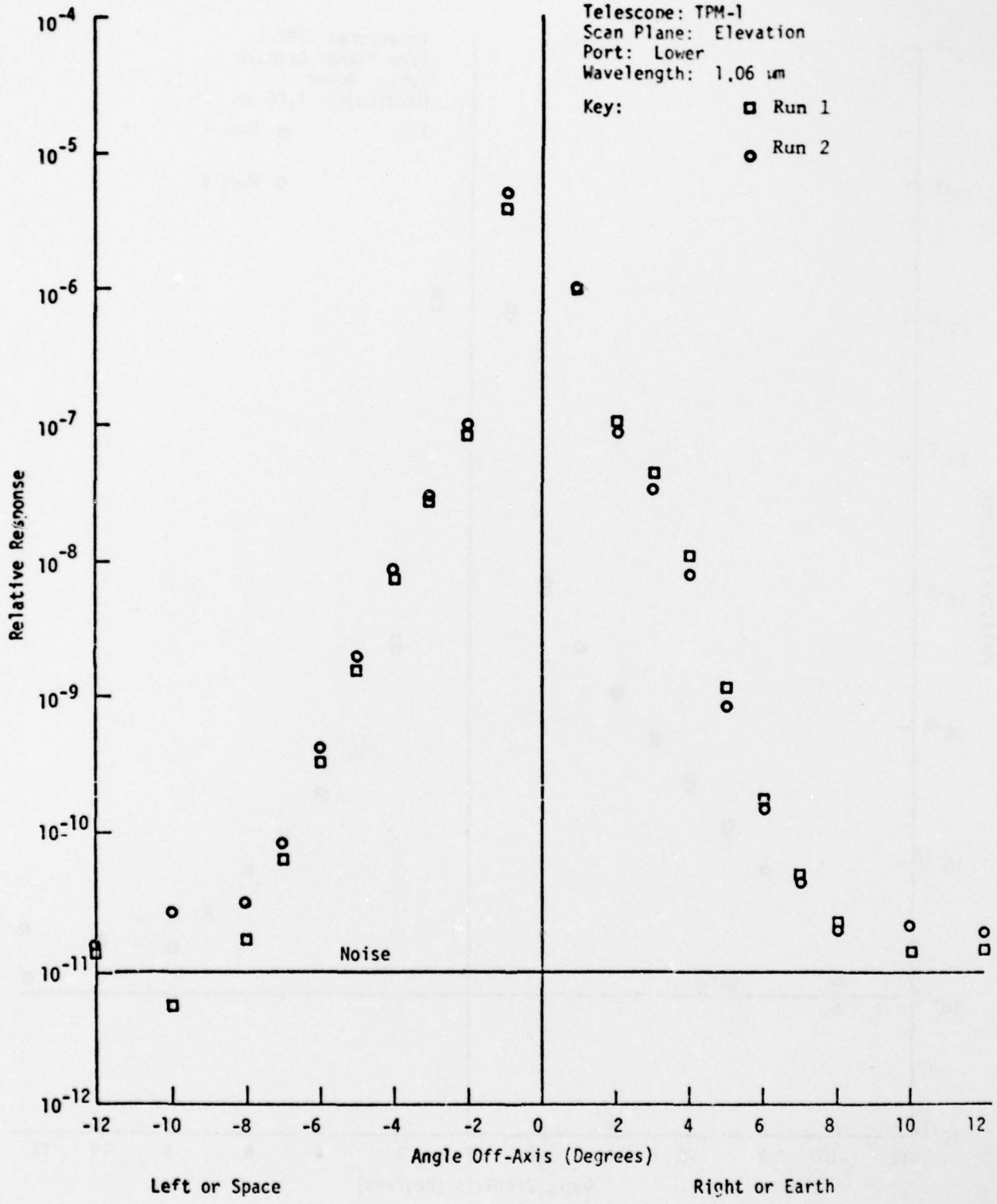

Figure 34 GRAPH 11 - OFF-AXIS REJECTION

77-1-12

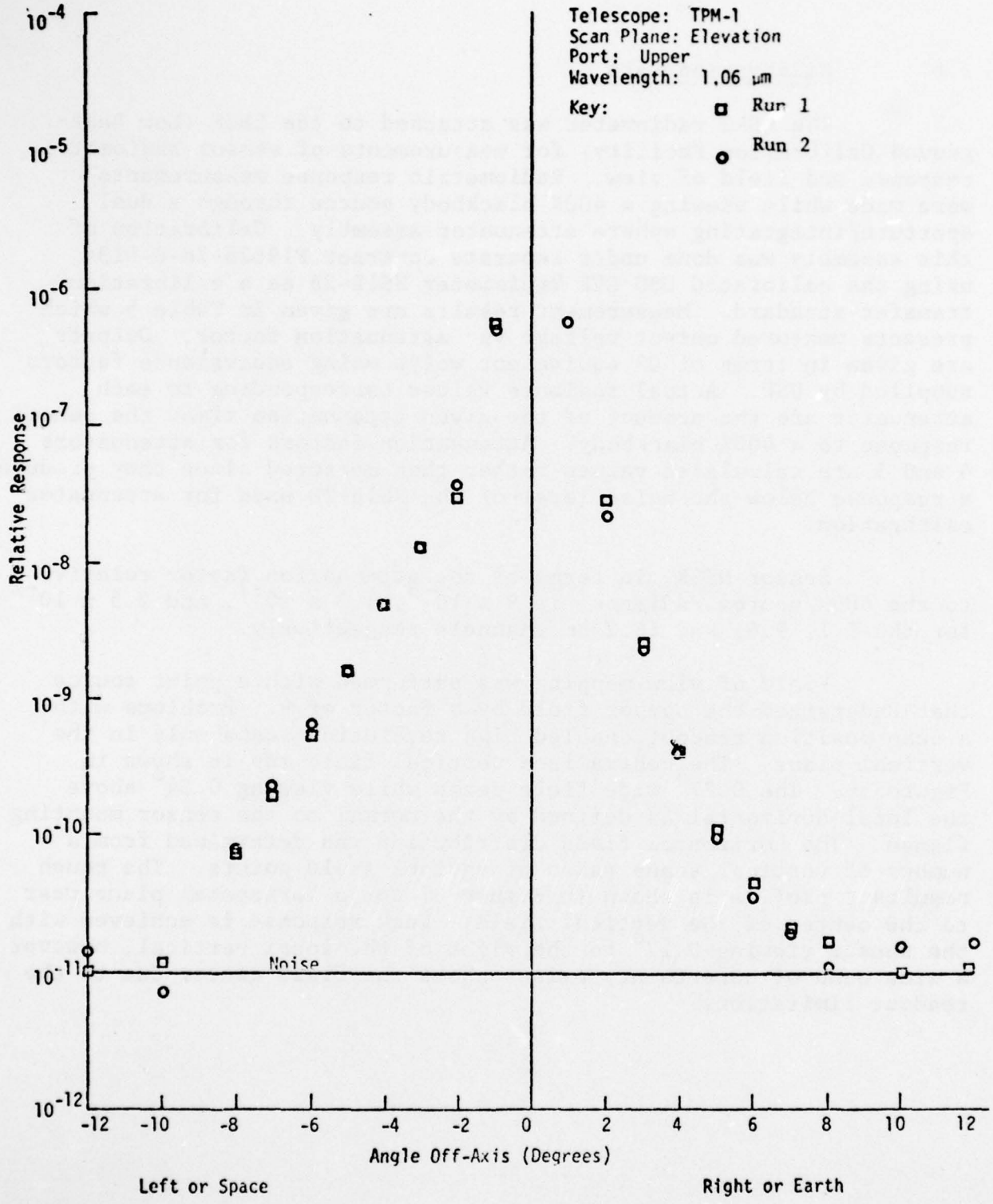

Figure 35 GRAPH 12 - OFF-AXIS REJECTION

77-1-12

3.6 Calibration Data

The HS-2 radiometer was attached to the LBCF (Low Background Calibration Facility) for measurements of sensor radiometric response and field of view. Radiometric response measurements were made while viewing a 400K blackbody source through a dual aperture/integrating sphere attenuator assembly. Calibration of this assembly was done under separate contract F19628-76-C-0134 using the calibrated USU CVF Radiometer HS1B-2B as a calibration transfer standard. Measurement results are given in Table 5 which presents measured output voltage vs attenuation factor. Outputs are given in terms of G3 equivalent volts using equivalence factors supplied by USU. Actual radiance values corresponding to each attenuator are the product of the given attenuation times the sensor response to a 400K blackbody. Attenuation factors for attenuators 4 and 5 are calculated values rather than measured since they produced a response below the noise level of the HS1B-2B used for attenuator calibration.

Sensor NESR, in terms of the attenuation factor relative to the 400K source radiance, is 9×10^{-8}, 1.3×10^{-7}, and 2.5×10^{-7} for the 5.1, 9.6, and 16.2 μm channels respectively.

Field of view mapping was performed with a point source that undersized the sensor field by a factor of 9. Problems with a scan position readout enabled high resolution scans only in the vertical plane. The centralized vertical field map is shown in Figure 36. The 0.27^{o} wide field peaks while viewing 0.34^{o} above the local horizontal as defined by the normal to the sensor mounting flange. The horizontal field distribution was determined from a number of vertical scans taken at various field points. The rough resultant profile is shown in Figure 37 for a horizontal plane near to the center of the vertical field. Peak response is achieved with the sensor viewing 0.17^{o} to the right of the local vertical, however a wide band of uncertainty exists about the field center due to the readout limitations.

Table 5

HS-2 SENSITIVITY PERFORMANCE

APERTURE	MINIMUM DESIGN TRANSMISSIONS	5.1μm	9.6μm	16.2μm
0	$1.0 \times 10^{-4} = 1.0$	G_1: 9.75×10^{-4}	2.3×10^{-3}	7.3×10^{-3}
		G_2: 7.5×10^{-3}	sat.	sat.
1	0.29	G_1: 4.3×10^{-4}	7.1×10^{-4}	2.5×10^{-3}
		G_2: 2.5×10^{-4}	6.3×10^{-4}	sat.
		G_3: 2.8×10^{-4}	sat.	sat.
2	0.03	G_1: NOISE	8.4×10^{-5}	3.0×10^{-4}
		G_2: 5.0×10^{-5}	5.8×10^{-5}	2.4×10^{-4}
		G_3: 4.9×10^{-5}	6.8×10^{-5}	sat.
3	0.002	G_2: NOISE	1.0×10^{-5}	6.2×10^{-5}
		G_3: 1.5×10^{-5}	1.0×10^{-5}	6.8×10^{-5}
4	2×10^{-4}	G_2: NOISE	NOISE	3.0×10^{-5}
		G_3: 5.8×10^{-6}	2.6×10^{-6}	3.0×10^{-5}
5	1×10^{-5}	G_2: NOISE	NOISE	2.8×10^{-5}
		G_3: 7.9×10^{-6}	2.9×10^{-6}	3.1×10^{-5}

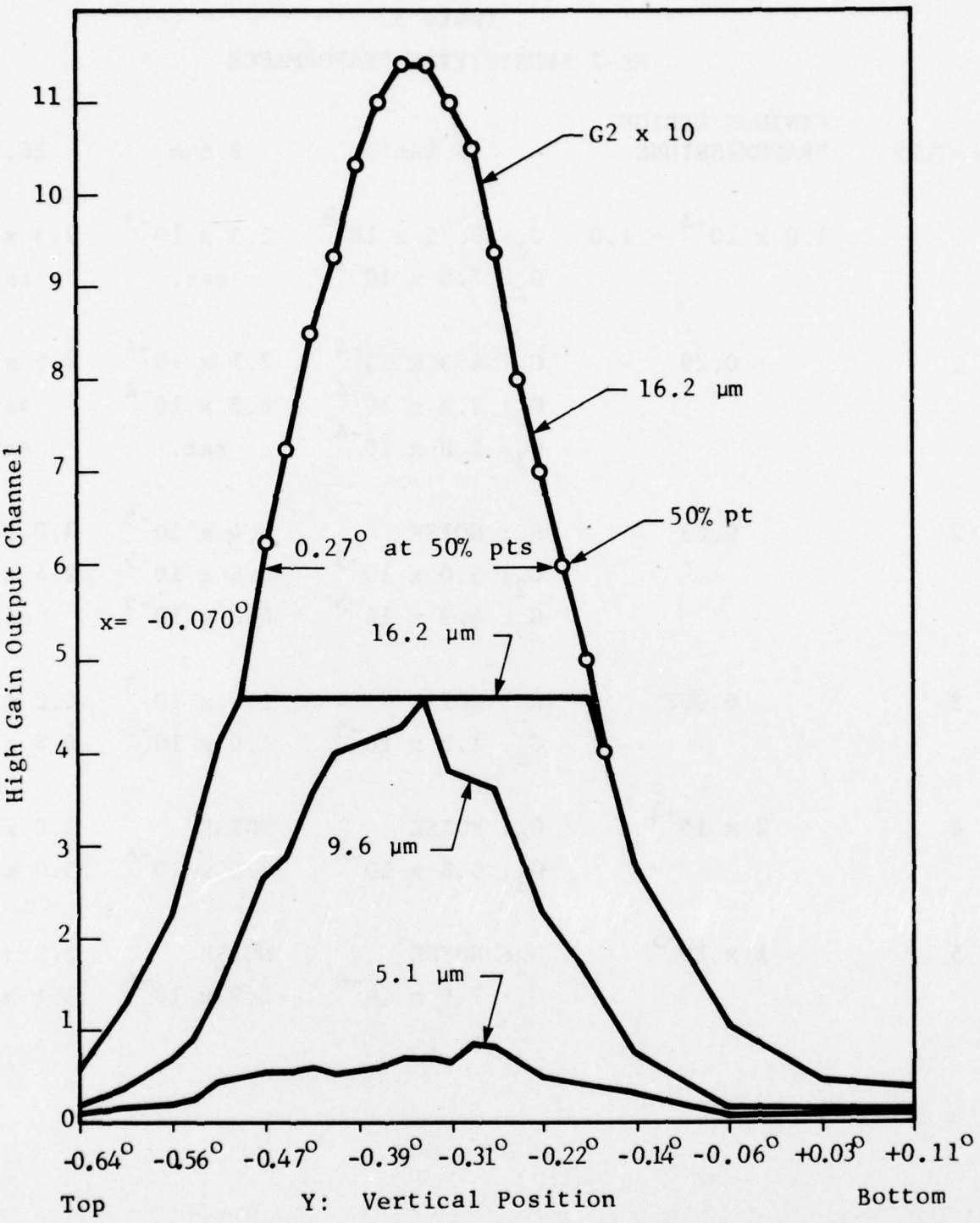

Figure 36 VERTICAL FIELD PROFILE

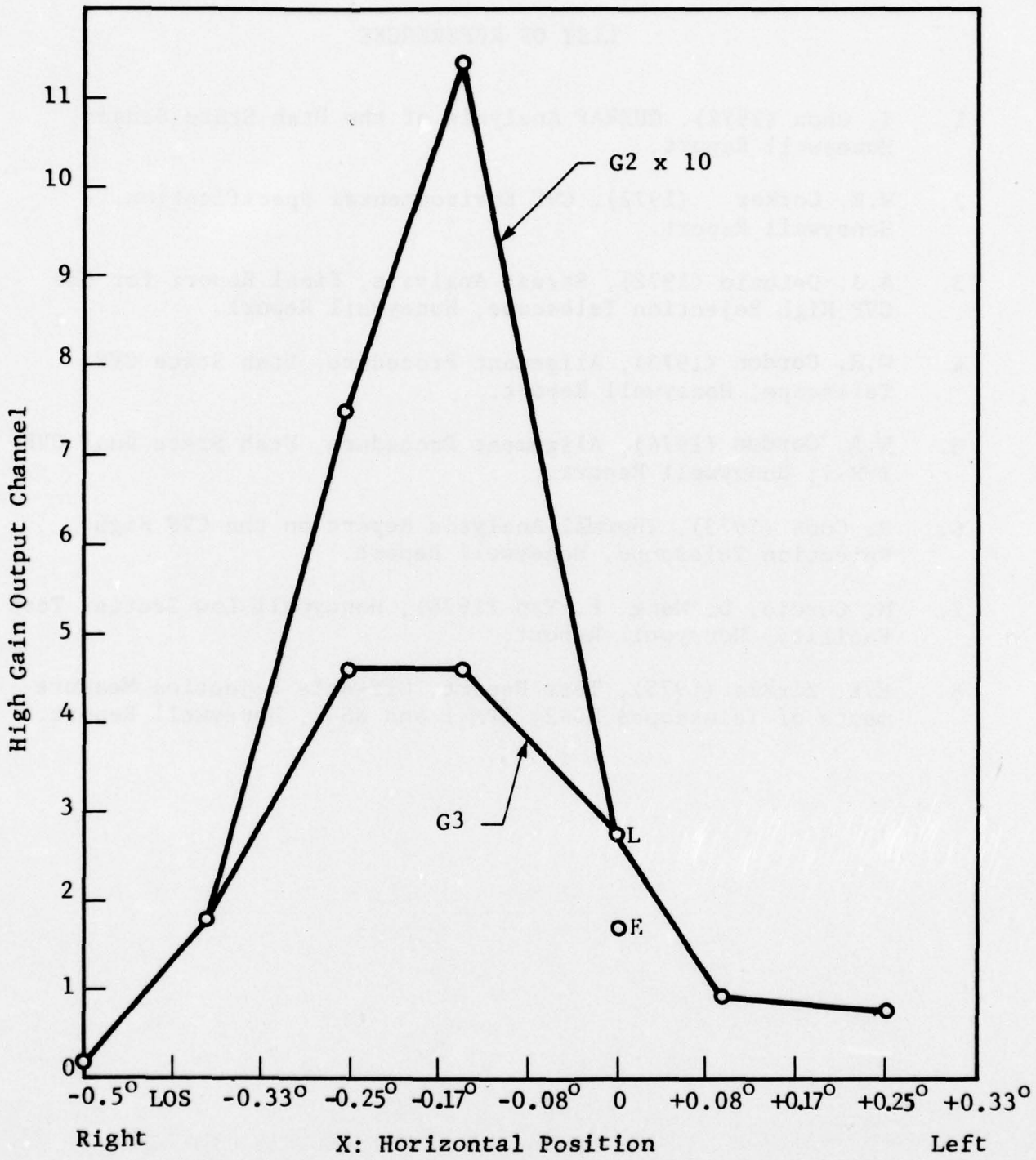

Figure 37 HORIZONTAL FIELD PROFILE

LIST OF REFERENCES

1. T. Chou (1972), GUERAP Analysis of the Utah State Sensor, Honeywell Report.

2. W.R. Corker (1972), CVF Environmental Specification, Honeywell Report.

3. A.J. DeLuzio (1972), Stress Analysis, Final Report for the CVF High Rejection Telescope, Honeywell Report.

4. W.R. Gordon (1973), Alignment Procedure, Utah State CVF Telescope, Honeywell Report.

5. W.R. Gordon (1974), Alignment Procedure, Utah State Dual CVF-TPM-1, Honeywell Report.

6. R. Coda (1973), Thermal Analysis Report on the CVF High Rejection Telescope, Honeywell Report.

7. M. Curcio, D. Wang, B. Yap (1974), Honeywell Low Scatter Test Facility, Honeywell Report.

8. R.E. Zirkle (1975), Test Report, Off-Axis Rejection Measurements of Telescopes HS-2, TPM-1 and NS-2, Honeywell Report.

Director
Defense Advanced Rsch Proj Agency
Architect Building
1400 Wilson Blvd.
Arlington, VA 22209
Attn: LTC W. A. Whitaker

Director
Defense Advanced Rsch Proj Agency
Architect Building
1400 Wilson Blvd.
Arlington, VA 22209
Attn: Major Gregory Canavan

Defense Documentation Center
Cameron Station
Alexandria, VA 22314
Attn: TC

Defense Documentation Center
Cameron Station
Alexandria, VA 22314
Attn: TC

Director
Defense Nuclear Agency
Washington, DC 20305
Attn: RAAE Charles A Blank

Director
Defense Nuclear Agency
Washington, DC 20305
Attn: TITL Tech Library

Director
Defense Nuclear Agency
Washington, DC 20305
Attn: TITL Tech Library

Director
Defense Nuclear Agency
Washington, DC 20305
Attn: TISI Archives

Director
Defense Nuclear Agency
Washington, DC 20305
Attn: RAEV Harold C. Fitz, Jr.

Director
Defense Nuclear Agency
Washington, DC 20305
Attn: RAAE Maj. J. Mayo

Director
Defense Nuclear Agency
Washington, DC 20305
Attn: RAAE G. Soper

Director
Defense Nuclear Agency
Washington, DC 20305
Attn: Major R. Bigoni

Dir of Defense Rsch & Engineering
Department of Defense
Washington, DC 20301
Attn: DD/S&SS (OS) Daniel Brockway

Commander
Field Command
Defense Nuclear Agency
Kirtland AFB, NM 87115
Attn: FCPR

Chief Livermore Division
FLD Command DNA
Lawrence Livermore Laboratory
P. O. Box 808
Livermore, CA 94550
Attn: FCPRL

Commander/Director
Atmospheric Sciences Laboratory
U. S. Army Electronics Command
White Sands Missile Range, NM 88002
Attn: DRSEL-BL-SY-A F. Niles

Atmospheric Sciences Laboratory
U.S. Army Electronics Command
White Sands Missile Range, NM 88002
Attn: H. Ballard

Commander
Harry Diamond Laboratories
2800 Powder Mill Road
Adelphi, MD 20783
Attn: DRXDO-NP, F.H. Wiminetz

Commander
U. S. Army Nuclear Agency
Fort Bliss, TX 79916
Attn: Mona-We

Director
BMD Advanced Tech Ctr
Huntsville, AL 35807
Attn: ATC-T, M Capps

Director
BMD Advanced Tech Ctr
Huntsville, AL 35807
Attn: ATC-O, W. Davies

Dep.Chief of Staff for Rsch, Dev.&ACQ
Department of the Army
Washington, DC 20310
Attn: MCB Division

Dep.Chief of Staff for Rsch,Dev&ACQ
Department of the Army
Washington, DC 20310
Attn: DAMA-CSZ-C

Dep.Chief of Staff for Rsch,Dev&ACQ
Department of the Army
Washington, DC 20310
Attn: DAMA-WSZC

Director
US Army Ballistic Research Labs
Aberdeen Proving Grounds,MD 21005
Attn: DRXBR-AM,G. Keller

Director
US Army Ballistic Research Labs
Aberdeen Proving Grounds,MD 21005
Attn: DRXRD-BSP, J. Heimerl

Director
US Army Ballistic Research Labs
Aberdeen Proving Grounds,MD 21005
Attn: John Mester

Director
US Army Ballistic Research Labs
Aberdeen Proving Grounds, MD 21005
Attn: Tech Library

Commander
US Army Electronics Command
Fort Monmouth, NJ 37703
Attn: Inst for Expl Research

Commander
US Army Electronics Command
Fort Monmouth, NJ 37703
Attn: DRSEL

Commander
US Army Electronics Command
Fort Monmouth, NJ 37703
Attn: Stanley Kronenberger

Commander
US Army Electronics Command
Fort Monmouth, NJ 37703
Attn: Weapons Effects Section

Commander
US Army Foreign Science & Tech Ctr
220 7th Street, NE
Charlottesville, VA 22901
Attn: Robert Jones

Chief
US Army Research Office
P. O. Box 12211
Triangle Park, NC 27709
Attn: Robert Mace

Commander
Naval Oceans Systems Center
San Diego, CA 92152
Attn: Code 2200 Ilan Rothmuller

Commander
Naval Oceans Systems Center
San Diego, CA 92152
Attn: Code 2200 William Moler

Commander
Naval Oceans Systems Center
San Diego, CA 92152
Attn: Code 2200 Herbert Hughes

Commander
Naval Oceans Systems Center
San Diego, CA 92152
Attn: Code 2200 Richard Pappert

Commander
Naval Oceans Systems Center
San Diego, CA 92152
Attn: Code 2200 Jurgen R. Richter

Director
Naval Research Laboratory
Washington, DC 20375
Attn: Code 7712 Douglas P. McNutt

Director
Naval Research Laboratory
Washington, DC 20375
Attn: Code 7701 Jack D. Brown

Director
Naval Research Laboratory
Washington, DC 20375
Attn: Code 2600 Tech Lib

Director Naval Research Laboratory
Washington, DC 20375
Attn: Code 7127 Charles Y. Johnson

Director
Naval Research Laboratory
Washington, DC 20375
Attn: Code 7700 Timothy P. Coffey

Director
Naval Research Laboratory
Washington, DC 20375
Attn: Code 7709 WAHAB ALI

Director
Naval Research Laboratory
Washington, DC 20375
Attn: Code 7750 Darrell F. Strobel

Director
Naval Research Laboratory
Washington, DC 20375
Attn: Code 7750 Paul Juluenne

Director
Naval Research Laboratory
Washington, DC 20375
Attn: Code 7750 J. Fedder

Director
Naval Research Laboratory
Washington, DC 20375
Attn: Code 7750 S. Ossakow

Director
Naval Research Laboratory
Washington, DC 20375
Attn: Code 7750 J. Davis

Commander
Naval Surface Weapons Center
White Oak, Silver Spring, MD 20910
Attn: Code WA501 Navy NUC Prgms Off

Commander
Naval Surface Weapons Center
White Oaks, Silver Spring, MD 20910
Attn: Technical Library

Superintendent
Naval Post Graduate School
Monterey, CA 93940
Attn: Tech Reports Librarian

Commander
Naval Electronics Systems Command
Naval Electronics Systems Command Hqs
Attn: PME 117

Commander
Naval Intelligence Support CTR
4301 Suitland Rd. Bldg 5
Washington, DC 20390
Attn: Document Control

AF Geophysics Laboratory, AFSC
Hanscom AFB, MA 01731
Attn: LKB Kenneth S. W. Champion

AF Geophysics Laboratory, AFSC
Hanscom AFB, MA 01731
Attn: OPR Alva T. Stair

AF Geophysics Laboratory, AFSC
Hanscom AFB, MA 01731
Attn: OPR-1 J. Ulwick

AF Geophysics Laboratory, AFSC
Hanscom AFB, MA 01731
Attn: OPR-1 R. Murphy

AF Geophysics Laboratory, AFSC
Hanscom AFB, MA 01731
Attn: OPR-1 J. Kennealy

AF Geophysics Laboratory, AFSC
Hanscom AFB, MA 01731
Attn: PHG JC McClay

AF Georphysics Laboratory, AFSC
Hanscom AFB, MA 01731
Attn: LKD Rocco Narcis

AF Geophysics Laboratory, AFSC
Hanscom AFB, MA 01731
Attn: LKO, R. Huffman

AF Weapons Laboratory, AFSC
Kirtland, AFB, NM 87117
Attn: Maj. Gary Ganong, Dym

Commander
ASD
WPAFB, OH 45433
Attn: ASD-YH-EX LTC Robert Leverette

SAMSO/AW
Post Office Box 92960
Worldway Postal Center
Los Angeles, CA 90009
Attn: SZJ Major Lawrence Doan

SAMSO/SW
P. O. Box 92960
Worldway Post Center
Los Angeles, CA 90009
Attn: AW

AFTAC
Patrick AFB, FL 32925
Attn: Tech Library

AFTAC
Patrick AFB, FL 32925
Attn: TD

HQ
Air Force Systems Command
Andrews AFB
Washington, DC 20331
Attn: DLS

HQ
Air Force Systems Command
Andrews AFB
Washington, DC 20331
Attn: Tech Library

HQ
Air Force Systems Command
Andrews AFB
Washington, DC 20331
Attn: DLCAE

HQ
Air Force Systems Command
Andrews AFB
Washington, DC 20331
Attn: DLTW

HQ
Air Force Systems Command
Andrews AFB
Washington, DC 20331
Attn: DLXP

HQ
Air Force Systems Command
Andrews AFB
Washington, DC 20331
Attn: SDR

HQ USAF/RD
Washington, DC 20330
Attn: RDQ

Commander
Rome Air Development Center
Griffiss AFB, NY 13440
Attn: JJ. Simons OSCS

Division of Military Application
US Energy Rsch & Dev Admin
Washington, DC 20545
Attn: DOC CON

Los Alamos Scientific Laboratory
P. O. Box 1663
Los Alamos, NM 87545
Attn: Doc Con for RA Jeffries

Los Alamos Scientific Laboratory
P. O. Box 1663
Los Alamos, NM 87545
Attn: DOC CON for CR Mehl Org 5230

Los Alamos Scientific Laboratory
P. O. Box 1663
Los Alamos, NM 87545
Attn: DOC CON for H V Argo

Los Alamos Scientific Laboratory
P. O. Box 1663
Los Alamos, NM 87545
Attn: DOC CON for M. Tierney J-10

Los Alamos Scientific Laboratory
P. O. Box 1663
Los Alamos, NM 87545
Attn: DOC CON for Robert Brownlee

Los Alamos Scientific Laboratory
P. O. Box 1663
Los Alamos, NM 87545
Attn: DOC CON for William Maier

Los Alamos Scientific Laboratory
P. O. Box 1663
Los Alamos, NM 87545
Attn: DOC CON for John Zinn

Los Alamos Scientific Laboratory
P. O. Box 1663
Los Alamos, NM 87545
Attn: DOC CON for Reference Library
Ann Beyer

Sandia Laboratories
Livermove Laboratory
P. O. Box 965
Livermore, CA 94556
Attn: DOC CON for Thomas Cook
ORG 8000

Sandia Laboratories
P. O. Box 5800
Albuquerque, NM 87115
Attn: DOC CON for W.D. Brown
ORG 1353

Sandia Laboratories
P. O. Box 5800
Albuquerque, NM 87115
Attn: Doc. Cont. for
L. Anderson ORG 1247

Sandia Laboratories
P. O. Box 5800
Albuquerque, NM 87115
Attn: Doc. Cont. for
Morgan Kramma ORG 5720

Sandia Laboratories
P. O. Box 5800
Albuquerque, NM 87115
Attn: Doc. Cont. for
Frank Hudson ORG 1722

Sandia Laboratories
P. O. Box 5800
Albuquerque, NM 87115
Attn: Doc. Cont. for ORG
3422-1 Sandia Repts. Coll.

Argonne National Laboratory
Records Control
9700 South Cass Avenue
Argonne, IL 60439
Attn: Doc.Cont. for AC Wahl

Argonne National Laboratory
Records Control
9700 South Cass Avenue
Argonne, IL 60439
Attn: Doc. Cont. for David W. Green

Argonne National Laboratory
Records Control
9700 South Cass Avenue
Argonne, IL 60439
Attn: Doc. Cont. for LIR SVCS Rpts Sec.

Argonne National Laboratory
Records Control
9700 South Cass Avneue
Argonne, IL 60439
Attn: Doc. Cont. for S. Garelnick

Argonne National Laboratory
Records Control
9700 South Cass Avenue
Argonne, IL 60439
Attn: Doc. Cont. for Gerald T. Reedy

University of California
Lawarence Livermore Laboratory
P. O. Box 808
Livermore, CA 94550
Attn: W. H. Duewer Gen L-404

University of California
Lawrence Livermore Laboratory .
P. O. Box 808
Livermore, CA 94550
Attn: Julius Chang L-71

University of California
Lawrence Livermore Laboratory
P. O. Box 808
Livermore CA 94500
Attn: G. R. Haugen L-404

University of California
Lawrence Livermore Laboratory
P. O. Box 808
Livermore, CA 94550
Attn: D. J. Wjerbles L-142

California, State of
Air Resource Board
9528 Telsta Avenue
Al Monte, CA 91731
Attn: Leo ZaFonte

California Institute of Technology
Jet Propulsion Laboratory
4800 Oak Grove Drive
Pasadena, CA 91103
Attn: Joseph A. Jello

U. S. Energy Rsch & Dev. Admin.
Division of Headquarters Services
Library Branch G-043
Washington, DC 20545
Attn: Doc. Cont. for Class Tech Lib

Department of Transportation
Office of the Secretary
TAD-44, 1, Room 10402-R
400 7th Street S. W.
Washington, DC 20590
Attn: Samuel C. Coroniti

NASA
Goddard Space Flight Center
Greenbelt, MD 20771
Attn: A Tempkin

NASA
Goddard Space Flight Center
Greenbelt, MD 20771
Attn: A. J. Bauer

NASA
Goddard Space Flight Center
Greenbelt, MD 20771
Attn: Technical Library

NASA
Goddard Space Flight Center
Greenbelt, MD 20771
Attn: J. Siry

NASA
600 Independence Avenue S. W.
Washington, DC 20546
Attn A. Gessow

NASA
600 Independence Avenue SW
Washington, DC 20546
Attn: D. P. Cauffman

NASA
600 Independence Avenue SW
Washington, DC 20546
Attn: LTC D. R. Hallenbeck Code SG

NASA
600 Independence Avenue SW
Washington, DC 20546
Attn: R. Fellows

NASA
600 Independence Avenue SW
Washington, DC 20546
Attn: Mr. A. Schardt

NASA
600 Independence Avenue SW
Washington, DC 20546
Attn: M. Tepper

NASA
Langley Research Center
Langley Station
Hampton, VA 23365
Attn: Charles Schexnayder MS-168

NASA
Ames Resch Center
Moffett Field, CA 90435
Attn: N-254-4 Walter L. Starr

NASA
Ames Research Center
Moffett Field, CA 94035
Attn: N-254-4 R Whitten

NASA
Ames Research Center
Moffett Field, CA 94035
Attn: N-254-4 Ilia G. Poppoff

NASA
Ames Research Center
Moffett Field, CA 94036
Attn: N-254-3 Neil H. Farlow

NASA
George C. Marshall Space Flight Ctr
Huntsville, AL 35812
Attn: C. R. Balcher

NASA
George C. Marshall Space Flight Ctr.
Huntsville, AL 35812
Attn: N. H. Stone

NASA
George C. Marshall Space Flight Ctr.
Huntsville, AL 35812
Attn: W. A. Oran

NASA
George C. Marshall Space Flight Ctr.
Huntsville, AL 35812
Attn: Code ES22 John Watts

NASA
George C. Marshall Space Flight Ctr.
Huntsville, AL 35812
Attn: W. T. Roberts

NASA
George C. Marshall Space Flight Ctr.
Huntsville, AL 35812
Attn: R. D. Hudson

NASA
George C. Marshall Space Flight Ctr.
Huntsville, AL 35812
Attn: R. Chappell

Albany Metallurgy Research Center
U. S. Bureau of Mines
P. O. Box 70
Albany, OR 97321
Attn: Eleanor Arshire

Central Intelligence Agency
Attn: RD/SI RM 5G48 HQ Bldg.
Washington, DC 20505
Attn: NED/OS I-2G4R HQS

Department of Commerce
National Bureau of Standards
Washington, DC 20234
Attn: Sec Officer for
Attn: James Devoe

Department of Commerce
National Bureau of Standards
Washington, DC 20234
Attn: Sec Officer Stanley Arramowitz

Depart.of Commerce
National Bureau of Standards
Washington, DC 20234
Attn: Sec Officer J. Cooper

Department of Commerce
National Bureau of Standards
Washington, DC 20234
Attn: Sec Officer George A. Sinnatt

Department of Commerce
National Bureau of Standards
Washington, DC 20234
Attn: Sec Officer K. Kessler

Department of Commerce
National Bureau of Standards
Washington, DC 20234
Attn: Sec Officer for M. Krauss

Department of Commerce
National Bureau of Standards
Washington, DC 20234
Attn: Sec Officer Lewis H. Gevantman

Department of Commerce
National Bureau of Standards
Washington, DC

National Oceanic & Atmospheric Admin.
Environmental Research Laboratories
Department of Commerce
Boulder, CO 80302
Attn: George C. Reid Aeronomy Lab

National Oceanic & Atmospheric Admin.
Environmental Research Laboratories
Department of Commerce
Boulder, CO 80302
Attn: Eldon Ferguson

National Oceanic & Atmospheric Admin
Environmental Research Laboratories
Department of Commerce
Boulder, CO 80302
Attn: Fred Fehsenfeld

Aero-Chem Research Laboratories, Inc.
P. O. Box 12
Princeton, NJ 08540
Attn: A Fontijn

Aero-Chem Research Laboratories, Inc.
P. O. Box 12
Princeton, NJ 08540
Attn: H. Pergament

Aerodyne Research, Inc.
Bedford Research Park
Crosby Drive
Bedford, MA 01731
Attn: F. Bien

Aerodyne Research, Inc.
Bedford Research Park
Crosby Drive
Bedford, MA 01731
Attn: M. Camac

Aeronomy Corporation
217 S Neil Street
Champaign, IL 61820
Attn: A. Bowhill

Aerospace Corporation
P. O. Box 92957
Los Angeles, CA 90009
Attn: N. Cohen

Aerospace Corporation
P. O. Box 92957
Los Angeles, CA 90009
Attn: Harris Mayer

Aerospace Corporation
P. O. Box 92957
Los Angeles, CA 90009
Attn: Sidney W. Kash

Aerospace Corporation
P. O. Box 92957
Los Angeles, CA 90009
Attn: T. Widhoph

Aerospace Corporation
P. O. Box 92957
Los Angeles, CA 90009
Attn: R. J. McNeal

Aerospace Corporation
P. O. Box 92957
Los Angeles, CA 90009
Attn: R. Grove

Aerospace Corporation
P. O. Box 92957
Los Angeles, CA 90009
Attn: Irving M. Garfunkel

Aerospace Corporation
P. O. Box 92957
Los Angeles, CA 90009
Attn: Thomas D. Taylor

Aerospace Corporation
P. O. Box 92957
Los Angeles, CA 90009
Attn: V. Josephson

Aerospace Corporation
P. O. Box 92957
Los Angeles, CA 90009
Attn: Julian Reinheimer

Aerospace Corporation
P. O. Box 92957
Los Angeles, CA 90009
Attn: R. D. Rawcliffe

AVCO-Everett Research Laboratory Inc.
2385 Revere Beach Parkway
Everett, MA 02149
Attn: Technical Library

AVCO-Everett Research Laboratory Inc.
2385 Revere Beach Parkway
Everett, MA 02149
Attn: George Sutton

AVCO-Everett Research Laboratory Inc.
2385 Revere Beach Parkway
Everett, MA 02149
Attn: C. W. Von Rosenberg, Jr.

Battelle Memorial Institute
505 King Avenue
Columbus, OH 43201
Attn: Donald J. Hamman

Battelle Memorial Institute
505 King Avenue
Columbus, OH 43201
Attn: Donald J. Ham

Battelle Memorial Institute
505 King Avenue
Columbus, OH 43201
Attn: Stoiac

Battelle Memorial Institute
505 King Avenue
Columbus, OH 43201
Attn: Richard K. Thatcher

Brown Engineering Company, Inc.
Cummings Research Park
Huntsville, AL 35807
Attn: N. Passino

The Trustees of Boston College
Chestnut Hill Campus
Chestnut Hill, MA 02167
Attn: Chairman Dept. of Chem.

Brown Engineering Company, Inc.
Cummings Research Park
Huntsville, AL 35807
Attn: Ronald Patrick

California At Riverside, Univ. of
Riverside, CA 92502
Attn: Alan C. Lloyd

California at Riverside, Univ. of
Riverside, CA 92502
Attn: James N. Pitts Jr.

California at San Diego, Univ. of
3175 Miramar Road
La Jolla, CA 92037
Attn: S. C. Lin

California University of
Berkeley Campus Room 318
Sproul Hall
Berkeley, CA 94720
Attn: Sec Officer for Harold Johnston

California University of
Berkeley Campus Room 318
Sproul Hall
Berkeley, CA 94720
Attn: Sec Officer for Dept. of Chem
W. H. Miller

California, State of
Air Resources Board
9528 Telstar Avenue
El Monte, CA 91731
Attn: Leo ZaFonte

Calspan Corporation
P. O. Box 235
Buffalo, NY 14224
Attn: C. E. Treanor

Calspan Corporation
P. O. Box 235
Buffalo, NY 14221
Attn: G. C. Valley

Calspan Corporation
P. O. Box 235
Buffalo, NY 14221
Attn: M. G. Dunn

Calspan Corporation
P. O. Box 235
Buffalo, NY 14221
Attn: W. Wurster

Colorado, University of
Office of Contracts and Grants
380 Administrative Annex
Boulder, CO 80302
Attn: A Phelps Jila

Colorado, University of
Office of Contracts and Grants
380 Administrative Annex
Boulder, CO 80302
Attn: Jeffrey B. Pearce LASP

Colorado, University of
Office of Contracts and Grants
380 Administrative Annex
Boulder, CO 80302
Attn: C. Peaty Jila

Colorado, University of
Office of Contracts and Grants
380 Administrative Annex
Boulder, Co. 80302
Attn: C. Lineberger JILA

Colorado, University of
Office of Contracts and Grants
380 Administrative Annex
Boulder, Co. 80302
Attn: Charles A. Barth LASP

Columbia University, The Trustees
In the City of New York
La Mont Doherty Geological
Observatory-Torrey Cliff
Palisades, N.Y. 19064
Attn: B. Phelan

Columbia University, The Trustees of
City of New York
116th Street & Broadway
New York, N.Y. 10027
Attn: Richard N. Zare

Columbia University, The Trustees of
City of New York
116th & Broadway
New York, N.y. 10027
Attn: Sec. Officer H.M. Foley

Concord Sciences
P.O. Box 119
Concord, Ma. 01742
Attn: Emmett A. Sutton

Denver, University of
Colorado Seminary
Denver Research Institute
P.O. Box 10127
Denver, Co. 80210
Attn: Sec. Officer for Mr. Van ZYL

Denver, University of
Colorado Seminary
Denver Reasearch Institute
P.O. Box 10127
Denver, Col. 80210
Attn: Sec. Officer for David Murcray

General Electric Company
Tempo-Center for Advanced Studies
816 State Street (P.O. Drawer QQ)
Santa Barbara, Ca. 93102
Attn: Dasaic

General Electric Company
Tempo-Center for Advanced Studies
816 State Street (P.O. Drawer QQ)
Santa Barbara, Ca. 93102
Attn: Warren S. Knapp

General Electric Company
Tempo-Center for Advanced Studies
816 State Street (P.O. Drawer)
Santa Barbara, Ca. 93102
Attn: Tim Stephens

General Electric Company
Tempo-Center for Advanced Studies
816 State Street (P.O. Drawer QQ)
Santa Barbara, Ca. 93102
Attn: Don Chandler

General Electric Company
Tempo-Center for Advanced Studies
816 State Street (P.O. Drawer QQ)
Santa Barbara, Ca. 93102
Attn: B. Cambill

General Elec. Co.
Space Division
Valley Forge Space Center
Goddard Boulevard
King of Prussia
P.O. Box 8555
Philadlephia, Pa. 19101
Attn: M. H. Bortner,
Space Science Lab

General Electric Company
Space Division
Valley Forge Space Center
Goddard Boulevard
King of Prussia
P.O. Box 8555
Philadelphia, Pa. 19101
Attn: J. Burns

General Electric Company
Space Division
Valley Forge Space Center
Goddard Boulevard
King of Prussia
P.O. Box 8555
Philadelphia, Pa. 19101
Attn: F. Alyea

General Electric Company
Space Division
Valley Forge Space Center
Goddard Boulevard
King of Prussia
P.O. Box 8555
Philadelphia, Pa. 19101
Attn: P. Zavitsands

General Electric Company
Space Division
Valley Forge Space Center
Goddard Boulevard
King of Prussia
P.O. Box 8555
Philadelphia, Pa. 19101
Attn: R. H. Edsall

General Electric Company
Space Division
Valley Forge Space Center
Goddard Boulevard
King of Prussia
P.O. Box 8555
Philadelphia, Pa. 19101
Attn: T. Baurer

General Research Corporation
P.O. Box 3587
Santa Barbara, Ca. 94105
Attn: John Ise, Jr.

Geophysical Institute
University of Alaska
Fairbanks, Ak. 99701
Attn: D. Henderson

Geophysical Institute
University of Alaska
Fairbanks, Ak. 99701
Attn: J. S. Wagner Physics Dept.

Geophysical Institute
University of Alaska
Fairbanks, Ak. 99701
Attn: B. J. Watkins

Geophysical Institute
University of Alaska
Fairbanks, Ak. 99701
Attn: T. N. Davis

Geophysical Institute
University of Alaska
Fairbanks, Ak. 99701
Attn: R. Parthasarathy

Geophysical Institute
University of Alaska
Fairbanks, Ak. 99701
Attn: Neal Brown

Lowell, University of
Center for Atmospheric Research
450 Aiken Street
Lowell, Ma. 01854
Attn: G. T. Best

Lockheed Missiles and Space Company
3251 Hanover Street
Palo Alto, Ca. 94304
Attn: John Kumer Dept. 52-54

Lockheed Missiles and Space Company
3251 Hanover Street
Palo Alto, Ca. 94304
Attn: John Kimer Dept. 52-54

Lockheed Missiles and Space Company
3251 Hanover Street
Palo Alto, Ca. 94304
Attn: John B. Cladis Dept. 52-12

Lockheed Missiles and Space Company
3251 Hanover Street
Palo Alto, Ca. 94304
Attn: Billy M. McCormac Dept 52-54

Lockheed Missiles and Space Company
3251 Hanover Street
Palo Alto, Ca. 94304
Attn: Tom James Dept 52-54

Lockheed Missiles and Space Company
3251 Hanover Street
Palo Alto, Ca. 94304
Attn: J. B. Reagan D/52-12

Lockheed Missiles and Space Comapny
3251 Hanover Street
Palo Alto, Ca. 94304
Attn: Martin Walt Dept 52-10

Lockheed Missiles and Space Company
3251 Hanover Street
Palo Alto, Ca. 94304
Attn: Richard G. Johnson Dept 52-12

Lockheed Missiles and Space Comapny
3251 Hanover Street
Palo Alto, Ca. 94304
Attn: Robert D. Sears Dept 52-14

Lockheed Missiles and Space Companh
3251 Hanover Street
Palo Alto, Ca. 94304
Attn: J. R. Wrinkler

Institute for Defense Analyse
400 Army-Navy Drive
Arlington, Va. 22202
Attn: Ernest Bauer

institute for Defense Analyse
400 Army-Navy Drive
Arlington, Va. 22202
Attn: Hans Wolfhard

Mission Research Corporation
735 State Street
Santa Barbara, Ca. 93101
Attn: D. Archer

Mission Research Corporation
735 State Street
Santa Barbara, Ca. 93101
Attn: D. Fischer

Mission Research Corporation
735 State Street
Santa Barbara, Ca. 93101
Attn: M. Scheibe

Mission Research Corporation
735 State Street
Santa Barbara, Ca. 93101
Attn: D. Sappenfield

Mission Research Corporation
735 State Street
Santa Barbara, Ca. 93101
Attn: D. Sowle

Photometric, Inc.
442 Marrett Road
Lexington, Ma. 02173
Attn: Irving L. Kofsky

Physical Dynamics Inc.
P.O. Box 1069
Berkeley, Ca. 94701
Attn: J. B. Workman

Physical Dynamics Inc.
P.O. Box 1069
Berkeley, Ca. 94701
Attn: A. Thompson

Physical Sciences, Inc.
30 Commerce Way
Woburn, Ma. 01801
Attn: Kurt Wray

Physical Sciences, Inc.
30 Commerce Way
Woburn, Ma. 01801
Attn: R. L. Taylor

Physical Sciences, Inc.
39 Commerce Way
Woburn, Ma. 01801
Attn: G. Caledonia

Physics International Company
2700 Merced Street
San Leandro, Ca. 94577
Attn: Doc Con for Tech Lib

Pittsburgh, University of
of the Comwlth Sys. of Higher Educ.
Cathedral of Learning
Pittsburgh, Pa 14213
Attn: Wade L. Fite

Pittsburgh, University of
of the Comwlth Sys. of Higher Educ.
Cathedral of Learning
Pittsburgh, Pa. 15213
Attn: Manfred A. Biondi

Pittsburgh, University of the
Comwlth Sys. of Higher Educ.
Cathedral of Learning
Pittsburgh, PA. 15213
Attn: Frederick Kaufman

Pittsburgh, University of the
Comwlth Sys. of Higher Educ.
Cathedral of Learning
Pittsburgh, PA. 15213
Attn: Edward Gerjuoy

Forrestal Campus Library
Box 710
Princeton University
Princeton, N.J. 08540
Attn: Arnold J. Kelly

R & D Associates
P.O. Box 9695
Marina Del Rey, CA. 90291
Attn: Richard Latter

R & D Associates
P.O. Box 9695
Marina Del Rey, CA 90291
Attn. R.G. Lindgren

R & D Associates
P.O. Box 9695
Marina Del Rey, CA 90291
Attn: Bryan Gabbard

R & D Associates
P. O. Box 9695
Marina Del Rey, CA 90291
Attn. H.A. Dry

R & D Associates
P. O. Box 9695
Marina Del Rey, CA 90291
Attn: Robert Lelevier

R & D Associates
P.O. Box 9695
Marina Del Rey,CA 90291
Attn: R.P. Turco

R & D Associates
P. O. Box 9695
Marina Del Rey, CA 90291
Attn: Albert L. Latter

R & D Associates
P. O. Box 9695
Marina Del Rey, CA 90291
Attn. Forest Gilmore

R & D Associates
P. O. Box 9695
Marina Del Rey, CA 90291
Attn. D. Dee

R & D Associates
1815 N. Ft. Myer Drive
11th Floor
Arlington, VA 22209
Attn: Herbert J, Mitchell

R & D Associates
1815 N. Ft. Myer Drive
11th Floor
Arlington, VA 22209
Attn: J.W. Rosengren

Rand Corporation
1700 Main St.
Santa Monica, CA 90406
Attn: Cullen Crain

Science Applications, Inc.
P. O. Box 2351
La Jolla, CA 92038
Attn: Daniel A. Hamlin

Science Applications, Inc.
P.O. Box 2351
La Jolla, CA 92038
Attn: David Sachs

Space Data Corporation
1331 South 26th St.
Phoenix, AZ 85034
Attn: Edward F. Allen

Stanford Rsch Institute International
333 Ravenswood Avenue
Menlo Park, CA 94025
Attn: M. Baron

Stanford Rsch, Institute International
333 Ravenswood Avenue
Menlo Park, CA. 94025
Attn: L. Leadabrand

Stanford Rsch Institute International
333 Ravenswood Avenue
Menlo Park, CA 94025
Attn: Walter G. Chestnut

Stanford Rsch Institute International
1611 North Kent Street
Arlington, VA 22209
Attn: Warren W. Berning

Stanford Rsch Institute International
1611 North Kent Street
Arlington, VA 22209
Attn: Charles Hulbert

Technology International Corporation
75 Wiggins Avenue
Bedford, MA. 01730
Attn: W.P. Boquist

United Technologies Corporation
755 Main Street
Hartford, CT. 06103
Attn: H. Michels

United Technologies Corporation
755 Main Street
Hartford, CT. 06103
Attn: Robert Hbullis

Utah State University
Logan, UT 84321
Attn: Doran Baker

Utah State University
Logan, UT. 84321
Attn: Kay Baker

Utah State University
Logan, UT 84321
Attn; C. Wyatt

Utah State University
Logan, UT 84321
Attn: D. Burt

Visidyne, Inc.
19 Third Avenue
Northwest Industrial Park
Burlington, MA. 08103
Attn: Henry J. Smith

Visidyne, Inc.
19 Third Avenue
Northwest Industrial Park
Burlington, MA. 01803
Attn: J.W. Carpenter

Visidyne, Inc.
19 Third Avenue
Northwest Industrial Park
Burlington, MA. 01803
Attn: T.C. Degges

Visidyne, Inc.
19 Third Avenue
Northwest Industrial Park
Burlington, MA. 01803
Attn: Charles Humphrey

Wayne State University
1064 MacKenzie Hall
Detroit, MI 48202
Attn: Pieter K. Rol,
Cham. Engrg & Mat. Sci.

Wayne State University
1064 MacKenzie Hall
Detroit, MI 48202
Attn: R.H. Kummler

Wayne State University
Dept. of Physics
Detroit, MI 48202
Attn: Walter E. Kauppila

Yale University
New Haven, CT. 06520
Attn: Engineering Dept.